UNIVERSITÀ
DEGLI STUDI
FIRENZE

DOTTORATO DI RICERCA IN SCIENZE BIOMEDICHE
Curriculum Oncologia Sperimentale e Clinica

CICLO XXX

COORDINATORE Prof. Dello Sbarba Persio

"Characterization of novel molecular targets and mechanisms in Philadelphia-negative Myeloproliferative Neoplasms"

Settore Scientifico Disciplinare MED/15

Dottorando
Dott. Calabresi Laura

Tutore
Prof. Vannucchi Alessandro Maria

Coordinatore
Prof. Dello Sbarba Persio

Anni 2014/2017

INDEX

ABSTRACT

The present thesis encompasses two researches projects I conducted during my PhD program in Clinical and Experimental Oncology. The common theme is represented by Philadelphia negative Myeloproliferative Neoplasms (MPNs), which include Essential Thrombocythemia (ET), Polycythemia Vera (PV) and Primary Myelofibrosis (PMF). MPNs are clonal disorders of hematopoietic stem cell and are characterized by an excessive production of terminally differentiated myeloid cells. Driver mutations in MPNs include *JAK2*^{V617F}, *CALR* and *MPL*.

The constitutive activation of JAK/STAT pathway by *JAK2*^{V617F} and other driver mutations in MPNs promotes deregulation of other intracellular signaling pathways including the PI3K/mTOR. We previously reported that drugs targeting the PI3K-pathway induce inhibition of MPN cells proliferation and the mTORC1 complex inhibitor RAD001 (Everolimus) demonstrated clinical efficacy in a phase I/II trial in MPN patients. In the first project I evaluated the effects of BKM120, a pan-PI3K specific inhibitor, alone and in combination with the JAK1/JAK2 inhibitor Ruxolitinib and RAD001, in different MPN models. I provided proof-of-principle that BKM120 preferentially inhibits *JAK2*^{V617F} mutated cells both in *in-vitro* and *in-vivo* models and impairs colony formation from MPN patients' CD34+ cells. Furthermore By triple combination of BKM120 and Ruxolitinib plus RAD001 produced strong synergism that preventing *JAK2*^{V617F} cells proliferation *in-vitro* as well as myeloproliferation in *JAK2*^{V617F} KI mouse. Such efficacy of the combined treatment is mediated by differential targeting of STAT5a/b isoforms phosphoresidues overall leading to a complete STAT5 inactivation. The experiments performed also unraveled the involvement of Phosphatase2A (PP2A) and its deregulated repressor Cancerous Inhibitor of Phosphatase 2a (CIP2A) in this signaling. Overall, results obtained reinforce the functional cross-talk between the JAK/STAT and PI3K/mTOR pathways in preclinical models of MPN and underlines the importance of maximal STAT5 inactivation to

produce magnified treatment effects, thereby providing a rationale for designing innovative strategies of treatment in MPNs.

As regards the second part of my PhD project, I focused on the most recently described driver mutations in *CALR*, whose functions and downstream targets are still largely unknown. There are several types of *CALR* mutations, the most frequent are a 52 bp (Type1) deletion and a 5 bp (Type2) insertion in exon 9. All described abnormalities cause a frameshift with generation of a novel C-terminal domain with a common novel sequence of 36 aminoacidic. I was successful in generating two new rabbit mutation-specific antibodies binding to the mutated CALR only. Furthermore, in order to create a novel tool allowing mechanistic analysis of mutated *CALR* in a hematopoietic setting, I used CRISPR/Cas9 technology to perform targeted site-specific genome editing In BCR/ABL mutated K562 cell line. I was successful in generating CRISPR/Cas9 K562 *CALR* Knock-Out (KO) and *CALR* mutated with 52 bd delection (Type1), that is an unique model where changes are to be entirely ascribed to *CALR* mutation and are not affected by endogenous *CALR*. Further characterization of K562 *CALR* KO and *CALR* Type1 showed no significant abnormalities in proliferation and cell cycle compartments compared to parental cells, while mutant cells had increased resistance to apoptosis. I showed that mutant CALR had a lower stability compared to wild-type counterpart and that nuclear localization is defective in the mutant protein. Since *CALR* mutations are restricted to MPN subtypes displaying aberrant megakaryopoiesis I also evaluated the effects of the mutations on the megakaryocytic commitment by culturing K562 with 10 nM PMA, a known inducer of megakaryocyte differentiation. I found that both *CALR* KO and Type1 cell lines showed accelerated and enhanced expression of CD41/CD61 differentiation markers compared to *CALR* wild-type cells; this was also confirmed in K562 KO cells stably expressing *CALR* Type1 and Type2 by lentiviral transduction. Moreover clonogenic assay with CRISPR/Cas9 genome edited CD34+ cells showed that the knock-out of the protein resulted in promotion of megakaryocytopoiesis, mimicking the effects of *CALR* mutations. Overall, these data indicate that such novel *CALR* mutated models and specific anti-CALR mutated antibodies are useful tools to study the pathogenic role of *CALR* mutations in MPNs facilitating clinical development of new diagnostic and therapeutic strategies.

PREFACE

During my PhD in Clinical and Experimental Oncology course at the University of Florence, I focused on some molecular aspects of Philadelphia-negative Myeloproliferative neoplasms (MPNs).

MPNs, including Essential Thrombocythemia (ET), Polycythemia Vera (PV) and Primary Myelofibrosis (PMF), are characterized by clonal proliferation of hematopoietic progenitor cells and dysregulated production of blood cells of different lineages. Driver mutations in MPNs are virtually mutually exclusive and include *JAK2*^{V617F}, *CALR* and *MPL*.

The exciting discovery of new genetic abnormalities in patients with myeloproliferative neoplasms holds the promise for advancing our understanding of the pathogenesis of these disorders as well as improving therapeutic management of the patients.

In this thesis, I am presenting the results of these two research topics:

In the first project I investigated the molecular basis of the functional crosstalk between the main signalling pathways activated by *JAK2* mutation, that include the JAK/STAT and PI3K/mTOR pathways, as well how to exploit the added value of target drug combination aimed at improving efficacy, and ameliorating toxicity, of treatments in MPNs.

As regard the second part of my PhD project, I focused on the most recently described MPN-associated driver mutations in *CALR*, whose function and downstream targets are still poorly known. To this end, I generated new cellular models of *CALR* mutations using target genomic editing and analysed the effects of mutations on cellular phenotypic traits.

These projects have been conducted in the laboratory of CRIMM-Center Research and Innovation of Myeloproliferative Neoplasms, Department of Experimental and Clinical Medicine of the University of Florence under the supervision of Prof. Alessandro Maria Vannucchi. The first of them has been recently published in *Oncotarget Journal*, the second one has been subject matter of communication at SIE

2017 (Italian Society of Hematology) and it will be present as poster at ASH 2017 (American Society of Hematology). A manuscript dealing with these studies is under preparation.

INTRODUCTION

MYELOPROLIFERATIVE NEOPLASMS

Chronic myeloproliferative neoplasms (MPNs) comprise several hematologic diseases that arise from the transformation of a pluripotent stem cell and are characterized by the clonal proliferation of one or more hematopoietic progenitors in the bone marrow and extramedullary sites.

The main clinical features of these diseases are the overproduction of mature, functional blood cells and a long clinical course (Campbell et al., 2006).

MPNs, first conceptualized in 1951 by William Dameshek, historically included Polycythemia Vera (PV), Essential Thrombocythemia (ET), Primary Myelofibrosis (PMF) and chronic myelogenous leukemia (CML) (Dameshek, 1951).

The association of the Philadelphia (Ph)-chromosome with CML in 1960 by Nowell and Hungerford, and the subsequent recognition of erythroleukemia as a variant of acute myeloid leukemia, distinguished the other three diseases (PV, ET and PMF) as "classic" Ph-negative myeloproliferative disorders. Dameshek was the first, in his seminal editorial published in 1951 in *Blood*, to recognize that these diseases should be classified as a set of phenotypically related "myeloproliferative disorders" characterized by bone marrow proliferation, "*perhaps due to a hitherto undiscovered stimulus*" (Levine et al., 2008). However, the finding that bone marrow and peripheral blood cells from MPN patients can produce erythroid colonies in vitro in the absence of added growth factors indicated the cell autonomous nature of these diseases (Prchal et al., 1974), and the clonal origin of peripheral blood cells of MPN patients was later proven by analyzing X-chromosome inactivation patterns (Adamson et al., 1976).

To underscore the clonal nature of myeloproliferative disorders and their propensity to evolve in Acute Myeloid Leukemia (AML), in 2008 the authors of the World Health Organization (WHO) *Classification of Tumours of Haematopoietic and Lymphoid Tissue* introduced the name "myeloproliferative neoplasms" (MPNs). The 2008 WHO classification for myeloid neoplasms, which incorporated novel information

derived from molecular discoveries in *BCR-ABL* negative "classic" myeloproliferative and clonal eosinophilic disorders, included five major entities: Acute Myeloid Leukemia (AML), Myelodisplastic Syndromes (MDS), Myeloproliferative neoplasms (MPN); the category of overlapping Myelodysplastic/Myeloproliferative Neoplasms (MDS/MPN) and Myeloid/Lymphoid neoplasms associated with eosinophilia and specific molecular abnormalities. The substitution of the attribute "neoplasm" for "disease" was a relevant, formal recognition that both "classic" and "non-classic" myeloproliferative diseases share a common stem-cell-derived clonal heritage. The incorporation of clonal markers such as *JAK2*^{V617F} mutation and similar activating, *PDGFRA*, *PDGFRB* or *FGFR1* rearrangements as well the acquisition of new histopathological information was consistent with the spirit of this revision (Tefferi et al., 2008; Vardiman et al. 2009). Although the 2008 WHO classification had undoubtedly the merit of promoting a systematic approach to these entities, taking into account clinical, morphological and molecular features, it presented controversial aspects such as the actual reliability of the proposed clinical parameters required for diagnosis, and, particularly, the diagnostic relevance and reproducibility of bone marrow morphology criteria. Moreover, the newly discovered molecular features have provided novel diagnostic and prognostic tools (Barbui et al., 2015; Barbui et al., 2016).

As a result, in 2016 the WHO updated the 2008-WHO classification for hematopoietic and lymphoid neoplasms (**Table 1**) and adressed these issues formally integrating the assessment of the so called "driver mutations" (namely, *JAK2*^{V617F}, *MPL*$^{W515K/L}$ and *CALR* mutations) as one of several major criteria in the diagnosis of PV, ET and PMF. This revision regard also the upgrading of bone marrow morphology as another major criterion for the diagnosis of these three major entities of MPNs (Arden et al., 2016).

Table 1: The 2016 World Health Organization (WHO) classification of myeloid neoplasms and acute leukemia. [For the full table referring to the source: Arber DA. et al*., The 2016 revision to the World Health Organization classification of myeloid neoplasms and acute leukemia*. Blood. 2016, Vol. 127, n. 20, pp. 2392].

WHO myeloid neoplasms and acute leukemia classification
Myeloproliferative neoplasms (MPN)
Chronic myeloid leukemia (CML), BCR-ABL1^{+}
Chronic neutrophilic leukemia (CNL)
Polycythemia vera (PV)
Primary myelofibrosis (PMF)
Pre-PMF, prefibrotic/early stage
Overt-PMF, overt fibrotic stage
Essenial thrombocythemia (ET)
Chronic eosinophilic leukemia, not otherwise specified (NOS)
MPN, unclassifiable
Mastocytosis
Myeloid/lymphoid neoplasms with eosinophilia and rearrangement of PDGFRA, PDGFRB, or FGFR1, or with PCM1-JAK2
Myeloid/lymphoid neoplasms with PDGFRA rearrangement
Myeloid/lymphoid neoplasms with PDGFRB rearrangement
Myeloid/lymphoid neoplasms with FGFR1 rearrangement
Provisional entity: Myeloid/lymphoid neoplasms with PCM1-JAK2
Myelodysplastic/myeloproliferative neoplasms (MDS/MPN)
Chronic myelomonocytic leukemia (CMML)
Atypical chronic myeloid leukemia (aCML), BCR-ABL1
Juvenile myelomonocytic leukemia (JMML)
MDS/MPN with ring sideroblasts and thrombocytosis (MDS/MPN-RS-T)
MDS/MPN, unclassifiable
Myelodysplastic syndromes (MDS)
MDS with MDS with single lineage dysplasia
MDS with ring sideroblasts (MDS-RS)
MDS with multilineage dysplasia
MDS with excess blasts
MDS with isolated del(5q)
MDS, unclassifiable
Provisional entity: Refractory cytopenia of childhood
Myeloid neoplasms with germ line predisposition
Acute myeloid leukemia (AML) and related neoplasms
AML with recurrent genetic abnormalities
AML with myelodysplasia-related changes
Therapy-related myeloid neoplasms
AML-NOS
Myeloid sarcoma
Myeloid proliferations related to Down syndrome
Blastic plasmacytoid dendritic cell neoplasm
Acute leukemias of ambiguous lineage
B-lymphoblastic leukemia/lymphoma
T-lymphoblastic leukemia/lymphoma

THE "CLASSIC" Ph-NEGATIVE MYELOPROLIFERATIVE NEOPLASM

As described above Polycytemia Vera (PV), Essential Thrombocythemia (ET) and Primary Myelofibrosis (PMF) represent the three main entities of the classic Ph-negative MPNs, that are among the most frequent hematologic neoplasms, usually affecting adults older than 60 years at initial diagnosis (Moulard et al., 2014). However, they can also be found in children, and in this instance, they raise specific diagnostic and management issues (Randi et al., 2006; Teofili et al., 2007). Epidemiological studies and meta-analysis about MPNs incidence and prevalence report highly variable annual incidence rates. Incidence rates per 100.000 inhabitants varies in the range of 0.74-0.86 for PV, 1.03 and 2.58 for ET and PMF, respectively (Titmarsh et al., 2014). Important risk factors are advanced age, male sex, and white race.

Clonal proliferation in MPNs is driven by somatic mutations in *JAK2*, *CALR* or *MPL*, but in the last years several reviews focused on familial clustering of these neoplasms in order to identify predisposition allele(s) (Kralovics et al., 2003). This concept was further strenghtened when a clear molecular distinction of true familial MPN from other familial syndrome such as familial erythrocytosis and hereditary thrombocythemia has become possible using clonality markers, cellular studies and *JAK2* mutation analysis. Currently the GGCC (also known as 46/1) haplotype is the strongest known predisposing factor for MPNs carryng $JAK2^{V617F}$ mutation (Jones et al., 2009; Olcaydu et al., 2009). More recently other genetic variation have been described, like *MECOM, TERT, JAK2, HBS1L-MYB, THRB-RARB* and *NR3C1* genes (Tapper et al., 2015).

The three clinical entities share a several common features, such as their origin in a multipotent hematopoietic stem cell, a relatively normal cellular maturation, a striking overlap in clinical presentation (apart from PMF, which has its own peculiar manifestations). The classification is based on which myeloid cell lineage is predominantly expanded in the blood; in PV and ET there are respectively elevated red cell mass and platelet number. PMF is a more complex disease and patients display

bone marrow fibrosis, variable myeloid cell number, extramedullary hematopoiesis and hepatosplenomegaly.

Patients with PV and ET have a high risk of thrombotic and/or haemorrhagic events and may progress to an accelerated myelofibrosis phase, while all three subtypes are associated with a long term risk of transformation to acute myeloid leukemia (AML) with a uniformly poor prognosis. The risk of leukemic transformation is highest in PMF, where it is estimated to be approximately 10-20% at 10 years. In PV the risk is 2.3% at 10 years and 7.9% at 20 years (Tefferi et al., 2014). Transformation to AML is considered relatively uncommon in ET (Vardiman et al., 2009).

POLYCYTHEMIA VERA

Polycythemia Vera (PV) is the most common myeloproliferative disease, characterized by abnormal expansion of erythroid lineage, variably associated with thrombocytosis and leukocytosis, in absence of a recognizable physiologic stimulation. The first clinician to provide a definition of the Polycythemia Vera was Vaquez in 1892 when he described it as a condition of "*persistent and excessive hypercellularity accompanied by cyanosis*" (Vaquez, 1892).

The incidence rate of PV is 0.86 cases per 100.000 people, but the true incidence may be higher because of asymptomatic cases. There is a little prevalence in male gender and the median age at diagnosis is 60 years (Stein et al., 2015).

The abnormal proliferation of PV is a conseguence of *JAK2* gain of function gene mutations, with the majority of patients (>95%) harboring the $JAK2^{V617F}$ mutation and an additional 3% of PV patients being positive for mutations in exon 12 of the *JAK2* gene (Kralovics et al., 2005; Levine et al., 2005; Scott et al., 2007). Recently other mutations or DNA variants involving 27 genes other than *JAK2*, *CALR* or *MPL* in patients with PV have been reported; the most frequent mutations included *TET2*, *ASXL1*, *SH2B3*, *SRSF2*, *IDH1/2*, *LNK* (Tefferi et al., 2016; Tefferi et al., 2010).

PV is characterized by bone marrow hyperplasia with hyperproliferation of erythroid lineage which is largely independent from erythropoietin (EPO). This is

confirmed by the evidence of *in-vitro* spontaneous formation of erythroid endogenous colonies (EEC) in absence of EPO stimulation (Prchal JF, 1974).

The main clinical manifestations of PV are consequences of excessive proliferation of red cells. Erythrocytosis causes augmented blood viscosity that leads to cerebral and peripheral microvascular involvment and related signs and symptoms; water-related pruritus is typical and affects 50% of patients. Costitutional symptoms such as weight loss, night sweats, and fever, are present at diagnosis in <30% of cases. Hepatomegaly, splenomegaly, cyanosis and arterial hypertension are common. The main complications are thrombotic events that can occur also in uncommon sites such as principal abdominal vessels. Increased plasma volume can lead to understimation or failure to identify the increased erythrocyte mass. Leukocytosis and thrombocytosis are present in more than 50% of cases. During evolution, the disease changes, and patients may present evolution in myelofibrosis (post-PV) and more rarely in acute myeloid leukemia. The most frequent cause of death in PV patients are cardiovascular event (41% of deaths).

PV diagnosis is based on updated WHO criteria 2016 (**Table 2**), as a result of new important mutational and clinical discoveries: in order to confirm the diagnosis of PV all three major criteria are required, or the first two major criteria and the minor criterion.

Table 2: The 2016 WHO diagnostic criteria for PV [Arber DA. et al., *The 2016 revision to the World Health Organization classification of myeloid neoplasms and acute leukemia*. Blood. 2016 , Vol. 127, n. 20, pp. 2394].

2016 WHO PV criteria
Major criteria
1. Hemoglobin >16.5 g/dL in men; Hemoglobin >16.0 g/dL in women or, Hematocrit >49% in men; Hematocrit >48% in women or, increased red cell mass (RCM)*
2. BM biopsy showing hypercellularity for age with trilineage growth (panmyelosis) including prominent erythroid, granulocytic, and megakaryocytic proliferation with pleomorphic, mature megakaryocytes (differences in size)
3. Presence of *JAK2*^{V617F} or *JAK2* exon 12 mutation
Minor criteria
Subnormal serum erythropoietin level

*More than 25% above mean normal predicted value.

ESSENTIAL THROMBOCITHEMIA

Essential Thrombocithemia (ET) is characterized by abnormal megakaryocytic proliferation with consequent increased peripheral platelets. The first report is from 1934 by Dr. Emil Epstein and Dr. Alfred Goedel (Epstein et al. 1934).

The incidence rate varies between 0.62-1.72 cases per 100.000 people and it is more common in females. It is more frequent between the fifth and seventh decades of life, although it may be present at any age.

ET is triggered by several mutations causing hyperactive cytokine signaling. The most common mutations are *JAK2*^{V617F} (50-60% of cases), *CALR* (15-35% of cases) and *MPL* mutations (4% of cases). The recent targeted study mentioned above identified *SH2B3, SF3B1, U2AF1, TP53, IDH2* and *EZH2* as adverse mutations (Tefferi et al., 2017; Tefferi et al., 2016). In case where no mutation is found (triple negative) essential thrombocytosis is largely a diagnosis of exclusion because isolated thrombocytosis may be the first manifestation of polycythemia vera, primary myelofibrosis or myelodysplastic disorders (Spivak et al., 2017). Other possible causes of reactive thrombocytosis have different prognosis and treatment.

Usually, ET is occasionally identified in the majority of patients, for example through an increased platelet count or thrombo-hemorrhagic symptoms, the most frequent complications in ET. Thromboembolic symptoms are the most severe manifestation in this pathology, especially when they occur in central nervous system arteries or in cardiovascular system. Other characteristic symptoms bound with thrombosis in ET are: erythromelalgia, deep vein thrombosis, with high risk of pulmonary embolism, and splanchnic veins thrombosis. Hemorrhagic events are less common than thromboembolic symptoms. Acquired form of von Willebrand disease induced by high platelet count in ET has been also reported: this makes worse prognosis in these patients.

In addition to thrombo-hemorrhagic symptoms other possible complications that must be considered are myelofibrotic transformation (post-ET) and leukemic transformation (Passamonti et al., 2008, Wolanskyi et al., 2006).

WHO developed new criteria for ET diagnosis in 2016 (**Table 3**). Diagnosis of ET requires meeting all four major criteria or the first three major criteria and the minor criterion.

Table 3: The 2016 WHO diagnostic criteria for ET [Arber DA. et al., *The 2016 revision to the World Health Organization classification of myeloid neoplasms and acute leukemia.* Blood. 2016 , Vol. 127, n. 20, pp. 2395].

2016 WHO ET criteria
Major criteria
1. Platelet count ≥ 450 × 10^9/L 2. BM biopsy showing proliferation mainly of the megakaryocyte lineage with increased numbers of enlarged, mature megakaryocytes with hyperlobulated nuclei. No significant increase or left shift in neutrophil granulopoiesis or erythropoiesis and very rarely minor (grade 1) increase in reticulin fibers 3. Not meeting WHO criteria for *BCR-ABL*[11] *CML, PV, PMF,* myelodysplastic syndromes, or other myeloid neoplasms 4. Presence of *JAK2, CALR*,or *MPL* mutation
Minor criteria
Presence of a clonal marker or absence of evidence for reactive thrombocytosis

Morphological features of megakaryocytes in ET are very important especially in patients with suspected ET but that are negative for somatic mutations. Marrow aspiration or biopsy show large, hyperlobulated and mature appearing megakaryocytes, without cells adhesion (this is an important difference vis-à-vis myelofibrosis which features megakaryocytes organized in clusters) or dysplastic features (also typical of MF).

PRIMARY MYELOFIBROSIS

Primary Myelofibrosis (PMF) is a clonal disorder of a multipotent hematopoietic progenitor cell of unknown etiology characterized by marrow fibrosis and osteosclerosis, extramedullary hematopoiesis, splenomegaly, anemia, neutrophilia and thrombocytosis or thrombocytopenia and leukopenia, immature granulocytes and increased CD34+ cells, erythroblasts and teardrop-shaped red cells in the blood, and constitutional symptoms due to inflammatory cytokine production. The first description of PMF dates back to 1879, when Heuck firstly reported about myelofibrosis in a paper titled "*Two cases of leukemia and peculiar blood bone marrow*

findings" (Heuck et al., 1879). Over the years, PMF has also been referred to by a variety of others terms, such as agnogenic myeloid metaplasia, myelosclerosis, idiopathic myeloid metaplasia and idiopathic myelofibrosis (Tefferi et al., 2007). The current designation PMF reflects our greater understanding of the origin of this disorder, and differentiates a *de novo* disease from myelofibrosis which is preceded by a history of PV or ET (post PV/ET myelofibrosis).

PMF is the least common and most aggressive myeloproliferative neoplasm, occurring in the majority of cases after the fifth decade of life, with a pick of incidence at 65-70 years old; however, several studies report it can occur also in childhood and adolescence (Cervantes et al., 2001). Clinically the manifestations are similar in both adults and young, but normally the frequency of indolent cases is higher in pediatric age. The estimated incidence of PMF is between 0.1 and 1.0 per 100.000 per year, with a higher prevalence in males than in females (Moulard et al., 2014).

The key mutational abnormalities associated with PMF are: *JAK2* mutations, especially V617F, that occur in almost 60% of PMF patients; *CALR* mutation, either 52-bp deletion and 5-bp insertion, in 20% of cases; and *MPL* in 7% of cases. Other somatic mutations have also been detected such as *TET2, ASXL1, DNMT3A, EZH2*, and *IDH1/2, SRSF2*, implicated in epigenetic regulation, and *TP53* and *CBL* (Lundberg et al., 2014). Additional adverse mutations identified in PMF include *CBL, KIT, RUNX1, SH2B3* and *CEBPA* (Tefferi et al., 2016).

The clonality of this disorder has been extensively observed in several studies in murine models. CD34+ cells play a key role of in peripheral blood migration and neoplastic megakaryocytopoiesis of PMF. The migration of CD34+ cells is probably a consequence of an epigenetic alteration due to the hypermethylation of the CXCR4 promoter. This modification induces reduced expression of CXCR4 on CD34+ cells and enhance their migration into the blood (Bogani et al., 2008). In addition, a study about the molecular profiling of CD34+ cells in PMF demonstrated that these cells have a higher expression of some genes, namely *CD9, GAS2, DLK1, CDH1, WT1, NFE2, HMGA2*, and *CXCR4*, that is abnormal for this kind of cells. These genes are indeed involved in the pathogenesis and in the clinical features of PMF (Guglielmelli et al., 2007).

Another characteristic of PMF is the enhanced bone marrow angiogenesis and blood flow, probably connected with an increasing of circulating endothelial cell progenitors

(Massa et al., 2005). Finally, we have to consider the different features of hematopoiesis dysfunction. Neoplastic proliferation is the main bone marrow alteration especially in granulocytic and megakaryocytic lineages, resulting in panmyelosis but few circulating mature blood cells, especially granulocytes and platelets. Likely, this is related to an exaggerated apoptosis of very early precursors. Anemia is a frequent finding in PMF as a result of insufficient erythropoiesis, short erythrocytes survival and splenic sequestration, as a consequence of hypersplenism. However, it is important to exclude other possible causes of bone marrow fibrosis.

Many patients are asymptomatic at the time of diagnosis, but some of them refer fatigue as a principal complaint in association with night sweats, fever, weight loss and bone pain. Inflammatory cytokines, like IL-1β, IL-6, IL-8, tumor necrosis factor (TNF)-α, TNF receptor II (TNFRII), and C-reactive protein show significantly higher concentration and play a role in the constitutional symptoms (Tefferi et al., 2008). In most of PMF cases it is possible to palpate a splenic enlargement. Dragging sensation, early satiety, left hypocondrial pain or left shoulder pain are a consequences of splenomegaly and splenic infarction, respectively.

Patients can show organ failure due to extramedullary hematopoiesis, and portal hypertension and varices, due to an enhanced hepatic blood flow, hepatic vein thrombosis or decreased hepatic vascular compliance (Jacobs et al., 1985).

Thrombotic risk is elevated in PMF patients, but not as much as in PV or ET. However almost 10% of cases developed a thrombotic event in the first four years from the diagnosis. The two main risk factors for thromboembolic events in PMF patients are elevated leukocyte count and age, but not platelet count (Buxhofer-Ausch et al., 2012).

The increasing marrow failure with transfusion-dependent anemia and increasing organomegaly due to extramedullary hematopoiesis is one of the most common complications in PMF. Leukemic transformation could also occur and has dismal prognosis because of the poor response of the treatment.

The 2016 revision of the World Health Organization (WHO) classification of myeloproliferative neoplasms defines two stages of primary myelofibrosis (PMF): prefibrotic/early (pre-PMF) (**Table 4**) and overt fibrotic (overt-PMF) (**Table 5**) phase. In comparison with overt PMF, patients with pre-PMF are more frequently female, younger, and have higher hemoglobin. By contrast, leukocytosis and blasts >1% in

peripheral blood are more frequent in overt-PMF as well as LDH level, clinical features (especially splenomegaly) and unfavorable karyotype. Diagnosis of pre-PMF as well as for overt-PMF requires meeting all three major criteria and at least one minor criterion. According to the International Prognostic Scoring System (IPSS), pre-PMF patients may be included in lower-category risk in comparison to patients with overt-PMF, more frequently classified in higher-category risk as demonstrated by Guglielmelli et al. (2017).

Table 4: The 2016 WHO diagnostic criteria for pre-PMF [Arber DA. et al., *The 2016 revision to the World Health Organization classification of myeloid neoplasms and acute leukemia*. Blood. 2016 , Vol. 127, n. 20, pp. 2395].

2016 WHO pre-PMF criteria
Major criteria
1. Megakaryocytic proliferation and atypia, without reticulin fibrosis > grade 1, accompanied by increased age-adjusted BM cellularuty, ranulocytic proliferation, and often decreased erythropoiesis. 2. Not meeting WHO criteria for *BCR-ABL*[11] *CML, PV, ET,* myelodysplastic syndromes, or other myeloid neoplasms 3. Presence of *JAK2, CALR* or *MPL* mutation or in the absence of these mutations, presence of another clonal marker, or absence of minor reactive BM reticulin fibrosis.
Minor criteria
Presence of at least 1 of the following, confirmed in 2 consecutive determinations: a. Anemia not attributed to a comorbid condition b. Leukocytosis ≥ 11 x 10^9/L c. Palpable splenomegaly d. LDH increased to above upper normal limit of institutional reference range

Table 5: The 2016 WHO diagnostic criteria for overt-PMF [Arber DA. et al., *The 2016 revision to the World Health Organization classification of myeloid neoplasms and acute leukemia.* Blood. 2016 , Vol. 127, n. 20, pp. 2396].

2016 WHO overt-PMF criteria
Major criteria
1. Presence of megakaryocytic proliferation and atypia, accompanied by either reticulin and/or collagen fibrosis grade 2 or 3. 2. Not meeting WHO criteria for *BCR-ABL*[11] *CML, PV, ET,* myelodysplastic syndromes, or other myeloid neoplasms 3. Presence of *JAK2, CALR* or *MPL* mutation or in the absence of these mutations, presence of another clonal marker, or absence of reactive myelofibrosis.
Minor criteria
Presence of at least 1 of the following, confirmed in 2 consecutive determinations: a. Anemia not attributed to a comorbid condition b. Leukocytosis ≥ 11 x 10^9/L c. Palpable splenomegaly d. LDH increased to above upper normal limit of institutional reference range e. Leukoerythoblastosis

MOLECULAR BASIS OF MYELOPROLIFERATIVE NEOPLASM

In the last decade, our understanding of the molecular aspects of Philadelphia-negative MPN has been dramattically revolutionized by the genetic discoveries in 2005 with the identification of the *JAK2*^{V617F} mutation (James et al., 2005; Kralovics et al., 2005; Levine et al., 2005; Baxter et al., 2005). Since then, several somatic mutation have been described, and their pathogenetic role is currently under investigation, but non of them appear to garner the disease specificity or pathogenetic relevance otherwise displayed by the Philadelphia chromosome in CML. Overall, it is now clear that among the numerous genetic culprits that can affect the neoplastic clone, three mutations (namely, *JAK2*^{V617F}, *MPL*$^{W515K/L}$ and *CALR* mutations) play a crucial role in driving the disease phenotype and affecting the clinical course of MPNs, so that they have been recently re-defined as “driver mutations” (Tefferi et al., 2015) (**Figure 1**). *JAK2*, *MPL* and *CALR* mutations are considered phenotypic driver since the expression of the mutated gene in cell lines caused cytokine independent or hypersensitive growth, as known to occur in primary cells from MPN patients, and in animal models phenotypes closely resembling a myeloproliferative disease were observed in

transgenic or conditional animals (Li et al., 2011). The subclonal mutations usually occur in hematopoietic cell subclones of variable size, often but not invariably together with one of the phenotypic driver mutations, and may either antedate or follow the acquisition of phenotypic driver mutations (Vainchenker et al., 2011). The order by which these mutations appear in the mutational phylogenesis of MPN contribute to the disease phenotype, while the prognostic relevance if any is far from being appreciated (Ortmann et al., 2015; Nangalia et al., 2015). Since these mutations are commonly represented also in myelodysplastic syndromes, other myeloid neoplasia and acute leukemias, they have no specific diagnostic value, while, on the other hand, they contribute remarkably to the prognosis of patients with PMF.

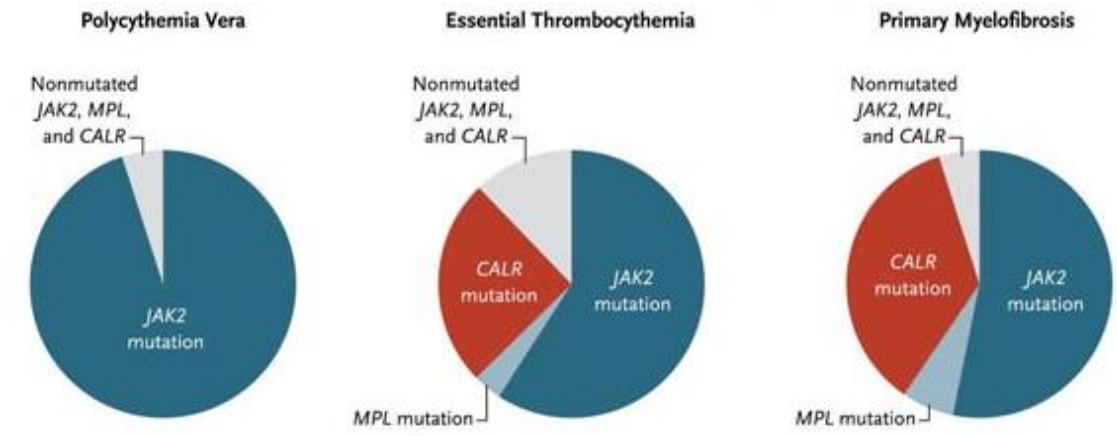

Figure 1: Distribution of *JAK2*, *CALR* and *MPL* mutations in MPNs (Klampft et al., 2013).

DRIVER MUTATIONS IN MPNs

***JAK2* MUTATIONS.** *JAK2* is the most common myeloproliferative neoplam driver gene. A member of the Janus tyrosine kinase family, JAK2 is responsible for signal transduction by the erythropoietin (EPO), thrombopoietin (TPO), granulocyte macrophage colony stimulating factor (GM-CSF), and granulocyte colony-stimulating factor (G-CSF) receptors in hematopoietic cells, as well as for signal transduction by many cytokine receptors, such as interleukin IL-3, IL-5, and IL-6 receptors (Verma et al. et, 2003). The cytoplasmatic domains of these receptors are docking sites for Janus Kinases (JAK). JAK2 is one of the four JAKs, it has a dual kinase structure and contain an N-terminal FERM domain, a Src-homology like domain (SH2), a pseudokinase domain

(JH2), and a C-term kinase domain (JH1)(**Figure 2**). The FERM and SH2 domains anchor JAK2 to cytokine receptors, JH2 regulates kinase activity, while JH1 is responsible for tyrosine phosphorylation. JH1 paired in tandem with a weakly active JH2, which normally inhibits JH1 kinase activity in the absence of ligand binding. Following the binding of cytokines to their receptor, a change in receptor conformation takes place so that JAK2 phosphorylates in trans Y1007 and Y1008 in the activation loop of JH1 domain, thus inducing JAK2 activation. JAK2 phosphorylates cytokine receptors and signal transducers and activators of transcription (STAT) bind to phosphorylated tyrosine residues on these cytokine receptors through their SH2 domains whereupon JAKs can themselves be phosphorylated by JAKs (Vainchenker et al., 2013). Phosphorylated STATs can translocate into the nucleus to be part of transcriptional complexes. In addition to activating STATs, JAKs also activate mitogen-activated protein kinase (MAPK)-extracellular signal-regulated kinase (ERK) and the phosphoinositide 3-kinase (PI3K)–AKT pathway. These three pathways induce survival, proliferation, and myeloid differentiation.

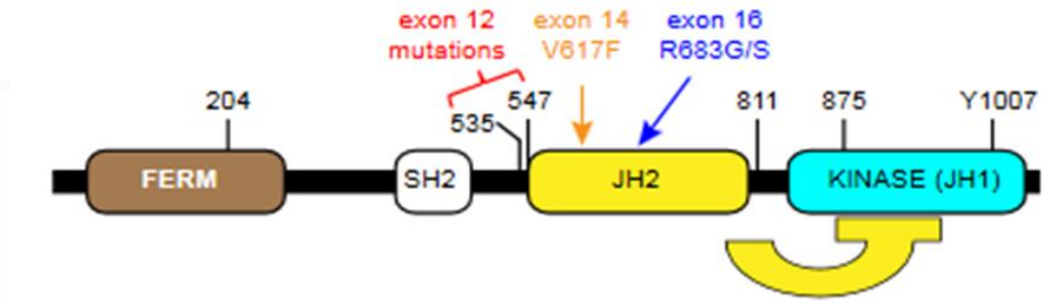

Figure 2: Domain structure of the Jak2 protein. Numbers indicate amino acid positions within the Jak2 protein. Arrows indicate the positions of the most frequently mutated regions. The auto-inhibitory effect of the JH2 domain is indicated in yellow. FERM = N-terminal Band 4.1, ezrin, radixin, moesin domain; JH1 and JH2 = Jak homology 1 and 2 domains; SH2 = Src homology 2 domain (Skoda et al., 2015).

In 2005, Dr. Skoda's, Dr. Vainchenker's and Dr. Gilliand's labs, using different approaches, discovered a recurrent acquired mutation in *JAK2* gene in a significant proportion of patients with MPN (James et al., 2005; Kralovics et al., 2005; Levine et al., 2005). This dominant gain-of-function mutation is a guanine-to-thymidine substitution at nucleotide 1,849 in exon 14 of the *JAK2* gene that results in a valine-to-phenylalanine substitution at codon 617 of *JAK2*. The *JAK2*^{V617F} mutation maps to the

JH2 pseudokinase domain, it rigidifies the α helix C of the domain, promoting the transphosphorylation of JH1, impairing its physiologic inhibitory influence. Tyr 1007 and Tyr 1008 in JH1 domain are phosphorylated, so that *JAK2*^{V617F} is constitutive active in the absence of cytokine (Silvennoinen et al., 2015).

In the heterozygous state, *JAK2*^{V617F}-bearing receptors are still responsive to growth factors. Only with *JAK2*^{V617F} homozygosity, usually due to 9p uniparental disomy, do these receptors become entirely autonomous with respect to growth factor.

Given that the mutant *JAK2*^{V617F} is constitutively activated, it promotes pro-survival and anti-apoptotic signals as well as cytokine-independent growth (Kundrapu et al., 2008). In fact, when *JAK2*^{V617F} is expressed in hematopoietic cells, several signaling pathways that are important for proliferation and survival are activated (Levine et al., 2005; Vainchenker et al., 2013).

In addition, mice transplanted with marrow cells transduced with a retrovirus expressing *JAK2*^{V617F} invariably developed erythrocytosis eventually associated with leucocytosis, splenomegaly and later changes suggestive of transformation to post-polycythemic myelofibrosis (Wernig et al., 2006; Lacout et al., 2006; Bumm et al., 2006; Zaleskas et al., 2006).

More recently, transgenic mice presenting an expression of mutated allele lower than wild-type one have been generated, and found to develop an ET-like phenotype (Tiedt et al., 2008; Shide et al., 2008); overall these data suggest that the *JAK2*^{V617F} mutation is an integral component of the myeloproliferative process that underlies the different classic MPNs.

JAK2 also serves as an endoplasmic reticulum chaperone for the erythropoietin and thrombopoietin receptors, transporting them to the cell surface, and increases the total number of thrombopoietin receptors by stabilizing the mature form of the receptor, enhancing receptor recycling, and preventing receptor degradation. However, in contrast to its effect on the erythropoietin receptor, *JAK2*^{V617F} appears to increase the quantity of immature MPL molecules while increasing MPL degradation through ubiquitination and reducing its cell-surface expression. In addition to functioning as a tyrosine kinase and chaperone, mutated JAK2 is sumoylated, permitting it to shuttle to the nucleus, where it deregulates gene transcription directly

through histone phosphorylation and indirectly by phosphorylating and inhibiting PRMT5, a histone arginine methyltransferase (Spivak, 2017).

The frequency of *JAK2*^{V617F} mutation is estimated at over 95% in PV and 50-60% in ET or PMF patients (Tefferi et al., 2010; Vainchenker et al., 2011). The mutation can be found on one or both alleles (homozygosity) as a result of a mitotic recombination process resulting in uniparental disomy that occurs in most patients with PV or PMF and a minority only of ET. Different studies suggested that in ET and PV, a higher allele burden is associated to disease progression to MF, but in contrast, a low allele burden is related to an inferior overall and leukemia-free survival in MF (Steensma et al., 2006; Guglielmelli et al., 2009; Vannucchi et al., 2011).

Approximately 3% of patients with PV have insertions or deletions in *JAK2* exon 12 at the interface of the JAK2 SH2 and JH2 domains, which enable constitutive kinase activation, possibly also by altering the interface between the JH2 and JH1 domains (Scott et al., 2011). The *JAK2* exon 12 phenotype is usually more benign than that of *JAK2*^{V617F}, often causing erythrocytosis alone, though a complete polycythemia vera phenotype can develop, as can homozygosity or coexistence with *JAK2*^{V617F} (Passamonti et al., 2011).

***CALR* MUTATIONS**. The gene that encodes calreticulin, is the second most common myeloproliferative driver gene. In 2013, whole-exome sequencing analyses contemporary performed by Dr. Green's and Dr. Kralovics's groups led to the identification of *CALR* exon 9 mutations in patients with MPNs who had no mutations in either *JAK2* or *MPL*. (Nangalia et al., 2013; Klampft et al., 2013). More details about calreticulin and its functions are outined in the introduction of my second PhD project.

Briefly, CALR is a multifunctional protein involved in glycoprotein folding and calcium homeostasis in the endoplasmic reticulum (ER), as well as in cellular functions such as proliferation, phagocytosis, immunogenic cell death and apoptosis (Gold et al., 2010).. Located on chromosome 19p13.2, *CALR* contains nine exones and mature CALR is a 46-kDa protein that consists of three structurally and functionally distinct domains: the globular N-terminal domain; the middle proline rich or P-domain; and the highly acidic C-terminal domain.

CALR mutations consist of a wide variety of deletions or insertions in exon 9. More than 50 different *CALR* mutations have been identified and classified according to their effect on DNA sequence: deletions have been designated as type 1 or type 1–like, of which L367fs*46, a 52-bp deletion, is the most common, and insertions as type 2 or type 2–like, of which K385fs*47, a 5-bp insertion, is the most common. Together, these account for 85% of the *CALR* mutations (**Figure 3A**); type 1 mutations are more common in PMF, whereas type 1 and type 2 occur with similar frequency in ET. Like *JAK2* and *MPL* mutations, mutated *CALR* is expressed in hematopoietic stem cells. It is a driver mutation primarily in ET and PMF; is occasionally homozygous as a result of 19 uniparental disomy, usually with type 2 mutations; is not mutually exclusive of $JAK2^{V617F}$; and causes PV in rare cases (Pietra et al., 2015; Vainchenker et al., 2017). Remarkably, all mutations cause a frameshift to a unique alternative reading frame resulting in a novel calreticulin C-terminal peptide sequence characterized by the acquisition of a minimal 36 amino acid stretch in place of 27 amino acifs that are lost from the normal sequence (**Figure 3B**). The C-terminal of mutant CALR lacks KDEL, a canonical endoplasmic reticulum retrieval motif, together with a switch from a negatively charged to a positively charged peptide sequence.

Recent studies have demonstrated that *JAK2/CALR* mutations and *MPL/CALR* mutations are not mutually exclusive (Ahmed et al, 2016; Tashkandi et al., 2017; Bernal et al., 2017). Comparing clinical outcomes of CARL mutation vs. JAK2 or MPL positive cases, the former seem to have more benign prognosis in terms of survival and lower risk of thrombosis due to lower hemoglobin levels and leukocytes count than JAK2 positives (Rumi et al., 2014; Rotunno et al., 2014).

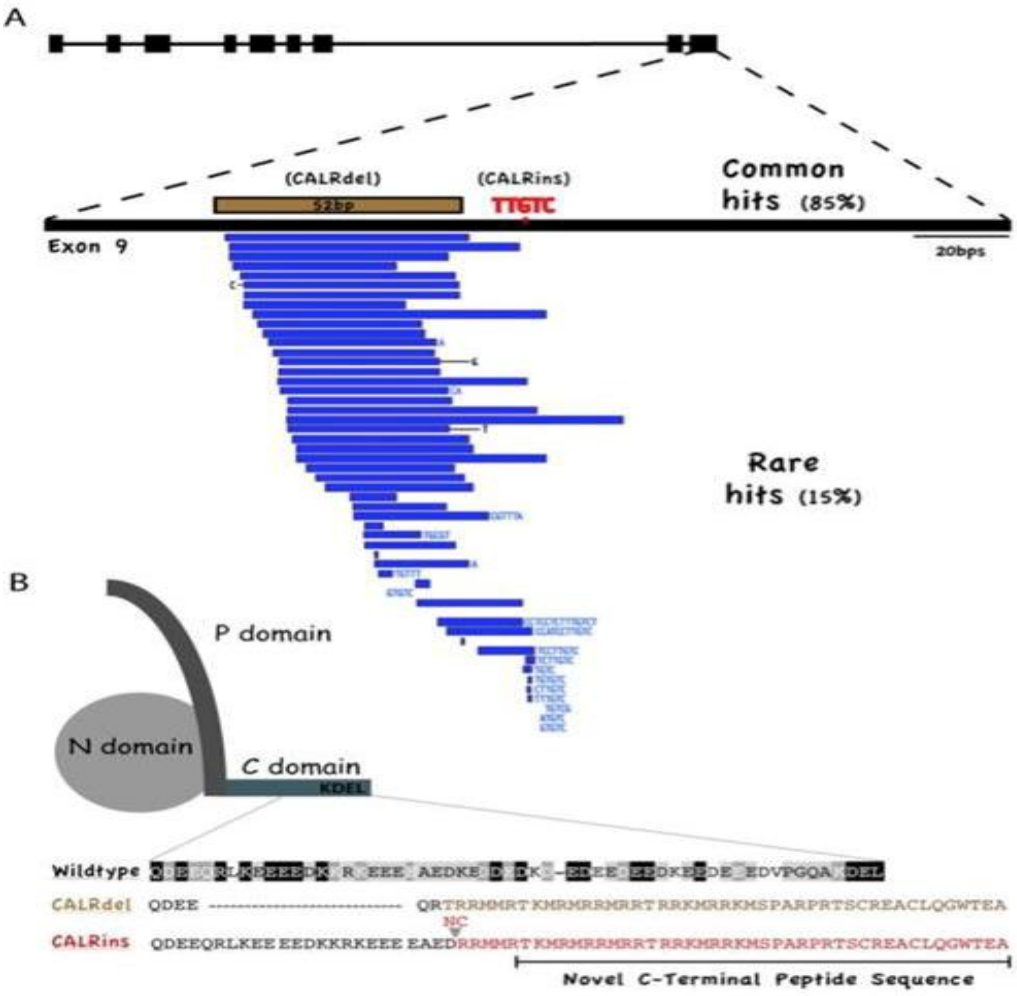

Figure 3: (A) Diagram showing the intron-exon structure of the gene *CALR*. Exon 9 is enlarged below with the two common *CALR* mutations—*CALR*del52 (brown bar) and *CALR*ins5 (red nucleotides) depicted above exon 9, and the numerous rare variants comprising deletions (blue bars), insertions (blue nucleotides) or complex insertions/deletions depicted below the exon. Black nucleotides are somatic point mutations reported with some rare deletions. **(B)** Model depicting the structural domains of wildtype (WT) CALR. The protein sequences show the terminal sequence of the WT protein, CALRdel52 and CALRins5. Black/Grey shading of WT protein sequence shows the degree of conservation of residues. Brown and red amino-acids represent the neomorphic C-terminus of mutant calreticulin in CALRdel52 and CALRins5, respectively. N-domain, lectin binding; P-domain, proline rich; C-domain, C terminal calcium-binding domain; KDEL, endoplasmic reticulum retention signal (Guglielmelli et al., 2014)

***MPL* MUTATIONS.** In 2006, Gary Gilliland's research team identified in some patients with PMF *JAK2* wild-type a new somatic point mutation in the gene Myeloproliferative Leukemia Virus Oncogene (*MPL*), coding for the thrombopoietin receptor (Pikman et al., 2006). *MPL* mutations are the least common myeloproliferative neoplasm driver mutations, occurring in <10% of PMF and ET. MPL is a unique type I hematopoietic cytokine receptor because it is the only one expressed in hematopoietic stem cells; it also has a reduplicated extracellular cytokine-binding

domain. Somatic *MPL* mutations occur most often in exon 10 and result in a switch from tryptophan to leucine or lysine or, less frequently, to arginine or alanine at amino acid 515 (MPL W515L/K or W515R/A) in the MPL juxtamembrane domain (Pardanani et al., 2006) (**Figure 4**).

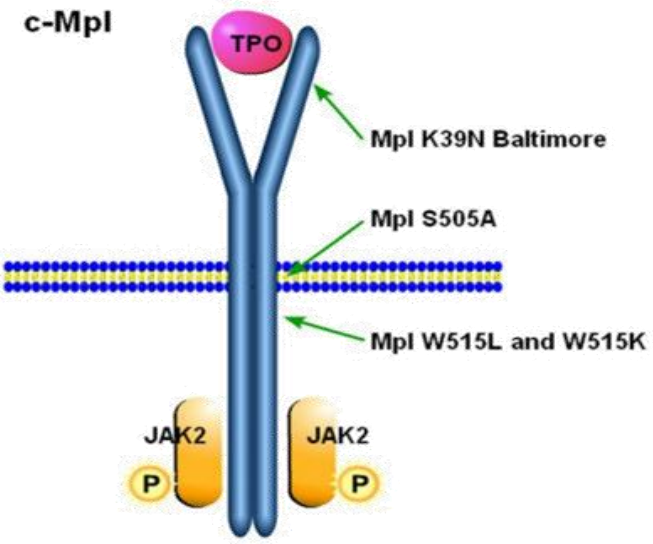

Figure 4: Polymorphism and mutations of the thrombopoietin receptor, c-Mpl. Two polypmorphisms, c-Mpl K39N and S505A, lead to constitutive activity of c-Mpl and thrombocytosis. Somatic mutations in the juxtamembranal domain of c-Mpl also lead to constitutive activity and have been found in patients with ET and PMF (Bennet et al., 2006).

They have been detected in 5% to 11% of patients with PMF and in up to 9% of *JAK2*^{V617F}-negative cases of ET (Beer et al. 2008; Vannucchi et al., 2007). A less common mutation, S505N, in the MPL transmembrane domain, in which serine is switched to asparagine, can be inherited or acquired and causes ET (Williams et al., 2007) *MPL* mutations force a change in receptor conformation, activating JAK2 in the absence of thrombopoietin binding. Like *JAK2* and *CALR* mutations, however, *MPL* mutations require a hematopoietic growth factor, in this case thrombopoietin, for complete kinase activation in the heterozygous state. Myeloproliferative neoplasm driver mutations also occur in the MPL extracellular distal cytokine domain. For example, *MPL* S204P/F are acquired mutations causing ET or PMF, whereas the germline *MPL* variants, K39N (*MPL Baltimore*) and P106L, cause a benign form of thrombocytosis in African-American and Arabic populations, respectively, which is most marked in the homozygous state. Interestingly in some patients, multiple MPL mutations or the

coexistence with *JAK2*^{V617F} allele were described (Guglielmelli et al., 2007; Vannucchi et al., 2008; Lasho et al., 2006).

In patients with ET, *MPL* mutations are associated with greater myelofibrotic transformation, but there is no difference in overall or leukemia-free survival between patients with *MPL* mutations and those with *JAK2*^{V617F}, and there appears to be no survival difference between patients with PMF who have *MPL* mutations and those who have *JAK2*^{V617F} mutations (Tefferi et al., 2010; Guglielmelli et al., 2007).

JAK2^{V617F} impairs MPL maturation, increasing the proportion of immature receptors in the plasma membrane; reduces MPL recycling; and increases its degradation. Impaired MPL cell-surface expression, which is also a feature of *CALR* and *MPL* mutations, results in elevated plasma thrombopoietin levels, as a result of reduced clearance of thrombopoietin from the plasma by megakaryocytes and platelets, and may also be involved in the emigration of involved hematopoietic stem cells from their marrow niches.

OTHER GENE MUTATIONS FREQUENTLY OCCURRING IN MPNs

In addition to the "phenotipic driver mutations" that are directly linked to hyperproliferation of hematopoietic cells, there is a growing list of somatic mutations found in 25-30% of patients with MPN that do not primarily act on proliferation, but can modify and enhance the effects of the phenotypic driver mutations. The identified genes encode for factors involved in epigenetic regulation (E*ZH2, ASXL1, TET2, DNMT3A, IDH1, IDH2*), the spliceosome complex (*SF3B1, SRSF2, U2AF1*) and rarely interfering with the JAK-STAT signaling pathway (*SH2B3/LNK*) (Vainchenker et al., 2011). Mutations in *TP53*, *TET2*, *SH2B3*, and *IDH1* are more frequently observed in leukemic blasts from transformed MPN patients, suggesting a role for these gene mutations in leukemic transformation (Abdel-Wahab et al., 2010). In addition, novel recurrent mutations occurring at low frequencies have been also found in *CHEK2, SCRIB, MIR662, BARD1, TCF12, FAT4, DAP3*, and *POLG* (Tenedini et al., 2014). The common feature of these gene mutations is that they alone do not cause a MPN phenotype. They are typically also found in other hematologic malignancies, such as

myelodysplastic syndrome (MDS) and acute leukemias. They have been proposed as "non phenotypic driver mutations" or perhaps "important passenger mutations" (Skoda et al., 2015). Many of these mutations are sequentially acquired in cells that already carry a mutation in one of the phenotypic driver genes, most frequently *JAK2*^{V617F}, and are thought to be involved in disease progression (Vainchenker et al., 2011). Interestingly, in some patients somatic mutations can precede the acquisition of the phenotypic driver mutations and constitute a potentially predisposing mutational event. Surprisingly, the same genes in some patients can be mutated before *JAK2*^{V617F}, and in other patients, after *JAK2*^{V617F} (Schaub et al., 2010). Thus, the order of events is not uniquely linked to the gene function. In the case of *TET2* mutations, the order of events, that is, whether the *TET2* mutation was acquired before or after *JAK2*^{V617F}, resulted in differences in phenotype and also in the rate of complications such as thrombotic events (Ortmann et al., 2015). Two recent studies examined the broad mutational landscape of patients with PV, ET, and PMF using exome sequencing or capture-based next-generation sequencing of a set of 104 genes (Lundberg P et al., 2014; Tenedini et al., 2014). Both studies found that after *JAK2*^{V617F} and *CALR*, the most frequent somatic mutations in MPN occur in genes involved in epigenetic regulation (*TET2, DNMT3A, ASXL1, and EZH2*). Mutations in other genes were found at lower frequencies, many of them in single individual patients, which will make it difficult to assess their functional and prognostic relevance. Poor survival and increased risk of leukemic transformation correlated with the increasing number of somatic mutations in individual patients (Guglielmelli et al., 2014). Among the rather rare mutation events, the *TP53* mutations stand out, because, when present, they are associated with poor prognosis and high risk of progression to acute myeloid leukemia (AML) (Harutyunyan et al., 2011). Overall, only about 10% of MPN patients are in the category of "triple negative," in which the driver mutation is still unknown. Triple-negative PMF patients appear to have a less favorable prognosis than patients with mutations in *JAK2, CALR* or *MPL* (Tefferi et al., 2014).

THERAPEUTIC ARMAMENTARIUM IN MPNs

Regarding the treatment, for decades the armamentarium to treat Philadelphia-negative MPNs was reduced to a small handful of cytotoxic drugs like hydroxyurea (HU); interferon; anagrelide; busulfan; and aspirin (Barbui et al., 2011). Since the discovery of the *JAK2*^{V617F} mutation 10 years ago followed by the discovery of many other genetic alterations (Vainchenker W et al., 2011), our knowledge of the pathophysiology of these disorders has dramatically changed. Current drug therapy in PV, ET and PMF is neither curative nor capable of prolonging life or preventing disease progression (Tefferi et al., 2015). Accordingly, treatment indications in PV and ET are primarily directed at prevention of thrombohemorrhagic complications and secondarily towards alleviation of symptoms and in PMF mostly at alleviation of symptoms with the possibility of cure limited to patients undergoing allogeneic stem cell transplant (ASCT) (Kroger et al., 2015).

The discovery of *JAK2*^{V617F} paved the way to JAK2 inhibitors. Ruxolitinib (INCB018424), is a JAK2/JAK1 inhibitor (Quintas-Cardama et al., 2010; Pardanani et al., 2011) and is approved by the US Food and Drug Administration (FDA) for the treatment of patients with myelofibrosis, based on the results of 2 pivotal phase III trials (COMFORT- COntrolled MyeloFibrosis study with ORal JAK inhibitor Treatment- I and -II) (Vannucchi et al. 2015) and with PV (Vannucchi et al., 2015; Passamonti et al., 2017) resistant or intolerant to hydroxyurea. Whatever the JAK2 status, Ruxolitinib therapy led to a rapid and sustained reduction of the spleen size (average of 30%), a sustained reduction of myelofibrosis-related symptoms and mutated allele burden after long-term treatment, improving quality of life in most patients (Harrison et al., 2012; Verstovsek et al., 2012). However, JAK2 is indispensable for hematopoiesis, particularly for red blood cell and platelet production. Therefore, it is not possible to strongly inhibit wild type JAK2 without inducing an anemia or a thrombocytopenia and presently no inhibitor is specific for *JAK2*^{V617F}. The lack of a clear disease-modyfing effect of Ruxolitinib (Mullally et al., 2010; Cardoso et al., 2015) might be ascribed to an underlying mutation complexity of clonal hematopoietic progenitors and/or to hyperactivated signalling pathways other than JAK/STAT, including in particular the PI3K/mTOR cascade (Nishioka et al., 2010; Ugo et al., 2004; Akada et al., 2010;

Krishnan et al., 2012). Evidences favouring the relevance of targeting PI3K/mTOR pathway in MPN derive from cellular and animal models (Bogani et al., 2013; Khan et al., 2013; Bartalucci et al., 2013); furthermore, in a phase I/II clinical trial in patients with myelofibrosis, the mTORC1 inhibitor RAD001 (Everolimus) demonstrated clinical effectiveness by reducing splenomegaly and improving constitutional symptoms (Guglielmelli et al., 2011). Other studies demonstrated an added efficacy by combining inhibitors of the PI3K/mTOR and JAK/STAT pathway (Pandey et al., 2015; Bartalucci et al., 2013). However, the molecular basis of the functional crosstalk between the JAK/STAT and PI3K/mTOR pathway in *JAK2*^{V617F} mutated cells remained poorly characterized.

Concurrent inhibition of PI3K/mTOR and JAK2 signalling pathways provides a complete inhibition of STAT5 phosphorylation in in-vitro and in-vivo MPN models.

BACKGROUND

As described in the introduction direct or indirect dysregulation of JAK2 signaling by somatically acquired mutations has emerged as a central pathogenetic driver of MPNs. The cytokine receptor JAK/STAT pathway is a key signaling pathway during hematopoiesis. As a consequence, it is no surprise to see that this pathway also plays a crucial role in the pathogenesis of these diseases.

PI3K/AKT/mTOR PATHWAY

Although the STAT proteins are important elements in the signaling by oncogenic JAK2, with STAT5 being the key player, constitutive activation of other pathways through the phosphatidylinositol 3-kinase (PI3K) and extracellular signal-regulated kinase (ERK) has been documented in MPNs (Kubota et al., 2004). Activation and autophosphorilation of Tyrosine Kinase Receptors (RTK) by the intracytoplasmic tyrosine portions facilitate their interaction with p85 (PI3K regulatory subunit). PI3K transfers the γ-phosphate from ATP to phosphatidylinositol 4,5-bisphosphate (PIP2) generating phosphatidylinositol (3,4,5)-trisphosphate (PIP3) and ADP. RTK can activate PI3K also through RAS protein, that binds and activates p110 subunit (PI3K catalytic subunit). PI3K is negatively regulated by phosphatases like PTEN; reduced expression of PTEN contributes to oncogenesis by activating PI3K. PIP3 recruits the protein kinase B/Akt through a link of the plekstrin homology domain (PH) next to the plasmatic membrane where Akt is phosphorylated and activated by the kinases PIP3-dependent 1 and 2 (PDK1- PDK2). Once activated, Akt phosphorylates several substrates involved in the regulation of many cellular processes including cell survival, proliferation, differentiation, apoptosis inhibition, autophagy as well as angiogenesis. All of these processes are being considered as crucial features for the establishment and the maintenance of the tumorigenic phenotype (Guertin et al., 2007). Akt resulted constitutively activated in *JAK2*^{V617F} mutated cells *in-vitro* (James et al., 2005; Bumm et

al., 2006) and in V617F transgenic (Shide et al., 2008) or knock-in mice (Akada et al., 2010). Akt is activated via PI3K in response to ligand engagement of the erythropoietin (EPO) receptor and has a role in normal erythroid differentiation. Akt supported erythroid differentiation in JAK2-deficient fetal liver progenitor cells through a mechanism downstream of EPO receptor (Ghaffari et al., 2006).

The main downstream target of Akt is the mTOR complex. It can integrate signals coming from outside and inside the cell, like signals correlated to the cellular energetic status, or the presence of nutritional substances and growth factors. Akt can directly phosphorylate and activate mTOR (mammalian Target of Rapamycin). The beginning of proteins transcription is regulated by phosphorylation of 4eBP1 protein: when 4eBP1 is not phosphorylated it binds eIF4E leading to the inhibition of transcription. After proliferating stimuli, 4eBP1 is phosphorylated by mTOR and other kinases: this induces the release of eIF4E that forms the transcription complex (Mendez et al., 1996; Rousseau et al., 1996). mTOR is the direct responsible of the 4eBP1 phosphorilation: it has been demonstrated that mTOR inhibition blocks 4eBP1 phosphorilation (Berretta et al., 1996; Dilling, 2002). mTOR proteins have pleiotropic functions and are involved in *mRNA* transcription regulation, protein translation and degradation and ribosomal biogenesis. mTOR exists in two complexes, mTORC1 and mTORC2. mTORC1 is formed by mTOR and RAPTOR, is sensible to Rapamycin and phosphorylates S6 kinase and 4eBP1, TORC1 is mainly involved in protein translation regulation and is found constitutively hyperactivated in a wide range of cancers and hematologic disorders (Foster et al., 2012); mTORC2 is formed by mTOR and RICTOR: it affects cytoskeleton changes and phosphorylates Akt leading to a positive feedback. The most recent evidence indicates a role also of mTORC2 in cancer development: many gliomas overexpress the mTORC2 subunit RICTOR, with a consequent enhanced mTORC2 activity that confers to cells increased proliferation and invasion potential (Hietakangas et al., 2009). Prostate cancer development induced by the loss of PTEN in mice, requires mTORC2 function (Guertin et al., 2009). The downstream effector p70S6K plays a critical role in cell growth; the p70S6K gene is found amplified in approximately 9% of primary breast cancer and elevated levels of its mRNAs are found in approximately 41% of tumors (Lluis et al., 2009). Several lines of evidence support the involvement of the PI3K/Akt/mTOR pathway in hematologic disorders: the

pathway results as constitutively activated in lymphoma (Lenz et al., 2010), myeloma (Peterson et al., 2009) and acts as principal mediator of FMS-like tyrosine kinase 3 signaling in acute myeloid leukemia (Brandts et al., 2005), and BCR/ABL signaling (Kharas et al., 2005). It has also been shown that transplantation of cells with a hyperactivated PI3K/mTOR pathway induces leukemia in mice (Feng et al., 2005; Dowling et al., 2010). PI3K signaling is of key importance in normal erythropoietin-induced erythroid differentiation and in spontaneous PV erythroid differentiation (Ugo et al., 2004); conceivably, several kinases which are part of this pathway such as Akt and mTOR have been reported constitutively phosphorylated in bone marrow (Grimwade et al., 2009), in megakaryocytes of MPN patients (Vicari et al., 2012) and in *JAK2*^{V617F} mutated cell lines (James et al., 2005).

AIM OF THE PROJECT

The aim of this project is to provide mechanistic explanation for the involvement of PI3K/mTOR signaling in cells harboring the *JAK2*^{V617F} mutation.

Exploring the hypothesis that complete dephosphorylation of STAT5 (involving different residues) might result in more pronounced inhibition of *JAK2*^{V617F} mutated cells, we wanted to evaluate the effects of different inhibitors, either alone or in combination, in different MPN models. To achieve maximal inhibition of STAT5 phosphorylation, we used as relevant drugs the pan PI3K inhibitor BKM120, that is being tested in a clinical trial in association with Ruxolitinib (Durrant. et al, 2015), and the mTORC1 complex inhibitor RAD001, already characterized in *in-vitro* models (Bogani et al., 2013).

The purpose was therefore to provide the rationale for designing innovative strategies, improving efficacy and ameliorating toxicity of treatments in MPNs.

METHODS AND MATERIAL

COMPOUNDS AND REAGENTS

PI3K/AKT/mTOR INHIBITORS

BKM120 (NVP-BKM120). BKM120 specifically inhibits class I PIK3 (p110α/β/δ/γ) (Brachmann et al., 2012; Maira et al., 2012) in the PI3K/AKT kinase (or protein kinase B) signalling pathway in an ATP-competitive manner, thereby inhibiting the production of the secondary messenger phosphatidylinositol-3,4,5-trisphosphate and activation of the PI3K signalling pathway. BKM120 has a potent anti-proliferative and pro-apoptotic activity in tumor cell lines and it shows good oral bioavailability in murine models and its specific activity, observed in cellular assays, also translates well in *in-vivo* models of neoplasms (xenograft), which present a significant inhibition of tumor growth with tolerated doses (Zheng et al ., 2012). Clinically, BKM120 has been shown to be safe at the maximum tolerated dose with a favorable pharmacokinetic profile (Ren et al., 2012; Rosich et al., 2013) and with anti-tumor activity.

RAD001 (Everolimus). It is an inhibitor of the serine-threonine kinase mTOR derived from Rapamycin (or Sirolimus, cyclic macrolactone produced by *Steptomices Hygroscopicus*; the formation of the active complex consists in the formation of the interaction complex between Rapamycin and FK506-binding protein 12 (FKBP12); this complex mediate anti-proliferative effects inhibiting catalytic activity of mTOR following binding on FRB domain). The RAD001 molecule is associated with high affinity with the FKBP12 molecule to generate an immunosuppressive complex that binds and inhibits mTOR activation, specifically TORC1. It thus exerts the action of inhibiting proliferation and factor-dependent growth by blocking the transition from G1 to phase S of cell cycle. The anti-neoplastic effect of RAD001 involves several mechanisms including inhibition of cell growth, apoptosis induction, inhibition of expression of genes controlling cell adhesion, migration and angiogenesis (Yee et al., 2006; Yang et al., 2010).

BEZ235. It is a dual inhibitor of both the PI3K class I and of the complexes 1 and 2 of the mTOR kinase. A dual inhibition should be more effective than the single inhibition of mTOR in controlling tumor growth, if the overgrowth is not controlled effectively by inhibition of the mTORC1 only (Maira et al., 2008; Serra et al., 2008). BEZ235 inhibits PI3K/Akt/mTOR signaling, induces inhibition of cell growth and apoptosis, both in human cell lines expressing *JAK2*^{V617F} and in CD34+ cells of patients with MPN (Fiskus et al., 2013; Blatt et al., 2012). The *in-vitro* anti-tumor activity of BEZ235 has been demonstrated in breast, prostate, rectal, glioblastoma, renal and pulmonary xenograft models. BEZ235 also acts in the blockade of proliferation of VEGF-stimulated endothelial cells.

PP242. It is a potent inhibitor of mTORC1 and mTORC2, also showing, when used at high concentrations, a minimal activity against a small range of tyrosine, (Apsel, 2008). PP242 unlike Rapamycin and its cytostatic derivatives, as RAD001, induces death of human and murine leukemic cells. PP242 *in-vivo* induces the effects of treatment with tyrosine kinase inhibitors more effectively than Rapamycin.

JAK2 INHIBITOR

Ruxolitinib (INCB018424). It is an inhibitor of tyrosine kinases JAK1 and JAK2; the JAK-STAT pathway is a key component of cytokine signalling and growth factors that regulate cell proliferation, hematopoiesis, and immune response. Deregulation of this pathway, upregulation of *JAK1* or *JAK2* or gain of function mutations (such as *JAK2*^{V617F}, *MPL*^{W515L}, and *JAK2* mutations on exon 12) are involved in MPN pathogenesis. Ruxolitinib binds and inhibits JAK1, JAK2 (both in wild-type and *JAK2*^{V617F}) and JAK3, though with lower affinity than the previous ones: the binding allows the inhibition of the cell signalling mediated by growth factors and the neoplastic cell proliferation (Verstovsek et al 2010, Quintás-Cardama et al., 2010).

BKM120 (NVP-BKM120, a selective pan class-I PI3-Kinase inhibitor), RAD001 (Everolimus, a mTOR specific allosteric inhibitor with activity against TORC1), BEZ235 (a double PI3K and mTOR inhibitor) and Ruxolitinib (INCB018424, a JAK1/JAK2 kinase ATP-competitive inhibitor) were kindly provided by Novartis (Basel, Switzerland);

PP242 was purchased from Sigma-Aldrich (St Louis, MO, US). For *in-vitro* studies stock solution were prepared in 100% dimethyl sulfoxide (DMSO; Sigma-Aldrich) to a concentration of 10 mM and further diluted to an appropriate final concentration in culture medium at the time of use. For *in-vivo* use, BKM120 was prepared in 10% N-methyl-2-pyrrolidone and 90% PEG300; Everolimus was formulated as a microemulsion pre-concentrate, it was diluted with plain water; Ruxolitinib was formulated in 0.5% hydroxypropyl methylcellulose.

Calyculin A (Santa Cruz Biotechnologies, Santa Cruz, CA, US) was dissolved in DMSO at 0.1 mM final concentration and established concentration was delivered to cultures two hours prior treatment.

CELL LINES AND CELL CULTURE

K562. This cell line was derived from the pleural effusion of a Caucasian woman of 53 years old affected by chronic myelogenous leukemia; the cells have a lymphoblastic morphology. They have a human diploid karyotype with 46 chromosomes in which there is the terminal deletion of the long arm of chromosome 22 (del (22) (q12)), Philadelphia (Ph) chromosome; there is also a reciprocal translocation of an unbalanced chromosome 17 on the long arm of one of chromosome 15. The majority of the mononuclear cells are undifferentiated and do not produce immunoglobulin, show no alkaline phosphatase activity and myeloperoxidase and they are not able to phagocytize inert particles (Baker et al., 2002). The cell line K562 is WT for the mutation $JAK2^{V617F}$.

HEL. This cell line was derived from the peripheral blood of a 30 year old man with acute erythroblastic leukemia (AML-M6) arose after treatment for Hodgkin's lymphoma. The cells show a rounded morphology, appear great, and occasionally giant and multinucleated; they show capacity for induced and spontaneous synthesis of globin. The HEL cell line presents in its genome multiple copies of the mutation $JAK2^{V617F}$ (Quentmeier et al., 2006).

SET2. This cell line was derived from peripheral blood of a 71 year old woman affected by essential thrombocythemia evolved into megakaryoblastic leukemia. The

cells are found mostly individually suspended and some of them grow losing adhesion. It can be note the rare presence of giant cells (Uozumi et al., 2000; Gozgit et al., 2008). The SET2 cell line are heterozygous for the mutation *JAK2*^{V617F}.

Ba/F3. This cell line was derived from the peripheral blood of BALB/c mice affected by pro-B leukemia. They are IL-3 dependent and show round morphology, some appear polymorphic, they meet individually suspended or occasionally in groups. They show a diploid karyotype mouse with 33% of polyploidy (40 (36-42) 2*n*) (Bosward et al., 1999).

WEHI-3B. This cell line was derived from a murine myelomonocytic leukemia of BALB/c mice. The cells are similar to macrophages, small and round. They grow both in adherence and in suspension and they produce IL-3.

The K562 and HEL cell lines used were obtained from the German Collection of Microorganisms and Cell Cultures (DSMZ, Braunschweig, Germany, www.dsmz.de). SET2 cells were purchased from the American Type Culture Collection (ATCC, Manassas, VA, US, www.atcc.org). Murine Ba/F3 and Ba/F3-EPOR cells expressing JAK2 wild-type (WT) or JAK2V617F (VF) were donated by Dr. R. Skoda (University Hospital of Basel, Switzerland). *JAK2*^{V617F}-Ba/F3-EPOR Luc+ cells (clone 8) were kindly provided by Dr. T. Radimerski (Novartis, Basel).

The cells lines were maintained in RPMI 1640 medium supplemented with 10% Fetal Bovine Serum (FBS; Lonza, Verviers, Belgium) (20% for the SET2 cells), 1% L-glutamine and 1% Penicillin-Streptomycin. Ba/F3 and Ba/F3-EPOR WT cell lines were supplemented with 10% WEHI pre-conditioned media as a source of IL-3. Recombinant human EPO (rhEPO; Sigma Aldrich) was added to *JAK2*^{WT} Ba/F3-EPOR cells, that require the cytokine for survival and proliferation, at final concentration of 1 U/mL. Cells were maintained at 37°C in 5% CO_2 humidified atmosphere.

PRIMARY HUMAN CELLS

For the evaluation of molecular targets and for cellular studies peripheral blood (PB) or bone marrow (BM) samples were obtained from PV or PMF patients, diagnosed according to the World Health Organization (WHO) criteria, under a protocol approved by Institutional Review Board of Azienda Ospedaliera-Universitaria Careggi and after obtaining a written informed consent. Briefly, in order to collect mononuclear cells (MNCs) 20 mL of PB was layered on Ficoll Hypaque (Lonza, Belgium) and centrifuged at 1600 rpm for 20 min at room temperature. It has been recovered the ring of mononuclear cells, which were washed in sterile PBS at 4°C, and centrifuged at 1200 rpm for 10 minutes at 8 °C for two times. The cells were counted using a Burker chamber with a dilution factor of 1:300.

CD34+ cells isolation. The purification of CD34+ cells from peripheral blood or cord blood was performed using immunomagnetic separation according to the Miltenyi procedure: the layer of mononuclear cells was washed with Buffer 1 (Ca-Mg free PBS, 2 mM EDTA), centrifuged at 1000 rpm for 10 minutes and then resuspended in Buffer 2 (Ca-Mg free PBS, 0.5% BSA, 2 mM EDTA) to a final volume of 300 µl containing up to 10^8 mononuclear cells. To this suspension were then added 100 µL of FcR blocking reagent (Human IgG) and 100 µL of MACS CD34 microbeads (microbeads super-paramagnetic conjugated to murine anti-human CD34 monoclonal antibodies (isotype: mouse IgG1) up to 10^8 of total cells; the whole was incubated for 30 minutes at 4°C and agitated every 10 minutes. After incubation, Buffer 2 was added up to a volume of 10ml and centrifuged at 1000 rpm for 10 minutes at 8°C. Very carefully was removed the supernatant and the pellet was resuspended in a final volume of 500 µl Buffer 2 up to 10^8 total cells. For separating CD34 positive cells was taken a column MACS MS+ ($2x10^8$ total cells, $1x10^7$ positive cells). After washing with 500 µl of Buffer 2, the column MACS MS+ was inserted in the magnetic support, the cell suspension was applied to the column which was then allowed to drain by gravity the CD34 negative fraction; then three washes of the column with 500 µl of Buffer 2 were performed. Then it was added further 500 µl of Buffer 2 in the column, which was quickly detached from the magnetic media to recover the CD34 positive fraction by

pressure with a piston-column. Sometimes it was necessary to perform additional steps of purification of CD34 positive fraction recovered in a new column.
Control CD34+ cells were obtained from discarded cord blood units.

CD34+ cells were plated at the concentration of $5x10^5$ cells/mL in IMDM medium (Iscove's Modified Dulbecco's Medium, Lonza, Belgium) with the addition of 20% Human Serum, Penicillin/Streptomycin 1% L-glutamine 1%; plus a cytokines cocktail allowing CD34+ proliferation: human SCF 50ng/mL; FLT3L 50ng/mL; human TPO 20ng/mL; human IL-3 10ng/mL; human IL-6 10ng/mL. After 6 days of culture the cells were washed in PBS, counted and apoptosis, proliferation and cell cycle have been evaluated after addition of various drugs.

COLONY ASSAY

It was used two semisolid media: a preparation of methylcellulose containing an optimal blend of cytokines (Methocult GF H4434, StemCell Technologies Inc, Vancouver, Canada) to induce the growth of myeloid colonies (with rhSCF, rhGM-CSF and rhIL-3) and erythroid colonies (with rhIL-3 and rhEPO); a preparation of methylcellulose "base" (MethoCult H4531, StemCell Technologies Inc, USA), without any cytokine, allowing the growth of the endogenous erithroid colonies (EEC) (**Table 6**). It was added $1.0x10^5$ MNCs/mL for the methylcellulose complete medium and $2.5x10^5$ MNCs/mL for the methylcellulose "base" medium to vials of 2.5 mL of semisolid (methylcellulose) medium, in IMDM culture medium (Lonza, Belgium), Penicillin/Streptomycin (Lonza, Belgium) and 2 mM L-glutamine (Lonza, Belgium); the cells were subsequently plated in Petri dishes (Tissue Culture Dish, 35x10 mm, Falcon, USA).

METHOCULT GF H4434	METHOCULT H4531
1.0% Methylcellulose in IMDM	1.0% Methylcellulose in IMDM
30% Fetal Bovin Serum (FBS)	30% Fetal Bovin Serum (FBS)
1% Bovine Serum Albumin (BSA)	1% Bovine Serum Albumin (BSA)
10-4 M 2-Mercaptoethanol	10-4 M 2-Mercaptoethanol
2mM L-glutamine	2mM L-glutamine
50ng/mL rh Stem Cell Factor	10% Agar Leukocyte Conditioned Medium
10ng/mL rh GM-CSF	
10ng/mL rh IL-3	
3 unit/mL rh Erythropoietin (EPO)	

Table 6: Description of semisolid media.

After 14 days of culture in an incubator at 37°C and 5% CO_2, colonies were counted and recognized as belonging to the myeloid or erythroid lineage according to conventional morphological criteria. The presence or absence of hemoglobin pigment were done by examination under an inverted microscope (**Figure 5**).

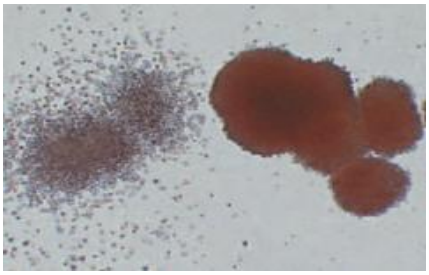

Figure 5: BFU-E and CFU-GM.

For the evaluation of the megakaryocytic colonies it was used MegaCult-C serum-free medium (Stem Cell Technologies Inc., Vancouver, Canada) (**Table 7**) to which it was added CD34 positive cells purified by immunomagnetic separation at a concentration of $1x10^3$ cells/mL in a final volume of 3.3 mL (consists of 0.4 mL of cell suspension, 1.7 mL of MegaCult non-C Medium supplemented with cytokines and 1.2 mL of Collagen Solution). It was then added to the medium 50 ng/mL of Thrombopoietin, 10 ng/mL of human IL-6 and 10 ng/mL of human IL-3.

COMPONENTS	FINAL CONCENTRATION
Collagen	1.1 mg/mL
Bovine Serum Albumin	1%
Recombinant Human Insulin	10 μg/mL
Human Transferrin	200 μg/mL
L-glutamine	2 mM
2-Mercaptoethanol	10^{-4} M
Iscov's MDM	

Table 7: Description of MegaCult-C serum-free medium.

After 12 days of culture in an incubator at 37°C and 5% CO_2, megakaryocytic colonies were recognized and counted (CFU-Mk) (**Figure 6**).

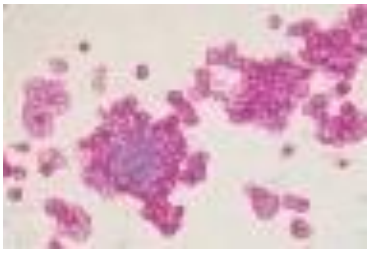

Figure 6: CFU-Mk.

CELL PROLIFERATION TEST (WST-1)

The evaluation of cell proliferation in presence of various amount of the drugs was performed using the colorimetric assay WST-1 (Cell Proliferation Reagent WST-1). The principle of this method is the increase in absorbance (450 nm) due to increased cell proliferation detectable by spectrophotometer. The tetrazolium salt WST-1 is turned in the Formazan molecule by the activity of mitochondrial enzymes. An expansion in the number of cells causes an increase in the activity of cellular mitochondrial dehydrogenases which leads to an increase in the Formazan formation, this increase is directly related to the number of metabolically active cells in the culture, so to the cell proliferation. 10 μL of WST-1 were added to 100 μL of cell suspension of HEL, K562, SET2, BaF3, CD34+ plated at a concentration of $2x10^5$ cells/mL ($3x10^5$ for CD34+ cells) in RPMI medium without phenol red on 96 multiwells (Falcon, USA) with escalating doses of the various drugs. The multiwells were

incubated for 3/4 hours at 37°C. The identification of the IC_{50} dose was detected using the software Origin 7.5. Each individual test was carried out in triplicate and the final datum was obtained as media of three tests. The spectrophotometer used was the instrument ELISA EL808 (Biotek) and data were analyzed with the Software Gen5 (Biotek).

ASSESSMENT OF CELL CYCLE AND APOPTOSIS

The cell cycle distribution was performed recovering $1x10^6$ cells after 18 hours of drugs treatment and washed twice with PBS by centrifugation at 1200 rpm for 5 minutes; subsequently the supernatant was aspirated, the cell pellet fixed with 500 µL of a 95% ethanol cold solution and then incubated on ice for 20 minutes. After washing with PBS, the cell pellet was resuspended in 500 µL of PBS containing 10 µg/mL of RNase (Roche) and incubated at 37°C for 20 minutes. The suspension was then transferred into a FACS tube and has been carried out a wash in PBS before addition of 500 µl of a propidium iodide (PI) solution at a concentration of 10 µg/mL and subsequent incubation on ice for 10 minutes. The addition of PI and subsequent incubation was performed protected from light. PI is an intercalating agent and a fluorescent molecule and when is bound to nucleic acids, the fluorescence excitation emission is detected. After incubation, we proceeded to the cytofluorimetric evaluation with FACS SCAN (Becton Dickinson) using the Cell Quest Pro software (Becton Dickinson) and a minimum of 30.000 events were acquired.

Quantification of apoptotic cells was accomplished using Annexin-V-FLUOS Staining kit (Roche, Basel, Switzerland). $1x10^6$ cells were removed from the wells after 48 hours of incubation with the various compounds and washed with PBS by centrifugation at 1200 rpm for 5 minutes. The pellet was resuspended in 100 µl of Incubation Buffer with the addition of 2µl of Annexin-V-FLUOS labeling solution (Roche) and 2µl of propidium iodide and incubated at room temperature for 15 minutes. Then 500 µl of Incubation Buffer were added and we proceeded to the

evaluation of at least 20.000 events in a FACS SCAN flow cytometer (Becton Dickinson). Data were processed with Flow-Jo software (Tree Star, Ashland, OR, USA).

CONFOCAL MICROSCOPY

Granulocytes from *JAK2*^{V617F} MPN patients and healthy donors were isolated by gradient using Ficoll Hypaque, resuspended in complete medium (RPMI 1640) ($3x10^5$ cells/mL) and seeded on polylysine-coated glass slides. Cells were then incubated at 37°C and CO_2 5% and then fixed in formaldehyde (4% in PBS pH 7.2). After fixing, cells were permeabilized with 0.1% Triton (Sigma) for 10 minutes, and incubated for 20 minutes at room temperature with goat serum (1 mg/mL). After, cells were incubated with antibody anti-phospho (p-) STAT5 Y694 (rabbit IgG, Cell Signaling), p-STAT5 S731 (rabbit IgG, Abcam, Cambridge, UK) or p-STAT5 S193 Ab (rabbit IgG, kindly given by Prof. Francesco Annunziato from University of Florence, Italy) for 40 minutes; cell were then incubated at room temperature with anti-rabbit IgG Alexa Fluor 488 conjugated Ab for 30 minutes (2 µg/mL), in buffer containing TOPRO-3 dye (0.2 µM) for the nuclear counter staining. Cells were then washed in PBS for 5 min, and the slides mounted with Vectashield mounting medium (Vector Laboratories Inc., Burlingame CA). Microscopic images were taken by a LSM 510 META Zeiss confocal microscope system (Carl Zeiss Inc., Jena, Germany), using 40X oil immersion lens, corresponding to a 400X magnification. For images analysis Confocor 2 (Zeiss) software was used.

TRANSFECTION

Gene silencing was performed by siRNA transfection according to Amaxa Nucleoflector® technology (Lonza). Briefly, 1 µl of siRNA was used to transfect $2\text{-}5x10^6$ cells, previously resuspended in a volume of 0.1 mL. The suspension was then immediately transferred to a flask containing a preheated culture medium. Transfection efficacy and cell viability were evaluated by flow cytometry with pmaxGFP® (AmaxaBiosystems). mTOR, PP1, PP2A, CIP2A and non-targeting control siRNAs were from Cell Signaling Technologies (Danvers, MA, US).

CELL LYSIS AND SDS-PAGE WESTERN BLOTTING

Cells were lysed in RIPA lysis buffer (50 mM pH 7.4 Tris-HCl, 150 mM NaCl, 1% NP-40, 1 mM EDTA) containing a proteinase inhibitor cocktail (Halt Protease Inhibitor Cocktail Kit, PIERCE, Rockford, IL, US). After sonication (Microson XL-2000, Minisonix, Farmingdale, NY, USA), the cell suspension was centrifuged at 14000 rpm for 15 minutes at 4°C and supernatant containing the extracted proteins was recovered. An aliquot of cell lysate was used for protein quantification using a BCA kit (Sigma-Aldrich). The proteins were resuspended in 4x Sample Buffer (Tris-HCl pH=6,8 250mM, glycerol 10%, SDS 8%, Bromophenol blue) and β-mercaptoethanol. After heating at 95°C for 10 minutes, the samples were applied on a polyacrylamide gel 4-12% (Invitrogen-Life Technologies, Carlsbad, Ca, USA). After the electrophoretic separation (SDS-PAGE) with running buffer (Tris 15 g/L, glycine 72 g/L, SDS 5 g/L, H2O milli-Q), the proteins were blot on PVDF membranes using iBlot 7-minute Blotting System (Invitrogen). The membranes were subsequent blocked for 1 hour at room temperature with 5% BSA in a solution of Tris Buffered Saline with 0.1% Tween 20 detergent (TBST). The next incubation with the primary antibody took place overnight at 4°C with a 1:1000 dilution of the antibody in a solution of TBST with 1% BSA. After incubation, three washes of the membranes were carried out to remove the excess of unbound antibody with a solution of TBST. Then, an incubation in the HRP-conjugated solution (with a dilution of 1:10000 in TBST with 1% BSA) was performed for one hour at room temperature. The membranes were successively rinsed three times for 5 minutes in TBST and incubated for 1 minute with ECL reagent. Western blotting images were acquired with ChemiDoc XRS+ (Bio-Rad, Hercules, CA, US) and analyzed with ImageJ software (50) for densitometric analysis.

The antibodies assayed in western blotting analysis were the following: p-STAT5 Y694, mTOR, p-4eBP1 (tyrosine 70), 4eBP1 and α-Tubulin (Cell Signaling Technology). p-STAT5 S731, STAT5 isoform A and B (STAT5a, STAT5b) (Abcam) and p-STAT5 S193 (from Prof. Annunziato), CIP2A and PP1 were from Santa Cruz Biotechnology. PP2A

was from Millipore (Merck Millipore, Darmstadt, Germania). Anti-rabbit HRP antibody was from Sigma-Aldrich and anti-mouse HRP antibody was from Millipore.

QUANTITATIVE REAL-TIME PCR (qRT-PCR)

Total RNA was extracted using TriPue Isolation Reagent (Roche Diagnostics) following the directions of the company. The RNA concentration and purity/integrity was determined with NanoDrop ND-1000 spectrophotometer (NanoDrop Techn., Wilmington, DE, USA) and reverse-transcribed to cDNA using one microgram of RNA.
cDNA was synthesized using High capacity cDNA Reverse Transcription kit (Applied Biosystems, Life Technologies; Carls-bad, CA) and quantitative real-time PCR (qRT-PCR) was carried out with SYBR Green PCR master mix (Applied Biosystems) on a StepOnePlus Real-time PCR System (Applied Biosystems) according to standard protocols.
The primers for the qRT-PCR analysis were as follows: for *CIP2A,* forward 5'-TGACCCTTCTGCTGCCTACA-3' and reverse 5'-GCCTTGGCAATCCTTTCACA-3'; for *Snail*, forward 5'-CCCAGTGCCTCGACCACTAT-3' and reverse 5'-CCAGATGAGCATTGGCA-3'; for miR375, forward 5'-CGAGCCGAACGAACAAAA-3' and reverse 5'-GACGAGCCCCTCGCACAA-3'; for *GAPDH,* forward 5'-GTCGGAGTCAACGGA-3' and reverse 5'-GGGTGGAATCATATTGGAACATG-3'. *GAPDH* was used as internal control. Relative gene expression was calculated according to the comparative cycle threshold (Ct) method.

MOUSE MODELS

All animal procedures were performed according to Italian laws in an animal facility (Di.V.A.L., University of Florence) under humanized conditions.

SCID Ba/F3 EPO-R *JAK2*^{V617F} – Luc+ mouse model (Figure 7). This mouse model is generated by tail vein injection in female beige SCID immunodeficient mice (4–6 weeks; Harlan, Indianapolis, IN, USA) of 3x10^6 murine leukemic pro-B Ba/F3-EPOR cells

expressing *JAK2*^{V617F} mutation and Luciferase enzyme (Luc+) (clone 8) kindly provided by Dr. Thomas Radimerski (Novartis Institute for Biomedical Research, Basel). At specified time points thereafter, mice were injected with Xeno Light D-luciferin (Caliper, Waltham, MA, USA) to generate a measurable bioluminescence signal that is proportional to leukemic burden (Luc+ cells); measurement was performed 15 min after luciferin injection using the Photon Imager apparatus (Biospace Lab, Paris, France). Baseline measurement performed on day 6 after Luc+ cells injection was used to establish individual bioluminescence level, then mice were randomly divided into three treatment cohorts of six mice each having comparable baseline disease burden (vehicle, 45 mpk BKM120, 60 mpk BKM120). Drugs were administered daily by gavage and imaging was performed at weekly intervals after the first drug dose; mice were followed daily for survival and euthanized when they developed hind limb paralysis or became moribund. This model was used to evaluate effectiveness doses and selectivity of drugs treatment.

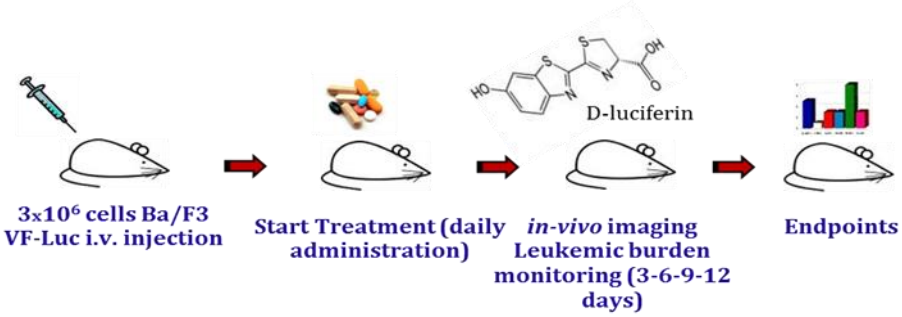

Figure 7: SCID Ba/F3 EPO-R *JAK2*^{V617F} – Luc+ mouse model**.**

The inhibitors and combinations in their effective concentrations were subsequently tested in the second mouse model.

C57Bl6/J *JAK2*^{V617F} KI mouse model (Figure 8). This mouse model was kindly provided by Dr. Jean-Luc Villeval (INSERM U1009, Institut Gustave Roussy, Villejuif, Paris, France) (Bartalucci et al., 2013). KI mice were generated with the insertion in mouse genome of inverted *JAK2*^{V617F} mutated sequence (L2) that is activated by the

mating with a VavCre transgenic mouse expressing Cre recombinase under the control of Vav promoter in hematopoietic and endothelial tissue (Schnutgen et al., 2003; Li et al., 2010). Progeny is heterozygous *JAK2*^{V617F} and develop a Chronic Myeloproliferative Neoplasms from birth with characteristic symptoms like high hematocrit values, high platelets and white blood cells count, splenomegaly and bone marrow fibrosis (Kubovcakova et al., 2013; Mullaly et al., 2010; Akada et al., 2010; Marty et al., 2010; Mullaly et al., 2012).

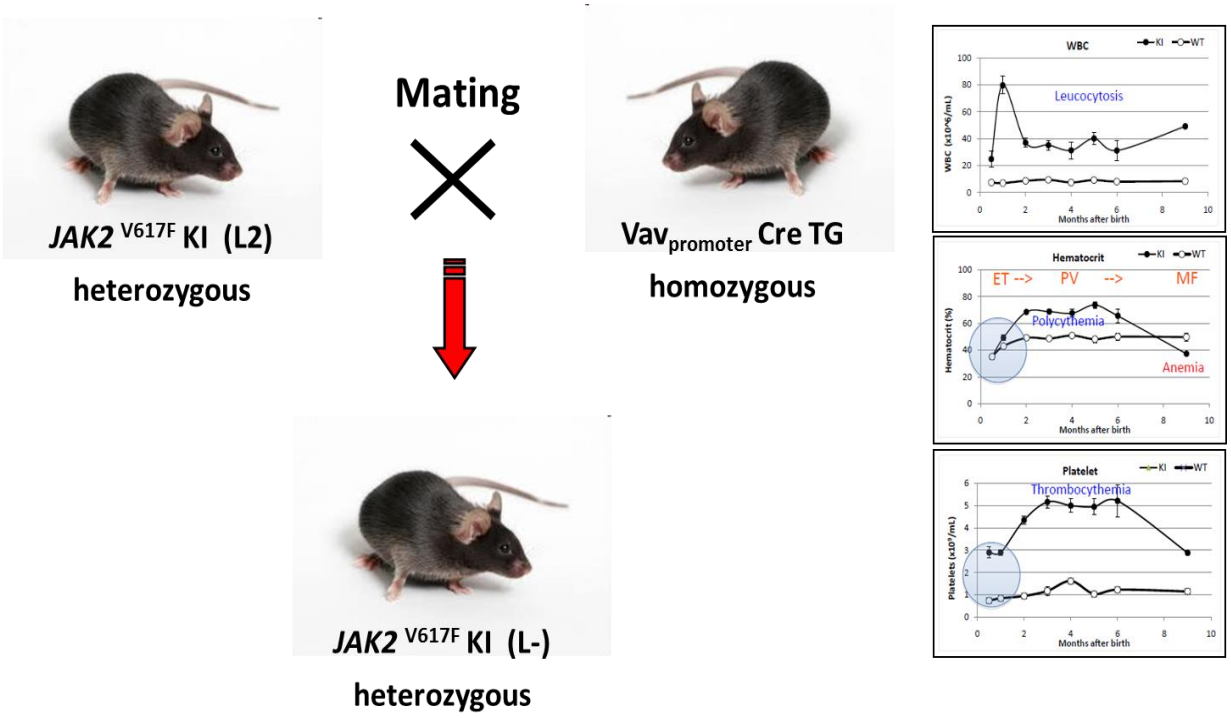

Figure 8: C57Bl6/J *JAK2*^{V617F} KI mouse model.

Three months-aged KI mice received the drugs for indicated periods administered by oral gavage and were euthanized by CO_2 inhalation. Hematic parameters were evaluated periodically: before, during and at the end of treatment by blood withdrawal from the retro-orbital vein; the blood count was performed by the Sysmex XE5000 (Sysmex, Hyogo, Japan) cell counter while the reticulocytes (number per high-power field, HPF) were counted in methylene blue-stained blood smears.

The spleen was collected and weighted; to accomplish for variations in body weight at baseline, a spleen index (*i.e.*, spleen weight/body weight ×100) was calculated. Cuts of the spleen, liver and bone marrow were fixed in PBS-buffered formalin (4%), paraffin embedded, sectioned and haematoxylin and eosin stained.

For murine colony assay, bone marrow cells were harvested from *JAK2*^{V617F} KI and *JAK2*^{WT} mice and plated at 1x10^4/mL in methylcellulose (MethoCult GF M3434, Stem Cell Technologies) supplemented with recombinant cytokines (SCF, mIL-3, hIL-6, hEPO). In experiments testing drugs and combination a 1:1 ratio of *JAK2*^{V617F} KI and *JAK2*^{WT} bone marrow mice cells was used. Single colonies were harvested on day 4 and genotyped by allele specific PCR in order to discriminate the JAK2 mutational status as previously described (Bartalucci et al., 2013).

STATISTICAL METHODS

The Mann-Whitney *U* or Fisher test was used for comparison using the SPSS software (StatSoft, Inc., Tulsa, OK, USA, www.statsoft.com) or Origin software (OriginiLab, Massachusetts, USA). Data were expressed as mean ± standard deviation (SD). The level of significance from two-sided tests was $P<0.05$. The analysis of drug synergism was performed by calculation of the combination index (CI), that is a measure of the interaction between two drugs. The CI was calculated according to the median-effect principle of the Chou and Talaly (Chou TC et al., 1977) method using CalcuSyn software 2.1 (BioSoft, Cambridge, UK). According to this formula, CI <0.90, 0.90< CI <1.10 and CI >1.10 were considered, respectively, synergistic, additive and antagonistic effects.

RESULTS

DIFFERENT STAT5 PHOSPHORYLATION PATTERNS FOLLOWING THE ACTIVATION OF JAK2 AND PI3K/mTOR PATHWAYS IN *JAK2^{V617F}* MUTATED CELLS.

In this first project we have been able to demonstrate how the activation of JAK2 and PI3K pathway in *JAK2^{V617F}* mutated cells originate unique STAT5 phosphorylation pattern. We previously reported that STAT5 phosphorylation in these cells was down-regulated after exposure to drug targeting the PI3K/Akt/mTOR pathway (Bogani et al., 2013; Bartalucci et al., 2013). So, in order to investigate the mechanisms by which inhibition of PI3K/mTOR signaling prevented STAT5 phosphorylation, we exposed for 24 hours the *JAK2^{V617F}* mutated SET2 human cell line to increasing concentrations of various drugs. Specifically, the compounds that we used were the JAK1/2 inhibitor Ruxolitinib and the following PI3K/Akt/mTOR inhibitors: the dual PI3K/mTOR inhibitor BEZ235, the pan-PI3K inhibitor BKM120, the mTORC1 inhibitor RAD001 and the mTORC1/2 inhibitor PP242. We than assessed the pattern of phosphorylated STAT5a and STAT5b residues following the treatment by western blotting analysis. As reported in the **Figure 9** Ruxolitinib caused reduction of p-Tyrosine (Y) residues (particularly p-Y694 than together with Y699 is the immediate target of activated JAK2 in human STAT5a and STAT5b, respectively), with irrelevant effects on serine residues. Conversely, all the PI3K/mTOR inhibitor induced a dose-dependent dephosphorylation of serine (S) residues of STAT5b, specifically S731 and S193, while p-tyrosine residues were unaffected.

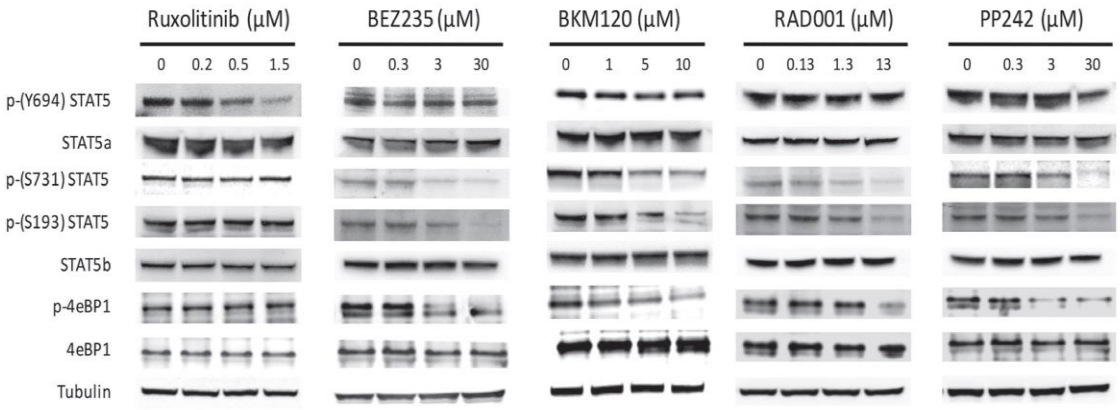

Figure 9: Effects of JAK1/JAK2 inhibitors and the PI3K/mTOR inhibitors in the modulation of the phosphorylation pattern of STAT5 in SET2 cell line. One representative experiment of at least four independent evaluations for the different targets. Tubulin was used for loading normalization.

To confirm the involvement of PI3K-pathway on STAT5 serine phosphorylation levels, an mTOR silencing was made using specific mTOR siRNA, or non-targeting control siRNAs (NTC) in SET2 cell line. As expected, the expression levels of mTOR and its target phospho-4eBP1 were almost completely abolished at 24 hours following siRNA transfection and we observed also a dephosphorylation of STAT5b serine residues, therefore excluding off-target effects of PI3K/mTOR inhibitors, without any change in the phosphorylated status of Y694 of STAT5a (**Figure 10**).

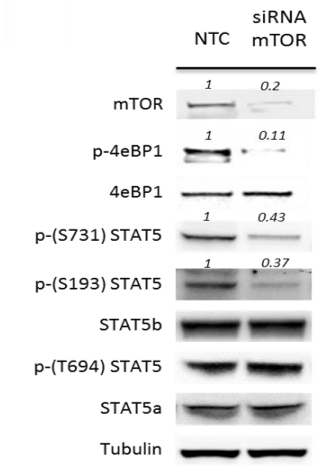

Figure 10: Effects of mTOR silencing by specific siRNA on the phosphorylation pattern of STAT5a/b in SET2 cell line. Tubulin was used for loading normalization. The numbers above each lane indicate results of densitometric analysis. Data are from one representative experiment out of three.

Finally, we explored the phosphorylated status of STAT5 tyrosine and serine residues in peripheral blood granulocytes of *JAK2*^{V617F} mutated MPN patients using confocal microscopy (**Figure 11**). After isolation of the cells by density gradient and probe with phospho-specific anti-STAT5 antibodies we found that phosphorylated Y694 as well as S193 and S731 residues were clearly marked in patients' cells as compared to control cell from healthy donor.

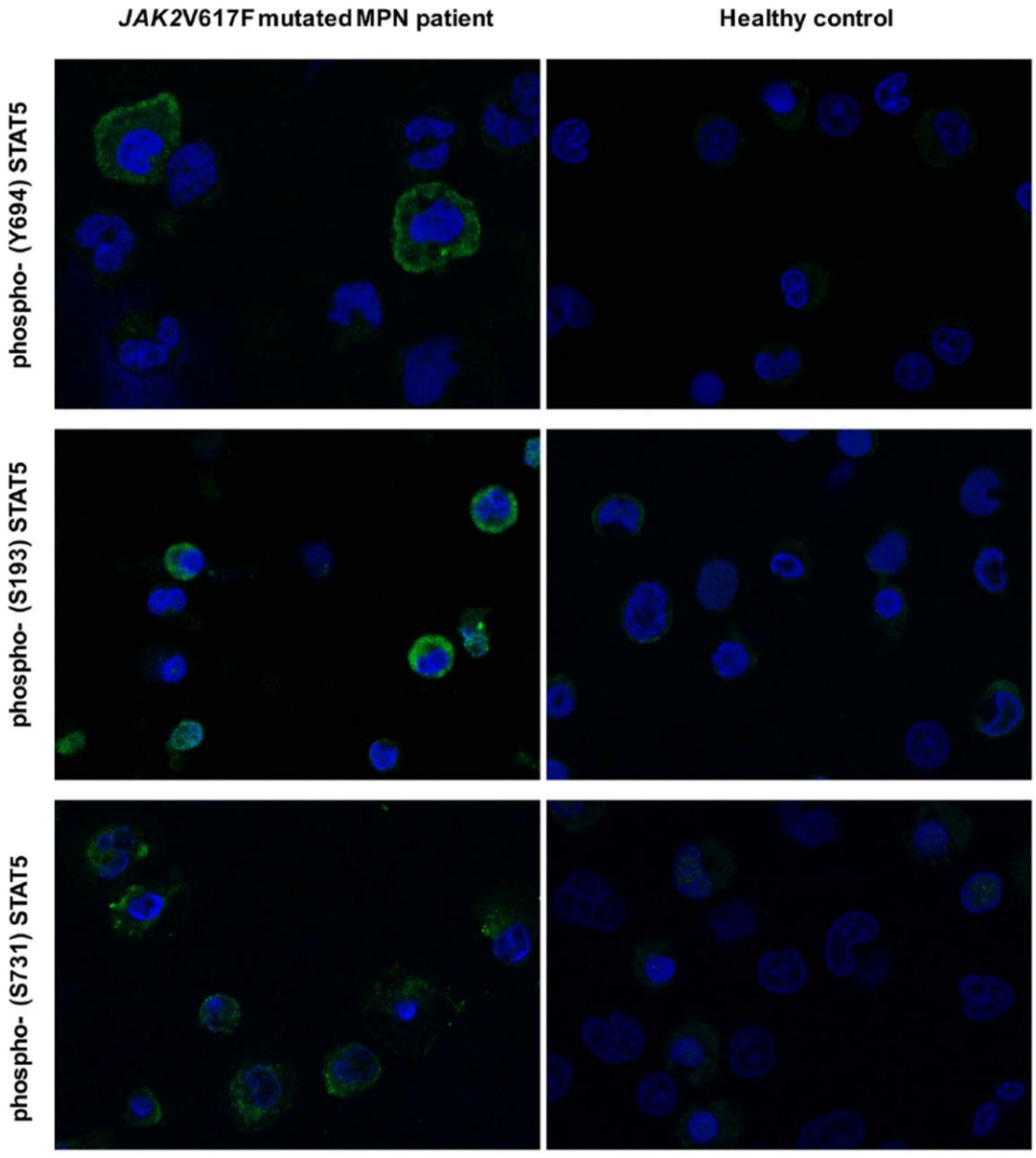

Figure 11: Confocal analysis of the phosphorylated status of STAT5a/b in granulocytes of JAK2^{V617F} mutated MPN patients and healthy donor. Topro-3 was used as nucleus marker. A representative experiment out of 5 is shown.

Overall, these findings indicate that in cells expressing the *JAK2*^{V617F} mutation, STAT5 is phosphorylated on both tyrosine and serine residues as the results of JAK2- and PI3K/mTOR-dependent mechanisms, respectively.

STUDY OF THE MECHANISMS REGULATING THE DE-PHOSPHORYLATION OF STAT5 INDUCED BY PI3K/mTOR INHIBITORS.

To understand how PI3K-pathway regulated STAT5 serine phosphorylation we focused on protein phosphatases, mainly represented by phosphatase 1 (PP1) and 2 (PP2A) that are the enzymes mainly responsible of protein de-phosphorylation (Perrotti et al., 2013; Ross et al., 2010; Mitra et al., 2012; Brush et al., 2004); the key protein is phosphatase 1 and its inhibitors. We started using the chemical phosphatases inhibitor Calyculin A (CA). The effects of the treatment was examined in SET2 cell line pre-treated for 2 hours with 10 nM of CA before the addiction of 5 µM of BKM120 for 24 hours. Calyculin A alone prompted a marked increase in phospho-S193 and S731 of STAT5b (2.1±0.4 and 1.3±0.2 fold increase, respectively and compared with untreated cells) and also abolished drug-induced dephosphorylation of these serine residues when BKM120 was added. It was notable that CA treatment did not affect at all the levels of phosphor-Y694 (**Figure 12A**).

Then we assessed the roles of PP1 and PP2A in drugs-mediated STAT5 dephosphorylation. For this we used specific siRNAs to silence either PP1 and PP2A in SET2 cells before the treatment with of 5 µM of BKM120. As shown in the **Figure 12B** only the down-regulation of PP2A was effective in abrogating drug-induced phospho-S193 and S731 STAT5b dephosphorylation.

Therefore, further information on mechanisms responsible for BKM120 mediated PP2A activation was provided by monitoring its main inhibitors, specifically the cancerous inhibitor of PP2A (CIP2A) and I2PP2A (also named SET) (Ciccone et al., 2015). We treated SET2 cells for 24 hours with different PI3K/mTOR inhibitors and with Ruxolitinib, next we measured the mRNA and protein levels of the two inhibitors by qRT-PCR and Western Blotting analysis.

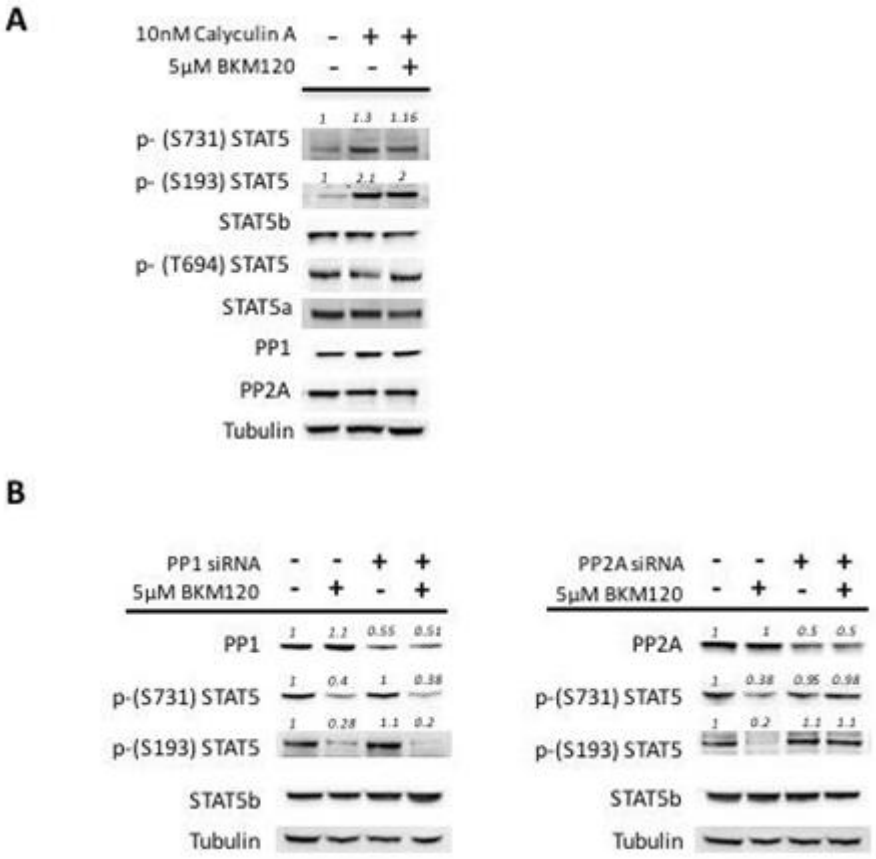

Figure 12: Effects of Calyculin A treatment before the addition of BKM120 **(A)** and PP1 or PP2A silencing by specific siRNA **(B)** on the phosphorylation pattern of STAT5a/b in SET2 cell line. Tubulin was used for loading normalization. The numbers above each lane indicate results of densitometric analysis. Data are from one representative experiment out of five.

As regards I2PP2A we found no change on its expression (data not show). On the contrary, relative mRNA and protein levels of CIP2A had a statistically significant decrease (ranging from -20% to -80% compared to controls) upon treatment with the PI3K/mTOR inhibitors, above all with BKM120 and the dual PI3K/mTOR inhibitor BEZ235, whereas Ruxolitinib was almost ineffective (**Figure 13A**).

BKM120-mediated decrease of CIP2A expression in SET2 cells clearly indicated its involvement in the mechanism of action of the inhibitor and was confirmed by using of specific siRNA. Western blot analysis of CIP2A silencing cells led to dephosphorylation of both serines 731 and 193 of STAT5b, without no effects on tyrosine 694 (**Figure 13B**).

As reported in the literature SNAI1 (Snail) and miR-375 (negatively regulated by SNAI1) are involved in *CIP2A mRNA* stability (Xu et al., 2014; Lin et al., 2014; Jung et al., 2013; Jung et al., 2014). To explore how the reduction of *CIP2A* levels determined by BKM120-treatment involved miR-375 we treated the *JAK2*^{V617F} mutated HEL and SET2

cell lines with the pan-PI3K inhibitor and with Ruxolitinib. We found that only BKM120 induced a marked upregulation of miR-375 mediated by a concurrent downregulation of SNAI1 (**Figure 13C**). Therefore, to investigate the role of CIP2A in primary *JAK2*^{V617F} mutated cells, in more detail, we assessed by qRT-PCR its *mRNA* levels in granulocytes isolated from the peripheral blood of MPN patients (3 PV and 9 MF) and healthy donors as controls (*n*=15). As reported in **Figure 13D** *CIP2A mRNA* resulted 3.28-fold higher in patients' granulocytes compared to healthy controls ($p<0.05$), further supporting abnormally increased CIP2A levels as a mechanism for reduced PP2A activity in patients' JAK2^{V617F} mutated cells. This has also been confirmed by the analysis of *CIP2A mRNA* levels in granulocytes from 14 patients with myelofibrosis who had been enrolled in a phase II clinical trial with the mTOR1 inhibitor RAD001 (Everolimus) (Guglielmelli et al., 2011). The *CIP2A mRNA* levels were quantified by qRT-PCR in samples collected after 3 months of treatment and, after being normalized to the pre-treatment value, were correlated with clinical outcome. Interestingly, we observed that all 7 patients who had a clinical response to treatment (defined by reduction of splenomegaly and symptomatic improvement) showed overt down-regulation of *CIP2A mRNA* levels in the range from -40% to -99.6% the baseline level, while conversely all the 7 patients who did not benefit from treatment (non responders) showed no changes or even an increase of *CIP2A mRNA* levels from baseline (**Figure 13E**).

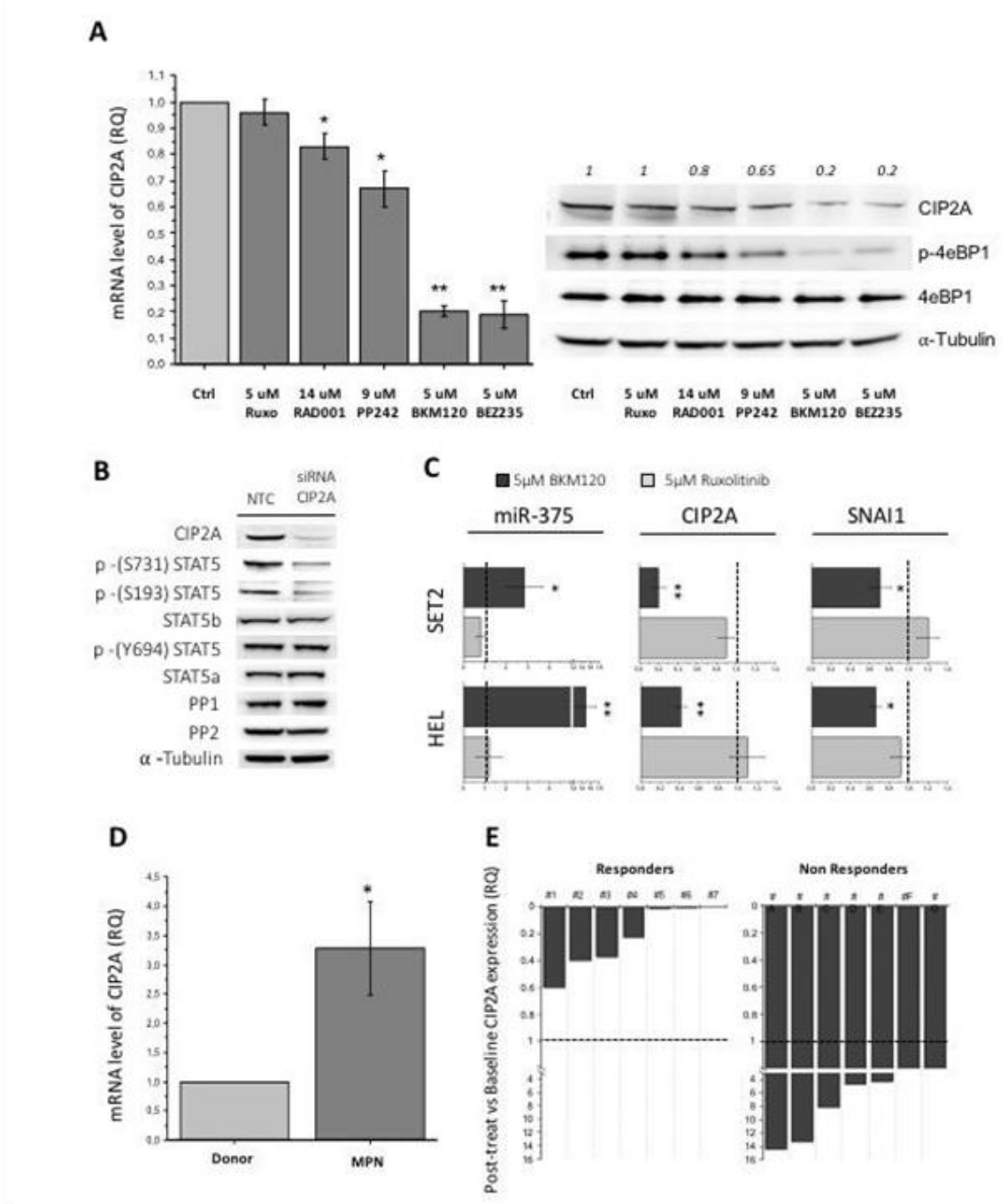

Figure 13: Expression of CIP2A affects the phosphorylation pattern of STAT5 serine residues. **(A)** Effects of PI3K/mTOR inhibitors treatment of SET2 cells in *CIP2A mRNA* levels, assessed by qRT-PCR (on the left) and western blotting (on the right) analysis. **(B)** Effects on the phosphorylation status of STAT5 S731, S193 and Y694CIP2A after CIP2A silencing by specific siRNA. **(C)** Levels of *miR- 375*, *CIP2A* and *SNAI1 mRNAs* in SET2 and HEL cells treated with BKM120 or Ruxolitinib. **(D)** *CIP2A mRNA* levels in granulocytes of 12 *JAK2*^{V617F} mutated MPN patients and 15 healthy controls. **(E)** Correlation of changes of *CIP2A mRNA* levels with clinical response to treatment in 14 patients with myelofibrosis who had received RAD001 for three months. All P values were determined by unpaired two-tailed Student's T test (*p<0.05, **p<0.01).

Therefore, we wanted to explore the hypothesis that pronounced dephosphorylation of STAT5, involving both serines and tyrosines residues, might result in more effective control of *JAK2*^{V617F} mutated cells. In this project we used as relevant drugs the pan-PI3K inhibitor BKM120, that is being tested in a clinical trial in association with Ruxolitinib (Durrant et al., 2015) and the mTORC1 complex inhibitor RAD001 (Everolimus), that was already employed as single agent in patients with myelofibrosis (Guglielmelli et al., 2011), and has been previously characterized in in-vitro models (Bogani et al., 2013).

STUDY OF THE EFFECTS OF THE PAN-PI3K INHIBITOR BKM120 ON CELL PROLIFERATION, CELL CYCLE AND APOPTOSIS.

In a preliminary set of experiments, we evaluated the efficacy of pan-PI3K inhibitor, BKM120, as single agent in *in-vitro* models of *JAK2*^{V617F} mutated cells, by measuring changes in cell proliferation, cell cycle and apoptosis. The human cell lines employed were the *JAK2*^{V617F} mutated HEL and SET2 and the BCR/ABL positive cell line K562, used as a control. The effects of inhibitors were also evaluated in Ba/F3 murine cell lines, stably transfected with a construct containing the *JAK2*^{V617F} (Ba/F3 V617F) gene or the *JAK2*^{WT} (Ba/F3 WT) gene: *JAK2*^{V617F} gene transfection in Ba/F3 determines the independence of IL-3 for survival and growth, unlike the wild-type lines, which requires this cytokine for supporting cell growth. These effects were also analyzed in the Ba/F3-dependent EPO (Ba/F3 EPOR) wild-type and its counterpart cytokine-independent *JAK2*^{V617F}.

As shown in the **Figure 14**, we found that BKM120 dose-dependently inhibited the proliferation of Ba/F3 VF and Ba/F3-EPOR VF cells at concentrations significantly lower than the WT counterparts: the IC_{50} were 364±200 nM and 1.100±207 for Ba/F3 VF and Ba/F3 EPOR-VF versus 5.300±300 nM and 3.122±100 nM for the Ba/F3 WT and Ba/F3-EPOR WT ($p<0.05$). Also the viability of human HEL and SET2 cells was affected by BKM120 with IC_{50} values of 2000±500 nM and 1000±300 nM, respectively. Conversely, in the *JAK2*^{WT} K562 line an IC_{50} value of 4500±800 nM was found ($p<0.05$).

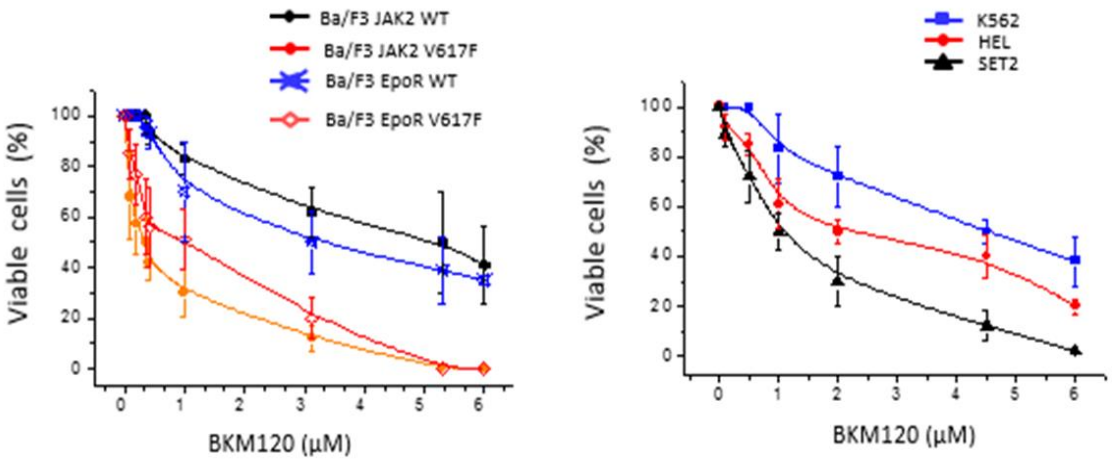

Figure 14: Effect of the BKM120 as single agent in the proliferation of *JAK2* WT and V617F mutated cell lines. Data were expressed as the Means ± SD (*n* = at least three experiment).

We then evaluated the effects of increasing drug amounts on the rate of cell division through the analysis of changes in cell cycle of *JAK2*^{V617F} mutated Ba/F3-EPOR cells and SET2 cells. A significant increase of G2/M phase and concomitant decrease of S-phase in murine and human mutated Ba/F3-EPOR and SET2 cell lines was documented ($p<0.01$ versus control cells) (**Figure 15**).

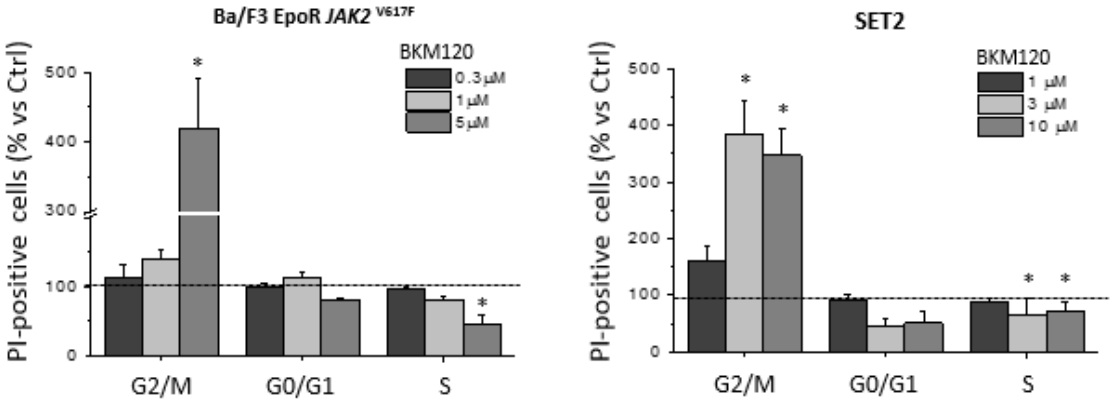

Figure 15: Effects of the BKM120 on the cell cycle distribution of *JAK2*^{V617F} mutated Ba/F3-EPOR and SET2 cells after 18 hours incubation with varying drug amounts. Data were expressed as the Means ± SD (*n* = at least three experiment).

We also found that BKM120 induced apoptosis in the Ba/F3-EPOR VF and SET2 cell line, although higher drug concentrations were required than for proliferation arrest (IC_{50} 1,8 µM and 10 µM respectively for Ba/F3-EPOR VF and SET2 cells)(**Figure 16**).

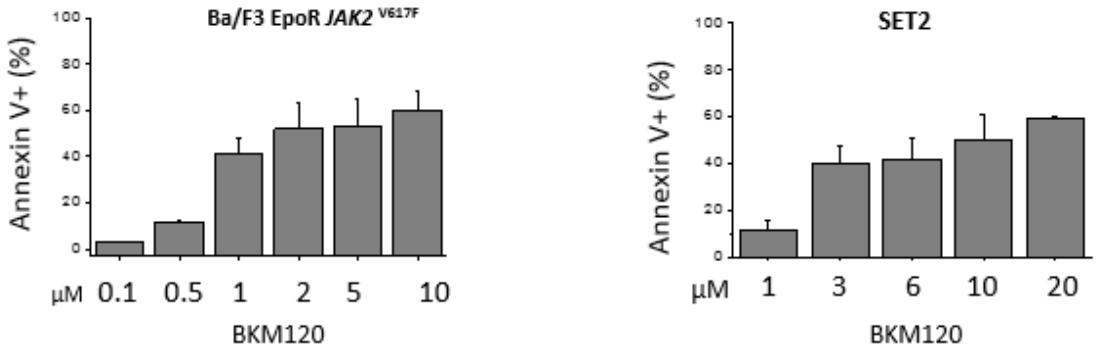

Figure 16: *JAK2^{V617F}* mutated Ba/F3 EPOR and SET2 Annexin V-positive cells after 48 hours incubation with varying drug amounts. Value were expressed as percent of Annexin V-positive cells (Means ± SD of at least three experiments, in duplicate) after substracting apoptotic cells measured in vehicle-only cultures.

STUDY OF THE EFFECTS OF BKM120 ON THE CLONOGENIC POTENTIAL OF THE HEMATOPOIETIC PROGENITOR CELLS OF MPN PATIENTS.

The efficacy of BKM120 as a single agent against primary MPN cells was evaluated by clonogenic assay. For this purpose were used mononuclear cells and CD34+ cells isolated from patients affected by PMF (*n*=7) and PV (*n*=10) all with *JAK2^{V617F}* mutation and healthy controls (*n*=7). Mononuclear cells were isolated and plated in methylcellulose in the presence of different concentrations of the drug and of cytokines favoring the growth of erythroid colonies (BFU-E) and granulocyte-macrophage (CFU-GM) colonies. In addition, CD34+ cells from patients with PV, PMF or from healthy controls were purified and plated in a collagen medium for the growth of megakaryocyte colonies (CFU-Mk). The IC_{50} values found were, in case of PV and PMF, respectively: 77±50 nM and 312±180 nM for CFU-GM (both $p<0.05$ vs controls), 187±76 nM and 148±63 nM (both $p<0.05$) for BFU-E and 14±1 nM and 18±8 (both $p<0.01$) for CFU-Mk, compared with 760±200 nM, 900±370 nM and >100 nM, respectively, in control subjects (**Table 8**).

	BFU-E IC_{50} (nM)	CFU-GM IC_{50} (nM)	CFU-Mk IC_{50} (nM)
Ctrl	900±370	760±200	>100
PV	187±76*	77±50*	14±1**
MF	148±63*	312±180**	18±8**

Table 8: Effects of BKM120 on the colony-forming activity of progenitor cells. All P value were determined by unpaired two-tailed Student's T test (*0.01< p < 0.05; **0.001< p < 0.01).

As regards the growth of EPO-independent erythroid colonies (EEC), $2.5x10^5$ mononuclear cells/mL derived from peripheral blood of patients with PV (*n*=5) were plated in a methylcellulose semisolid medium in the absence of EPO. The EEC developed in the presence of increasing concentrations of the various drugs were enumerated after 10-12 days and expressed as a percentage of the clonogenic growth compared to control plates containing DMSO only (**Figure 17**). Endogenous erythroid colonies were dose-dependently inhibited by BKM120 with an IC_{50} value of 9±4 nM.

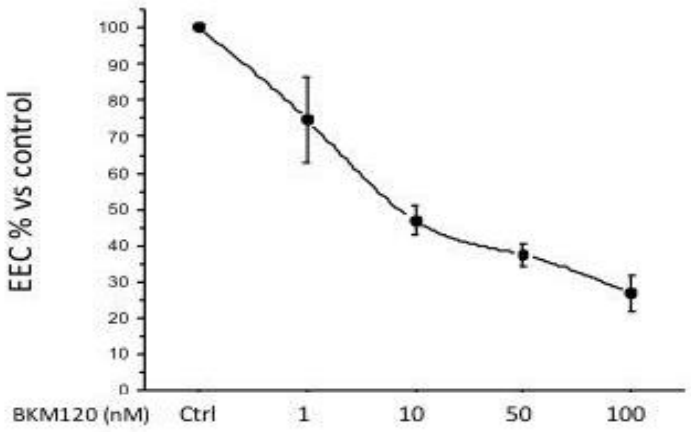

Figure 17: Effects of BKM120 on the EPO-indipendent endogenous erythroid (EEC) colonies growth.

STUDY OF THE EFFECTS OF BKM120 ON SURVIVAL OF MICE INJECTED WITH Ba/F3 *JAK2^{V617F}*-LUC+ CELLS.

To corroborate *in-vivo* the findings of efficacy shown *in-vitro* we first used the *JAK2^{V617F}*-Ba/F3-EPOR Luc+ mouse model. This model allowed to evaluate the effects of the pan-PI3K inhibitor and to identify an optimal dose of treatment that maximizes effects while maintaining the drug-intrinsic toxicity below the critical threshold. The assay relies upon the fast, uncontrolled proliferation of Ba/F3-EPOR VF cells, stably transfected with luciferase, after systemic injection in immunodeficient mice; the progression of disease is monitored by bioluminescence at predefined time points.

Mice were randomized to treatment groups 6 days after injection with $3x10^6$ Ba/F3-EPOR VF Luc+ cells based on the bioluminescence signals; this point constitutes the baseline lecture before starting mice treatment. They received two different doses of BKM120, 45mpk and 60mpk, and were followed by bioluminescence analysis at weekly intervals. In vehicle mice Ba/F3 *JAK2^{V617F}*–Luc+ cells colonize bone marrow and spleen first, followed by abdomen and the whole body, as shown by in-vivo imaging pictures took at day 14 and day 21 after injection. Images revealed a lesser degree of cell proliferation and dissemination in BKM120 treated mice compared to controls (**Figure 18A**). The mean bioluminescence signal of different groups was quantified by counts per minute and highlights that mice receiving 60mpk BKM120 showed a signal significantly lower than 45mpk BKM120 and placebo groups ($p<0.05$), reflecting effective inhibition of Ba/F3 *JAK2^{V617F}*-Luc+ cells proliferation (**Figure 18B**).

Kaplan-Meier analysis showed that survival of mice treated with 60 mpk and 45 mpk was significantly longer (mean lifespan post-treatment of 20.8±4.9 and 20.3±7.8 days respectively) than mice receiving vehicle (mean lifespan of 14.2±6.6) accounting for a 31.1% and 28.8% increase of lifespan compared to untreated mice ($p<0.05$) (**Figure 19C**).

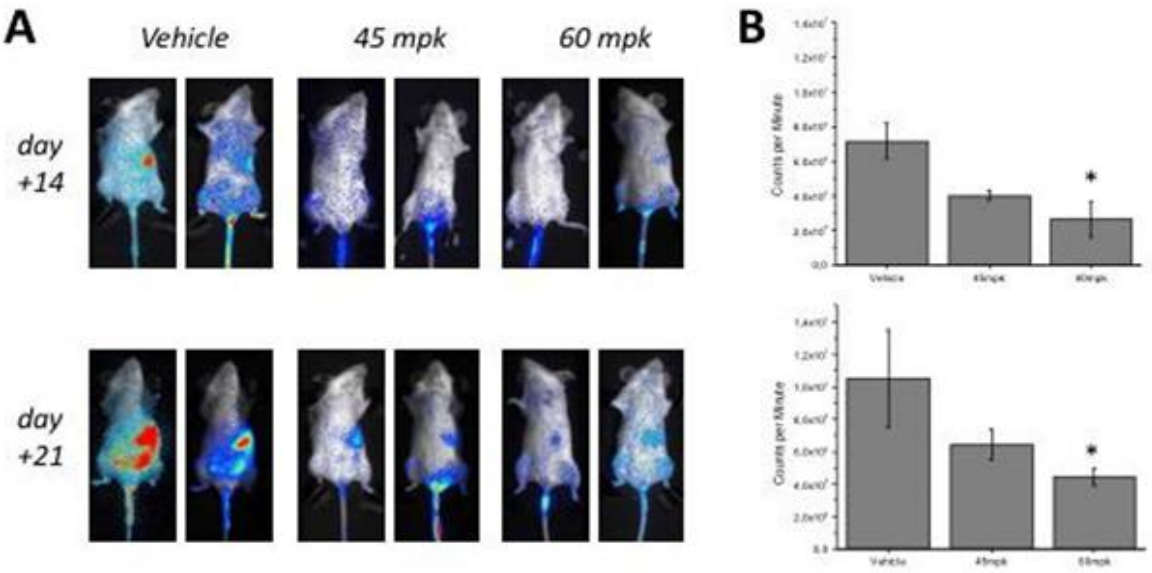

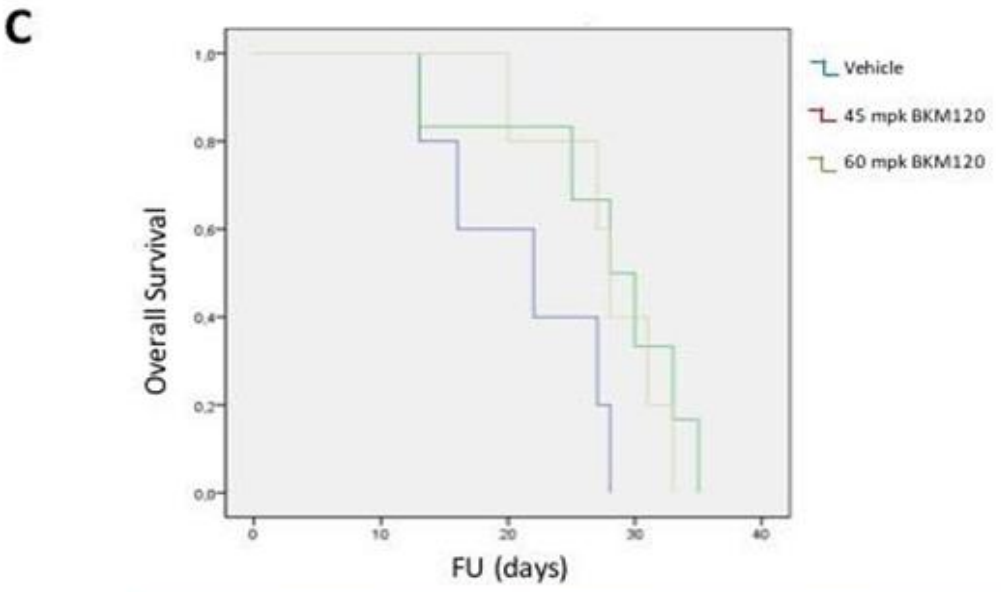

Treatment Cohort	Mean Lifespan post-Injection	Mean Lifespan post-Treatment	Mean Lifespan increment vs Veh
BKM120 60 mpk	27.8±4.9	20.8±4.9	+ 31.1 %
BKM120 45 mpk	27.3±7.8	20.3±7.8	+ 28.8 %
Vehicle	21.2±6.6	14.2±6.6	\

Figure 18: Treatment with BKM120 reduces dissemination of leukemic cells and improves survival in a *JAK2*^{V617F}-driven mouse model. (**A**) SCID mice injected with 3x10^{6} *JAK2*^{V617F} Ba/F3-EPOR Luc+ cells were randomized into three treatment groups (vehicle, BKM120 45mpk and 60mpk). (**B**) Bioluminescence activity expressed as counts per minute (cpm; Mean ± SD of three experiments) was measured on day 7 of treatment. (**C**) Kaplan-Meier survival curves in mice receiving 60mpk and 45mpk of BKM120; the table reports the individual values and the percentage increment of survival compared to control group ($p<0.05$).

STUDY OF THE EFFECTS OF COMBINING BKM120, RAD001 AND RUXOLITINIB IN DIFFERENT MPN MODELS.

Based on these results demonstrate the efficacy of BKM120 as single agent in different MPN models, we next evaluated the effects of concurrent inhibition of the JAK2 and PI3K pathway by combination of Ruxolitinib with BKM120 and RAD001.

Therefore, we evaluated the effects of triple drug combination on the viability of Ba/F3 VF and SET2 cell lines; to determine potential synergy, we calculated the combination index (CI) according to Chou and Talalay (Chou T-C et al, 2010). As shown in the **Table 8**, the IC_{50} values were significantly lower when we used the triple combination compared to single treatment and the calculated CI indicated strong synergistic activity in both cell lines ($p<0.05$).

Ba/F3 *JAK2*V617F

Single Drug IC_{50} (nM)			Combination IC_{50} (nM)			C.I.
BKM120 1100±207	RAD001 651±50	Ruxo 200±20	BKM120 299±13	RAD001 193±7	Ruxo 96±10	0.25

SET2

Single Drug IC_{50} (nM)			Combination IC_{50} (nM)			C.I.
BKM120 1300±160	RAD001 6500±110	Ruxo 1000±89	BKM120 1000±45	RAD001 5000±160	Ruxo 500±71	0.3

Table 8: Ba/F3 *JAK2*^{V617F} and SET2 cells treated with BKM120, RAD001 and Ruxolitinib as single drugs and in combination. The IC_{50} value of each condition was calculated. The Combination Index (CI) lower than 1, according to Chou and Talalay, indicates a high synergism of the triple drug combination.

We next analysed by western blot the effects on the phosphorylation of tyrosine and serine residues of STAT5 a and b as well as of 4eBP1 and the levels of CIP2A in SET2 cells treated with a suboptimal amounts of BKM120, RAD001 and Ruxolitinib as single agent or in combination. We found that drug combination produced greater inhibition of phosphorylated S731, S193 and Y694 of STAT5 compared to single treatment (**Figure 19A**).

This combination was then evaluated in clonogenic assay by plating bone marrow mononuclear cells isolated from six *JAK2*^{V617F} patients in semisolid medium in presence of single drugs or two different doses of the combination. The combination of Ruxolitinib 50 nM, BKM120 150 nM and RAD001 150 nM resulted in synergistic inhibition of colony formation compared to control cultures (62.6%) as well as to single drugs (29.3%, 33% and 27.3% respectively in the presence of BKM120, RAD001 and Ruxolitinib) (**Figure 19B**).

To strengthen data supporting a relatively greater selectivity of the triple drugs combination towards *JAK2*^{V617F} mutated cells, we next performed, clonogenic assay using bone marrow progenitors from *JAK2*^{V617F} KI mice and the corresponding *JAK2*^{WT} genotype. The two sources of bone marrow cells were mixed 1:1 ratio and plated in semisolid medium in the presence of BKM120, RAD001 and Ruxolitinib, 30 nM each. Individual colonies harvested at day 4 of culture were genotyped by allele specific PCR and we found that triple treatment reduced the proportion of *JAK2*^{V617F}-positive colonies from 50% at baseline to 18% on day 4 ($p<0.05$) (**Figure 19C**).

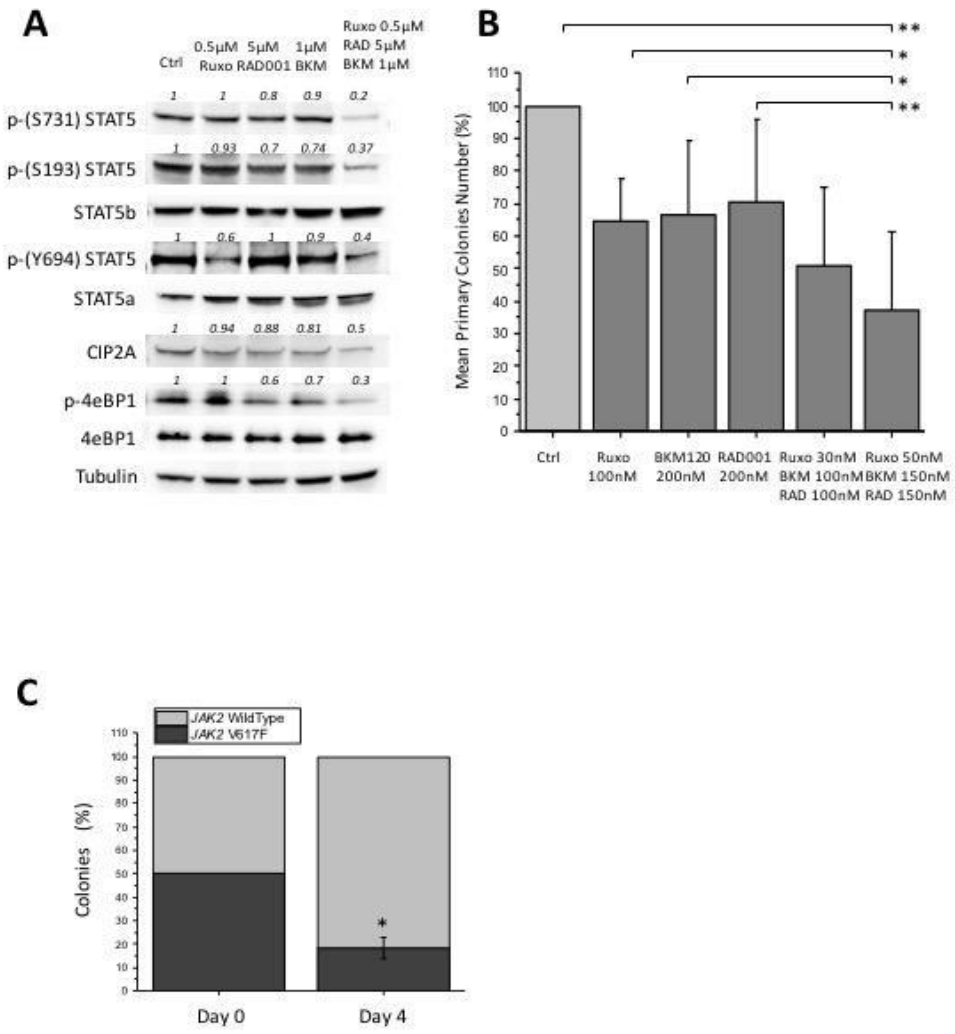

Figure 19: Effects of triple drugs combination in different MPN models. (**A**) Effects on the phosphorylation of S731, S193 and Y694 of STAT5 and of 4eBP1, and the levels of CIP2A, assessed by western blotting in SET2 cells. (**B**) Effects on colony formation of bone marrow mononuclear cells from *JAK2*^{V617F} patients plated in presence of single agents or in combinations. It was expressed as percent of the number of colonies enumerated in control dishes (no drug). (**C**) Effects on clonogenic assay with bone marrow cells of *JAK2*^{V617F} KI and WT mice mixed in a 1:1 ratio in the presence of BKM120 plus RAD001 and Ruxolitinib. All *P values* were determined by unpaired two-tailed Student's T test (*p<0.05, ** p<0.01).

STUDY OF THE EFFECTS OF THE COMBINATION TREATMENT WITH BKM120, RAD001 AND RUXOLITINIB IN *JAK2^{V617F}* CONDITIONAL KI MICE.

To evaluate *in-vivo* the effects of the triple drugs combination we used *JAK2^{V617F}* conditional KI mice. These mice develop a progressive myeloproliferative disease starting from the first months after birth, characterized by marked erythrocytosis with thrombocytosis and leukocytosis, and splenomegaly, that mimics PV in early phase and evolves into myelofibrosis at later stages (Marty et al., 2010). KI mice received daily, for 16 days of treatment, 3 mg/kg body weight (mpk) RAD001, 60mpk Ruxolitinib or 60mpk BKM120, as single drugs or in triple combination at half of the dose. Control mice received vehicle only with the same schedule as treated ones. The treatment was well tolerated and the body weight loss was <10% of baseline in all treatment groups. We documented a prompt, dramatic reduction of spleen weight (**Figure 20A**) in mice receiving the three drugs concurrently, compared to the groups that were treated with the single agents. The mean spleen index in mice of the combination group was 1.1 compared with 3.6 in control vehicle-treated mice, 2, 2.3 and 3.4 respectively for BKM120, Ruxolitinib and RAD001 ($p<0.01$). Histology showed a marked reduction of megakaryocytes and myeloid cells infiltrating the spleen in mice treated with the drug combination (**Figure 20B**). The mean reticulocyte count decreased from 48, 50, 29 and 33 per HPF in the vehicle, RAD001, Ruxolitinib and BKM120 group, respectively, to 11/HPF in the combination group ($p<0.01$; **Figure 20C**). Although not statistically significant, there was a trend towards reduced leucocyte and platelet counts in treated mice compared with vehicle group (**Figure 20D**).

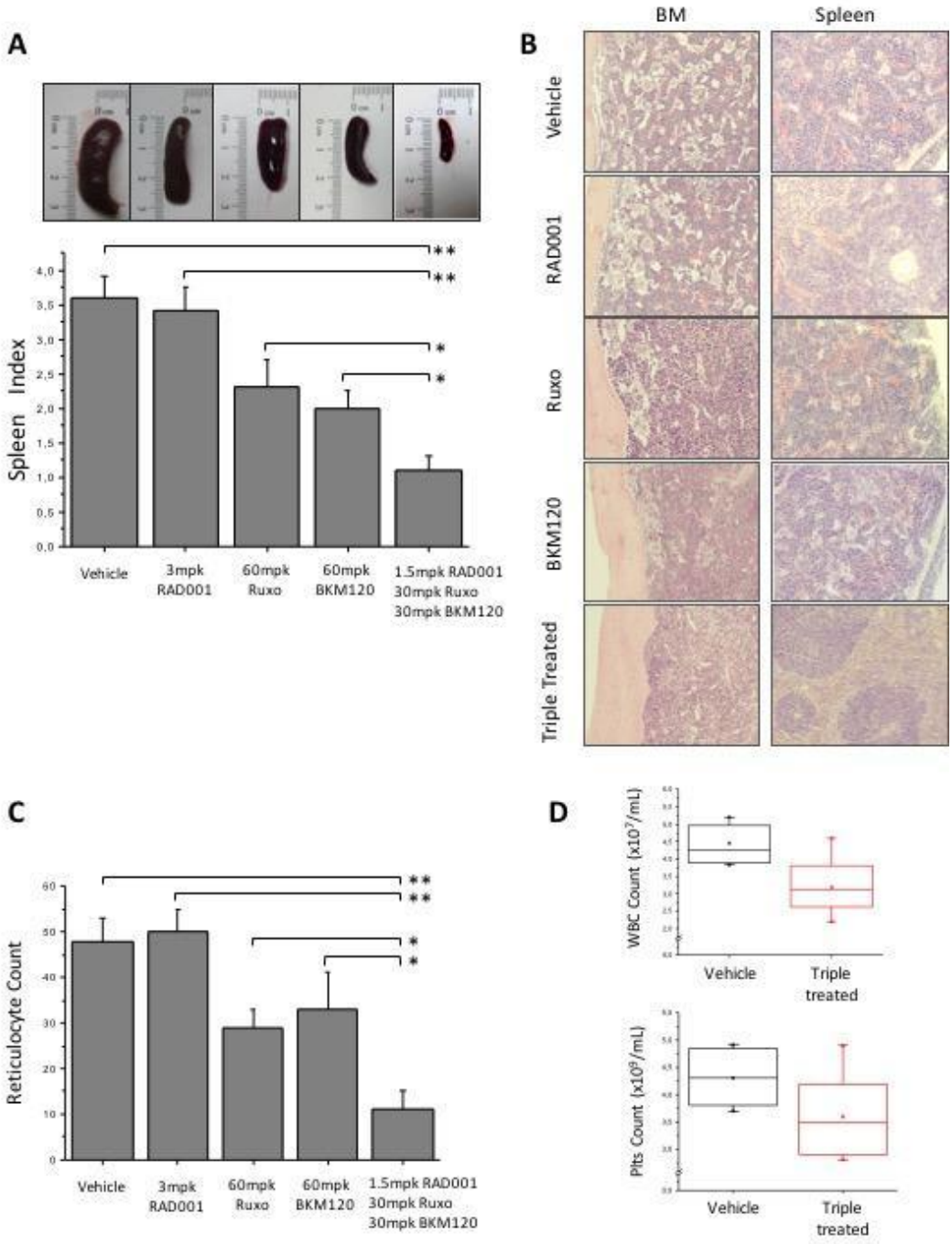

Figure 20: Effects of BKM120, RAD001 and Ruxolitinib, single or in triple combination, in *JAK2*^{V617F} knock-in mice. 10 mice for each treatment cohort were analyzed. **(A)** Effects of triple treatment on spleen size (upper panel) and spleen index (calculated as ratio of spleen and body weight x100) compared to other treatment groups and controls. **(B)** Hystopathology of the spleen and bone marrow in control and treated mice. Picture were taken with a LEICA DM LS2 microscope using a N-Plan × 20 objective. **(C)** The number of reticulocytes per 10 high power fields in peripheral blood smears. **(D)** The number of white blood cells and platelets in the peripheral blood of mice treated with drugs combination; values in mice receiving each single drug were comparable to controls and are not shown. All P values were determined by unpaired two-tailed Student's T test (* $0.01<p<0.05$, ** $0.001<p<0.01$).

DISCUSSION

Dysregulation of the JAK2/STAT pathway represents a central mechanism in the pathogenesis of myeloproliferative neoplasms, through either direct, as in patients harboring mutations of *JAK2*, or indirect, as in the case of *MPL* or *CALR* mutations, involvement of JAK2, that in turn leads to sustained phosphorylation of STAT5.

Inhibition of the constitutively activated JAK/STAT pathway in $JAK2^{V617F}$ mutated cells by the JAK1/JAK2 inhibitor Ruxolitinib resulted in clinical benefits in patients with myeloproliferative neoplasms (Harrison et al., 2016; Vannucchi et al., 2015). Even if it was able to produce improvements in splenomegaly and constitutional symptoms in patients with myelofibrosis, it is not enough by itself to contrast STAT5 hyperactivation and to modify the course of disease. The fact that Ruxolitinib is not $JAK2^{V617F}$ specific and inhibits $JAK2^{WT}$ as well might contribute to its limited activity.

As published before, others cellular pathways concur to the dysregulated signaling observed in MPN models and their inhibition might be considered as a treatment strategy to enhance JAK/STAT targeting (Levine RL et al., 2005; Kralovics R et al., 2005; Baxter EJ et al., 2005; Bartalucci et al., 2013).

In this project we focused on the importance of a maximal inhibition of STAT5 to dampen constitutive MPN signaling by the concomitant inhibition of the dysregulated PI3K/Akt/mTOR pathway. Together with reported clinical benefits, experimental evidences demonstrated the ability of PI3K/mTOR inhibitors to de-phosphorylate serine residues of STAT5 while Ruxolitinib mainly exerts de-phosphorylation of Tyr-694, both important for STAT5 activation.

Data reported in this study demonstrate that the deregulated serine phosphorylation of STAT5b may be due to the defective activity of the protein phosphatase 2A as the consequence of increased inhibition exerted by the allosteric inhibitor CIP2A; furthermore, it is shown here for the first time, to the best of our knowledge, that CIP2A is over-expressed in MPN patients compared to healthy controls.

The use of different PI3K-pathway inhibitors including BKM120 leads to a various degree of CIP2A downregulation (not observed after Ruxolitinib treatment) in

JAK2^{V617F}-mutated SET2 cell line with consequent reduced STAT5 activation and was correlated with a better response to treatment in MPN patients. Based on these observations, we hypothesize that the reduced expression of CIP2A by PI3K inhibitor, enforces PP2A action in de-phosphorylating its target kinases such as STAT5 and results in a reduced activation of the transcription factor. Taking together, these data indicate that the inhibition of key kinases of PI3K/mTOR pathway resulting in the downregulation of CIP2A is under the control of a microcircuit that includes Hif1α and its target SNAI1 (Karar et al., 2012; Hirasawa et al., 2013; Xu et al., 2015), with consequent enhanced expression of miR-375 and transcriptional downregulation of its target CIP2A.

As showed by the combination studies in preclinical models of MPN, the concurrent inhibition of JAK2 and PI3K/mTOR pathways leads to a more complete inhibition of STAT5 phosphorylation, preventing *JAK2*^{V617F} cells proliferation rate *in-vitro* as well as myeloproliferation in *JAK2*^{V617F} KI mouse (assessed by improvement of splenomegaly, blood cells count and a reduced number of circulating reticulocyte). In particular, the complete inhibition of PI3K/mTOR pathway is achieved at best by the combination of BKM120 and RAD001 that synergize with Ruxolitinib improving efficacy, and ameliorationg toxicity (with the reduction of administered doses compared to single drugs exposure).

This project focused on the STAT5 hyperactivation and the mechanism beyond its inhibition strategy based on a combined and synergic treatment capable to simultaneously inhibit JAK2 and PI3K/mTOR crosstalk as summarized in **Figure 21**, providing a rationale for future applications in the management of MPN.

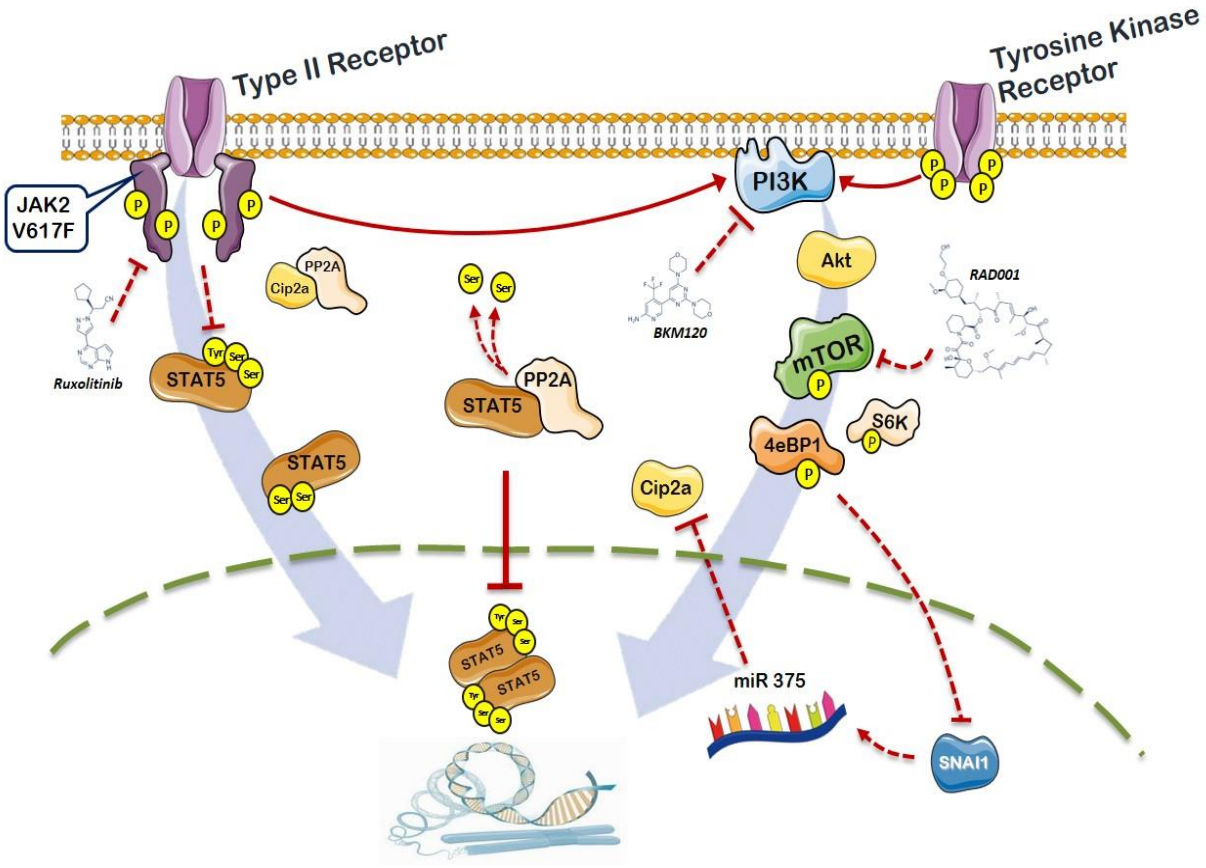

Figure 21: Representation of the JAK2/PI3K crosstalk and PP2A/CIP2A axis. *JAK2^{V617F}* mutation causes a constitutive phosphorylation of the transcription factor STAT5. Activated STAT5 proteins dimerize and translocate into the nucleus to act as transcription factors of target genes. As known, Ruxolitinib causes a de-phosphorylation of tyrosine-694 on STAT5a and we demonstrated that PI3K/mTOR inhibitors induce a de-phosphorylation of activating serine residues of STAT5b. Cells with the *JAK2^{V617F}* mutation express abnormally increased levels of CIP2A (PP2A inhibitor), that resulted down-regulated by PI3K/mTOR inhibitors via a microcircuit that includes SNAI1 and miR-375. The Jak2/PI3K-pathway cross-talk described, offers a better view on the MPN biological landscape and the opportunity to target concomitantly different key kinases to achieve a more effective inhibition of activated STAT5, thereby providing a rationale for clinical trials.

Characterization of CALR mutations in the Myeloproliferative Neoplasms: new tools to understand mechanisms and develop diagnostic and therapeutic strategies

BACKGROUND

CALRETICULIN IN MPN: WHAT WE KNOW.

In the first part of this thesis I already introduced briefly the most recently described MPN-associated driver mutations in *Calreticulin* (*CALR*) gene.

These mutations were described for the first time in December 2013, by two independent groups, in the majority of *JAK2*- and *MPL*- unmutated ET and PMF patients (50-60% ET and 75% PMF) (Nangalia et al., 2013; Klampfl et al., 2013).

The *CALR* gene is located in the short arm of chromosome 19 (19p13.2). It contains 9 exons and spans 4.2 kb. So far, more than 50 different types of *CALR* mutations have been identified, all of which occur in exon 9. With the exception of a few non-recurrent point mutations (Wu et al., 2014), almost all of these mutations are small insertions and delection. The commonest mutations accounting for 85% of mutated cases are a 52 base-pair (bp) deletion (CALRdel52/Type 1; c.1092_1143del; L367fs*46; 45-53% of all cases) or a 5 base pairs (bp) insertion (CALRins5/Type 2; c.1154_1155insTTGTC; K385fs*47; 32-41% of all cases) (**Figure 22**). Interestingly, the frequency of type 1 mutation is significantly higher in PMF than in ET, suggesting a specific role of this mutations in myelofibrotic transformation (Rumi et al., 2014; Cabagnols et al., 2015). Most of the mutations are heterozygous mutation. Homozygous *CALR* mutations are very rare and they are most 5-bp insertions (Nangalia et al., 2013; Klampfl et al., 2013). It was found initially that *CALR* and *JAK2* mutations were mutually exclusive. However, *CALR* and *JAK2* co-mutations have been reported recently in a few MPN cases across different ethnic groups, although the frequency of co-mutation is usually below 1% (Park et al., 2015; Tefferi et al., 2014; Lundberg et al., 2014; McGaffin et al., 2014).

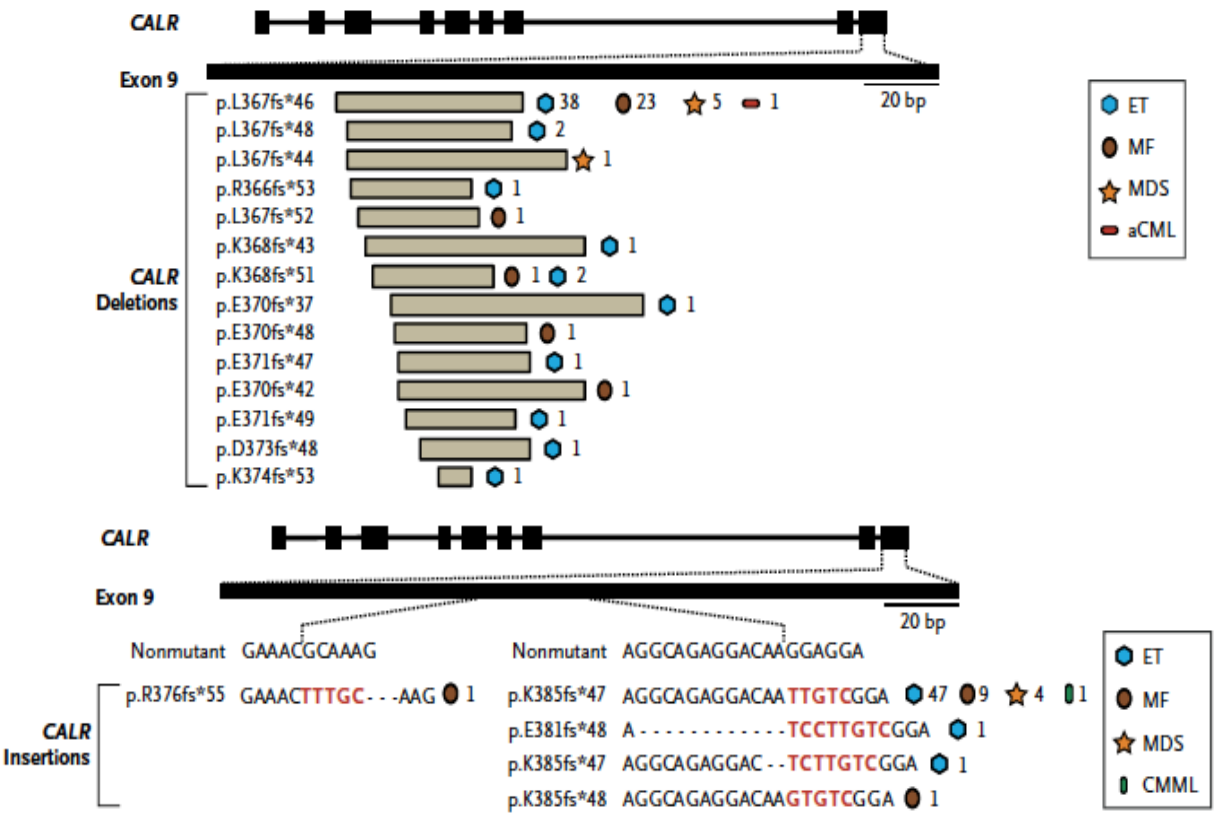

Figure 22: *CALR* Mutations in Myeloproliferative Neoplasms. Genomic location of *CALR* Delections (at the top) and *CALR* insertions (at the bottom) (Nangalia et al., 2013).

Remarkably, all mutations are exclusively +2/-1 base-pair frameshifts that cause a +1 frameshift in the reading frame, and thus generate a novel amino acid sequence (characterized by the acquisition of a minimal 36 amino acid stretch in place of 27 amino acids that are lost from the normal sequence) common to all mutant CALR proteins on their C-terminal end (**Figure 23**). As a result, mutant CALR proteins contains a number of positively charged amino acids; such variability may be associated with qualitatively different phenotypes of *CALR*-mutated MPNs.

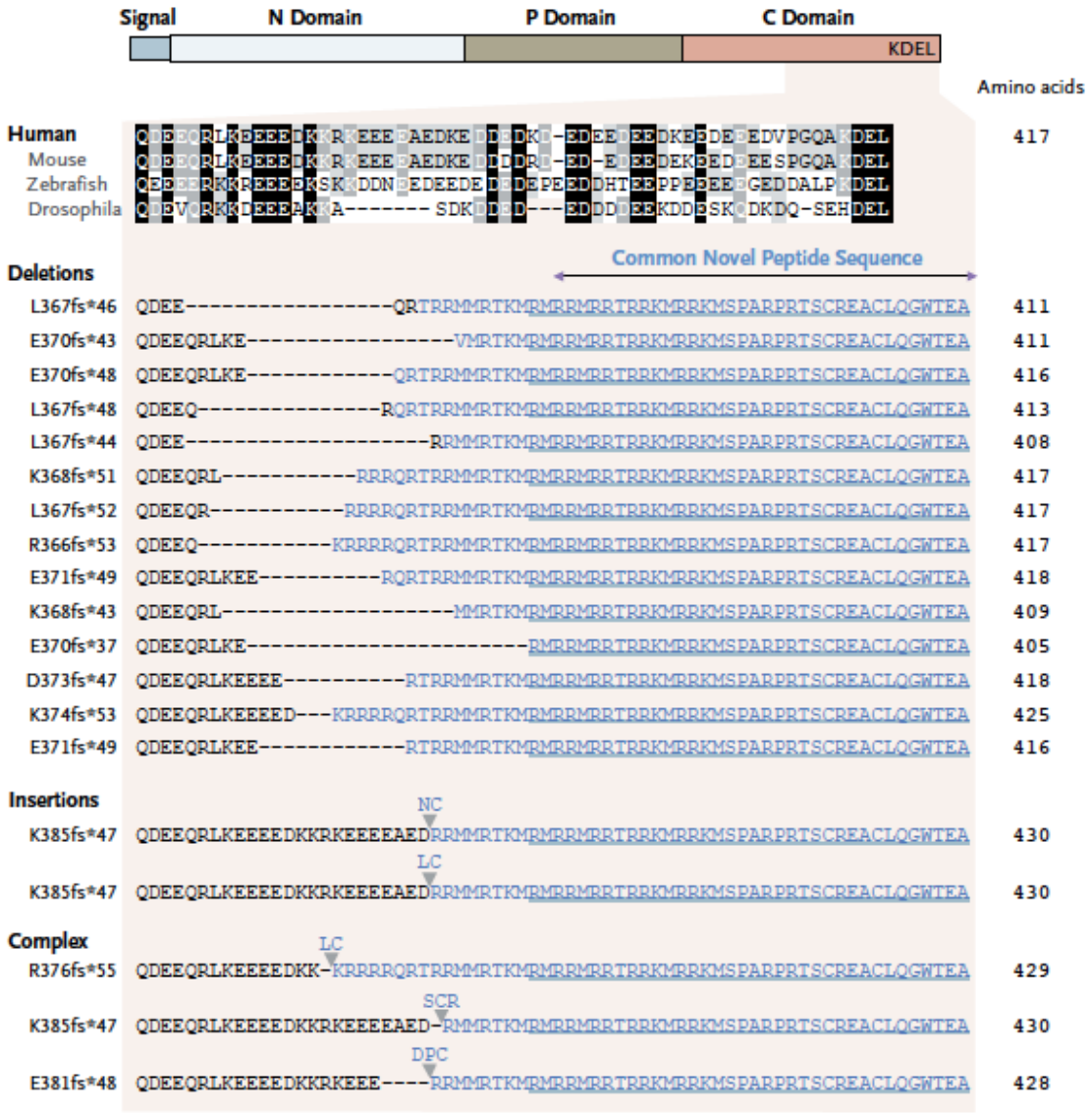

Figure 23: Altered protein reading frame with novel C-terminal associated with *CALR* mutations. Functional domains of CALR protein and the range of frameshift insertion and deletion mutations in *CALR* exon 9 are shown, all of which result in a common +1 base-pair-altered reading frame and predict a novel C-terminal peptide sequence lacking the KDEL motif (Nangalia et al., 2013).

CALR is a developmentally highly conserved luminal ER (endoplasmic reticulum) chaperone protein that ensures the proper folding of newly synthetized glycoproteins; it has also been implicated in several other roles both within and outside of the ER, including calcium homeostasis, immunogenic cell death, proliferation, phagocytosis, apoptosis as well as the assembly and cell surface expression of major histocompatibility complex (MHC) class I molecules (Michalak et al., 2009; Chao et al., 2012). Given its many functions, it is not surprising that homozygous *CALR* knock-out mutation is embryonic lethal in mice. The CALR is a 46 kDa protein that consists of multiple domains. The first 17 amino acids comprise a signal peptide sequence that is cleaved upon entering the ER (Denning et al., 1997). This sequence is followed by the

amino-terminal domain (N-domain; residues 1-180), which contains amino acids required for carbohydrate binding, zinc binding, and chaperone activity (Kapoor et al., 2003; Guo et al., 2003). Next comes the proline-rich P-domain (residues 181-290), which binds to calcium and ERp57 that cooperates with CALR for protein folding (Martin et al., 2006). The last C-domain (residues 291-400) shows a capacity for calcium storage and includes an ER retention signal sequence, the KDEL (Nakamura et al., 2001; Araki et al., 2017) (**Figure 24**).

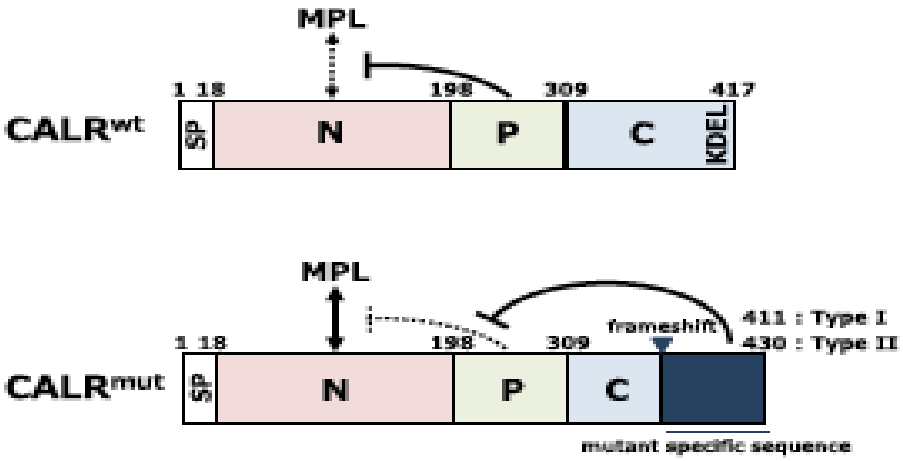

Figure 24: Domain structure of wild-type (WT) and mutant (MUT) CALR. CALR WT consists of a signal peptide (SP), N-domain (N), P-domain (P), and C-domain (C) with the ER-retention signal KDEL. Because of +2/−1 frameshift mutation, all types of CALR MUT lose KDEL sequence and gain a novel positively charged amino acid tail. The mutant-specific C-terminal domain interferes with the P-domain and allows interaction between the N-domain and MPL for activation (see the text as follow). The numbers refer to the positions of amino acid residues in the amino acid sequence.

Mutant calreticulin novel protein C-terminus differs from the wild-type protein in two ways. First, a Golgi-to-ER retention signaling motif (KDEL) responsible for retrieving and retaining chaperone proteins back to the ER is lost in the mutant protein. Preliminary evidence from localization studies of exogenous overexpression of mutant CALR in target cells, as well as localization studies of myeloid cells from CALR mutated patients has shown that mutant CALR largely retains its localization within the ER (Guglielmelli et al., 2014). Second, the largely negatively charged and acidic C-terminus of the wild-type protein is replaced by a basic and positively charged novel peptide sequence, and this has been predicted to alter the calcium-binding capacity of the protein. It is conceivable that loss of homeostatic calcium regulation by mutated calreticulin may contribute to MPN pathogenesis (Shivarov, 2014); the embryonic

lethality of CALR ablation has been attributed to loss of calcium binding activity more than its chaperone function.

CALR mutations have been shown to be acquired at the level of the hematopoietic stem cell (HSC) and clonal characterization of MPN samples has shown that mutated CALR is present in the earliest clone, which is consistent with it being an initiating event in these malignancies. As our group previously reported, mutant CALR is highly expressed in, and largely restricted to, the megakaryocyte lineage in primary patient bone marrow trephine biopsies immunostained with an antibody selective to mutant CALR's novel C-terminus (**Figure 25A**). Interestingly, we also found that wild-type CALR had a megakaryocyte-restricted expression pattern (as shown the immunostaining in **Figure 25B**; confirmed also by the analysis of gene expression profile in purified CD34+ cells, erythroblasts, megakaryocytes and neutrophils – not shown) which may explain why the mutant form is associated with MPNs characterized predominantly by abnormal megakaryopoiesis (Vannucchi et al., 2014).

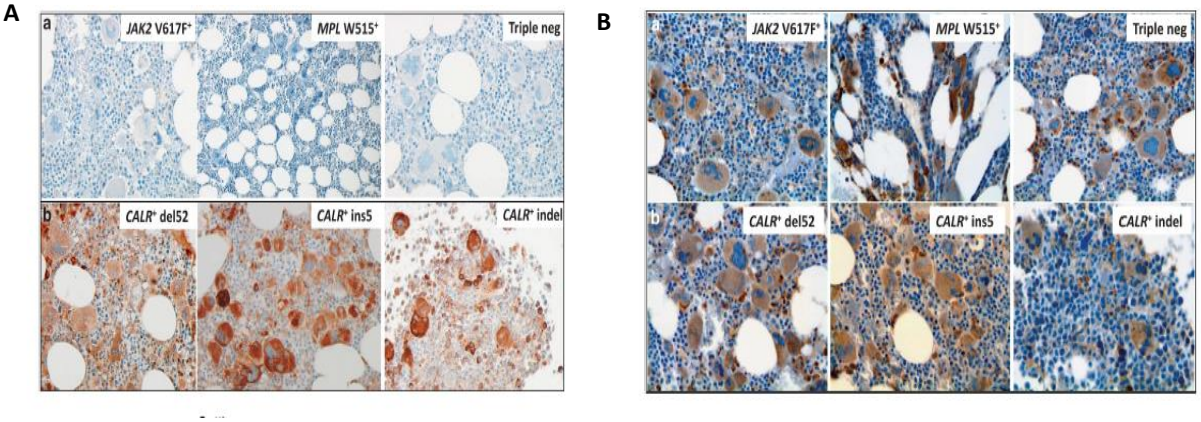

Figure 25: Immunostaining of bone marrow biopsies with: **(A)** the anti-mutated CALR antibody and **(B)** the anti-wild-type calreticulin antibody (that label both CALR wild-type and mutant proteins). Representative sections from *CALR*-unmutated ET/PMF patients (J*AK2V617F* mutated, *MPLW515L* mutated and triple-negative mutation) and from *CALR*-mutated patients (*CALR*del52, *CALR*ins5 and *CALR*indel) are shown in panel **a** and panel **b**, respectively.

As regards the results from the *in-vitro* experiments many groups have tried, in the last few years, to understand the mechanisms underlying the oncogenic properties of CALR mutant.

The initial publication on *CALR* mutations has shown that overexpression of mutated CALR in the IL-3-dependent murine Ba/F3 cell line makes cells independent and hypersensitive to IL-3; such enhanced growth was inhibited by the JAK2 inhibitor SAR302503, indicating the involvement of JAK/STAT signaling, as supported by

increased STAT5 phosphorylation in mutated compared with wild-type cells (Klampfl et al., 2013).

Later studies have established, by transducing CALR del52 or ins5 into cell lines (as the murine Ba/F3 and human UT-7 cell line) that depend on the presence of the cytokine for proliferation, how CALR mutants induce cytokine-independent growth and activate MPL with subsequently activation of JAK2/STATs as well as mitogen-activated protein kinase and phosphatidylinositol-3 kinase signaling (**Figure 26**) (Balligand et al., 2016; Chachoua et al., 2016; Elf et al., 2016; Marty et al., 2016; Nivarthi et al., 2016; Araki et al., 2016).

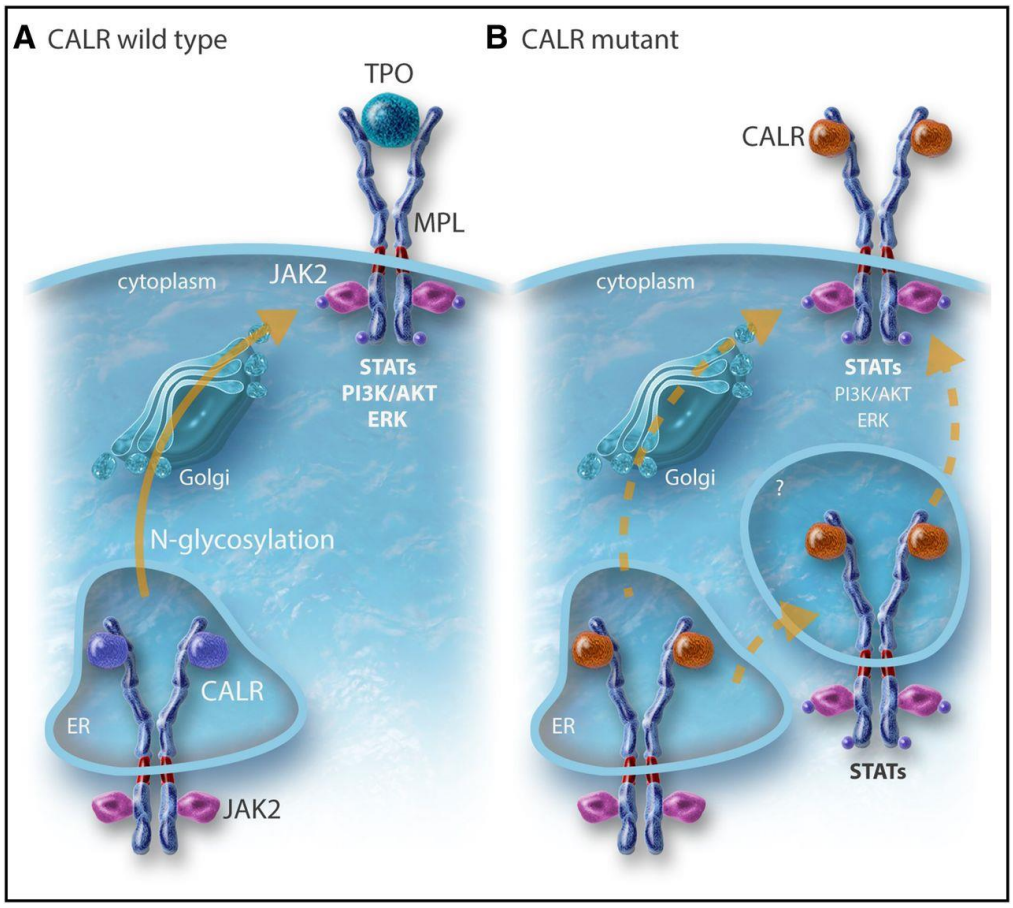

Figure 26: The Model for the constitutive activation of the thrombopoietin (TPO) receptor, MPL, by CALR mutant. **(A)** CALR WT binds to MPL in the ER by interaction of its lectin domain with MPL N-glycosylation, controls the quality of the proteins, and then comes away from the receptor, which traffics to the cell surface mainly by the conventional route to the cell surface. A completely glycosylated MPL (mature form) is expressed at the cell surface where it binds TPO to be activated. CALR mutants bind to MPL in the ER by the same interaction as the WT but the interaction is reinforced by the new C terminus**. (B)** The CALR mutant remains bound to MPL and probably traffics to the membrane both conventionally and unconventionally (autophagosomes and pre-Golgi) to the membrane. This leads to the presence of an immature MPL form on which the mutant CALR is bound. In cell lines, this leads to activation of mainly the STAT pathway. In cell lines, MPL that binds mutant CALR can only be slightly activated by TPO (Vainchenker et al. 2017).

Mutant CALR requires both its mutant C terminus and MPL for oncogenic transformation. Interestingly, it was found that CALR binds to the N-glycosylated residue of the extracellular domain of MPL in the ER, and the lectin-binding activity of CALR mutants as well as the new tail are required for MPL activation. This binding is reinforced by the new C-terminus and its positive charges, which lead to activation of the TPO receptor (Chachoua et al., 2016; Elf et al., 2016; Araki et al., 2016). It is unknown at which cellular compartment MPL is activated, but there is evidence that CALR mutants behave as an abnormal chaperone and traffics with MPL to the cell surface (Staerk et al., 2006). In this case, MPL activation can occur anywhere from the ER to the cell surface. Moreover, CALR mutants are secreted and may induce cytokine secretion by monocytes (Garbati et al., 2016). CALR mutants also appear to slightly activate the G-CSFR, but not the other cytokine receptors (Araki et al., 2006; Marty et al., 2016; Elf et al., 2016; Chachoua et al., 2016). Additionally, Araky et al. showed the cell surface localization of mutant calreticulin with no paracrine activation capacity and demonstrated also that MPL is required for TPO-independent megakaryocytopoiesis in induced pluripotent stem cell-derived hematopoietic stem cells (HSCs) harboring a *CALR* mutation (Araki et al., 2016).

The oncogenic property of mutant CALR has also been examined *in-vivo* using early murine models. Two of these (Elf et al., 2016; Marty et al., 2106) utilized a retroviral transduction method while Shide et al. (Shide et al., 2017) employed a transgenic model expressing human CALR under the H2Kb promoter. All of these studies addressed specifically the CALR Type 1 (del52) mutation given its prevalence in humans. The phenotypes of all three models were remarkably similar: mice displayed an isolated thrombocytosis with no significant effects on erythrocyte or leukocyte counts consistent with an ET phenotype and with the results of the *in-vitro* studies that indicated that mutant CALR exclusively activates MPL whose expression and function is limited to megakaryocyte and stem cells, but not in cells of other lineages. While the models by Elf et al. showed no fibrosis, Marty et al., observed increased platelet and megakaryocyte counts and a progressive fibrosis in the bone marrow and spleen by 6 months following transplantation, which is consistent with the clinical features observed in patients with MPN (Pietra et al., 2016). Bone marrow analysis revealed a general expansion of $Lin^{-}Sca1^{+}cKit^{+}$ (LSK) and signaling lymphocyte activation

molecules, $Lin^{-}CD41^{-}CD48^{-}CD150^{-}$ (SLAM) populations, and competitive transplantation assays revealed an out-growth of *CALR* Type 1 cells in comparison to wild-type cells, indicating a competitive advantage. Both, Marty et al. and Shide et al., independently assessed the *CALR* Type 2 (ins5) mutational phenotype. This model displays a more modest thrombocytosis in comparison to *CALR* Type 1 and no progression to fibrosis. Their findings resemble in humans, in that *CALR* Type 1 mutations tended to be associated with more progressive ET/MF disease while those with *CALR* Type 2 mutations were not enriched in chronic ET (Cabagnols et al., 2015; Tefferi et al., 2014). These groups also assessed the effect of whole CALR exon 9 deletion and, in this case, no significant phenotype was observed, suggesting that the functional genotype of *CALR* mutants occurs as a result of the altered peptide sequence itself rather than from a loss of the intrinsic function of the encoded portion of exon 9. Survival was unaffected independent of mutation.

Through, as it is a very recent discovery, we are still far from a solid definition of genotype/phenotype correlation of *calreticulin* mutations in patients with myeloproliferative neoplasms and the mechanisms by which this signaling perturbation may occur remains largely to clarify.

There are many questions remained to be answered. The understanding of the mechanisms by which *CALR* mutations causes MPNs has remained unknown. More elaborated in vitro transfection experiments are required to fulfill this facet, as well as animal models with conditional knock-in of *CALR* mutations, that will help clarify phenotypic traits.

AIMS OF THE PROJECT

The molecular mechanism that links CALR mutations with the disease is not fully understood. At the same time, it is necessary to underline the limitations of the available experimental tools employed for that purpose. *In-vitro* models generated by insertion of *CALR* mutations, in fact, are hybrid cell systems in which the massive expression of the endogenous wild-type *CALR* gene significantly mitigates the possible effects of the mutations introduced. An additional bias of such models is the random introduction into the coding sequence genome of the mutated *CALR* sequence as well as the expression of the mutated sequence regulated by a non-physiological promoter. More elaborated *in-vitro* transfection based experiment, as well as *in-vivo* models with conditional knock-in of *CALR* mutations are required to fulfill this facet.

The aim of this study was therefore to generate a valid and versatile model, overcoming all the above mentioned limitations, able to increase the knowledge of the *CALR* mutations' functions in hematopoiesis and its role in MPN pathogenesis. A model mimicking with faithful approximation the biological landscape that is found in the patients, at the same time providing a model for the development of diagnostic and therapeutic strategies for the management of *CALR* mutated MPNs, would be highly desirable.

To achieve this goal we employed the recent and innovative CRISPR/Cas9 technology, that provides a system to study the effects of the *CALR* mutations in a physiological context, putting the protein expression under the control of the endogenous promoter and without the superimposed expression of the wild-type one.

Using this model, we were able to characterize the effects of *CALR* mutations on the protein cellular localization and on the activation of known downstream pathways.

Another purpose of this project was then to generate a tool which could improve and facilitate routine diagnosis and monitoring of *CALR* mutated MPNs. We aimed at preparing specific antibodies against mutated *CALR*.

Overall, the main objectives of this study were the generation of new “tools” to increase the knowledge of *CALR* mutations role in MPN pathogenesis, its significance in cellular phenotypic traits, facilitating discovery of novel diagnostic and therapeutic strategies.

METHODS AND MATERIAL

THE CRISPR/Cas9 GENOME EDITING SYSTEM

Targeted human genome editing enables functional studies of genetic variation in biology and disease, and holds tremendous potential for clinical applications. Recently, a new tool based on the type II bacterial Clustered Regularly Interspaced Short Palindromic Repeats (CRISPR)-associated protein 9 endonuclease (Cas9) has been developed as an efficient and versatile technology for genome editing in eukaryotic cells and whole organisms (Cong et al., 2013; DiCarlo et al., 2013; Friedland et al., 2013; Gratz et al., 2013; Hwang et al., 2013; Mali et al.; 2013; Wang et al., 2013). First observed in *Escherichia Coli* in 1987 by its striking eponymous genomic structure (Ishino et al., 1987), it is a prokaryotic RNA-programmable endonuclease system that provides natural immunity in bacteria against invading viruses and plasmids (Wiedenheft et al., 2012).

Their function was not confirmed until 2007 by Barrangou et al., who demonstrated that *Streptococcus Thermophilus* can acquire resistance against a bacteriophage by integrating a genome fragment of an infectious virus into its CRISPR locus (Barrangau et al., 2007). In 2008, Brouns et al. identified a complex of Cas protein that in Escherichia Coli cut the CRISPR RNA within the repeats into spacer-containing RNA molecules (Brouns et al., 2008), which remained bound to the protein complex. In the same year, Marraffini and colleagues showed that a CRISPR sequence of *Staphylococcus epidermidis* targeted DNA and not RNA to prevent conjugation (Maraffini et al., 2008). All these findings confirmed the proposed RNA-interference-like mechanism of CRISPR-Cas immunity. A 2010 study provided direct evidence that CRISPR-Cas cuts both strands of phage and plasmid DNA in *S. thermophiles* (Garneau et al., 2010).

The hallmark of the CRISPR/Cas system consists of CRISPR arrays composed of spacers interspersed with direct repeats (around 20-50 base-pairs long) and *cas* genes present in the operons (Bhaya et al., 2011). In CRISPR/Cas-mediated immunity, bacteria and archaea react to viral or plasmid attack in the adaptive phase by first integrating short fragments of foreign nucleic acid (called protospacers) into the host chromosome at the proximal end of the CRISPR array. In the expression phase, CRISPR loci are transcribed into precursor CRISPR RNA (pre-crRNA) and further processed into a library of short CRISPR RNAs (crRNAs) that can recognize and pair with complementary sequences from invading viral or plasmid targets (Carte et al., 2008; Deltcheva et al., 2011; Wang et al., 2011). In the final interference phase, crRNAs are packaged with trans-activating crRNA (tracrRNA) and Cas proteins to form ribonucleoprotein complexes that together detect and destroy foreign sequences (Brouns et al., 2008; Hale et al., 2008; Jore et al., 2008). Protospacer-encoded portion of the crRNA directs Cas9 to cleave complementary target-DNA sequences, if they are adjacent to short sequences known as protospacer adjacent motifs (PAMs). Protospacer sequences incorporated into the CRISPR locus are not cleaved presumably because they are not next to a PAM sequence (**Figure 27A**).

Three types (I-III) of CRISPR mechanisms have been identified across a wide range of bacterial and archael hosts, of which type II is the most studied.

It has been recently demonstrated that the type II CRISPR system from *Streptococcus pyrogenes* can be engineered to induce Cas9-mediated double-stranded breaks (DBSs) in a sequence-specific manner *in-vitro* by providing a synthetic guide RNA (gRNA) composed of crRNA fused to tracrRNA (Jinek et al., 2012) (**Figure 27B**). So, in the simplest and most widely used form of this system only two components must be introduced into and expressed in cells to perform genome editing: the Cas9 nuclease and the gRNA. Moreover, the system has been successfully adapted to function in human cells with the use of human codon optimized Cas9 and customizable 20 nucleotides at the 5’ end of the gRNAs (**Figure 27C**) (Cho et al., 2013; Cong et al., 2013; Jinek et al., 2013; Mali et al., 2013).

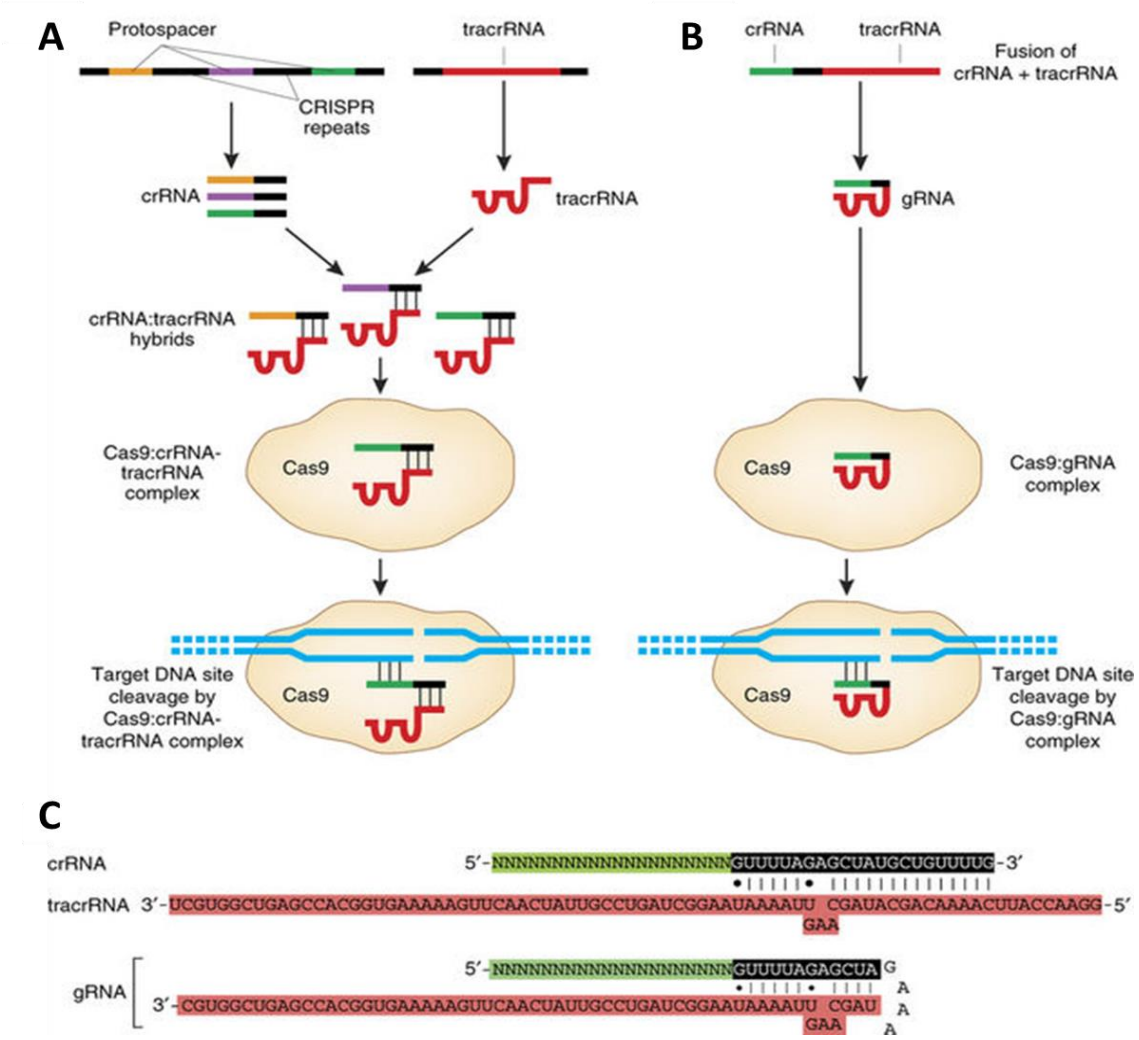

Figure 27: CRISPR-Cas platform. **(A)** Natural bacterial system is composed of incorporate foreign DNA sequences into CRISPR arrays, which then produce crRNAs bearing "protospacer" regions that are complementary to the foreign DNA site. crRNAs hybridize to tracrRNAs and this pair of RNAs can associate with the Cas9 nuclease. crRNA-tracrRNA:Cas9 complexes recognize and cleave foreign DNAs bearing the protospacer sequences. **(B)** The most used engineered CRISPR-Cas system utilizes a fusion between a crRNA and part of the tracrRNA sequence. This single gRNA complexes with Cas9 to mediate cleavage of target DNA sites that are complementary to the 5′ 20 nt of the gRNA and that lie next to a PAM sequence. **(C)** Example sequences of a crRNA-tracrRNA hybrid and a gRNA (Sander et al., 2014).

Once the gRNA identifies its 20-bp target followed by a PAM (protospacer-adjacent motif) sequence–NGG, Cas9 nuclease then cleaves the target sequence, creating a DSB (Jinek et al., 2012). The resulting DSB will either generate nonspecific mutations knocking out a gene through the error-prone NHEJ (Non Homologous End Joining) pathway, or produce specific modifications dictated by an exogenous repair template through the HDR (Homology Directed Repair) pathway (Urnov et al., 2010; Chen et al., 2011) (**Figure 28**). This system is easier to be used than previous editing systems such as ZFNs (Zinc-finger nucleases) or TALENs (Transcription activator-like effector

nucleases), bases on recognition between proteins and DNA. Based on RNA-DNA complementary base-pairing, CRISPR/Cas9 platform greatly enhances the ease of genome engineering through the creation of desired DSBs targeted by RNA sequences that are easy to design, synthesize, and deliver, holding great promise for multiplexed genome editing.

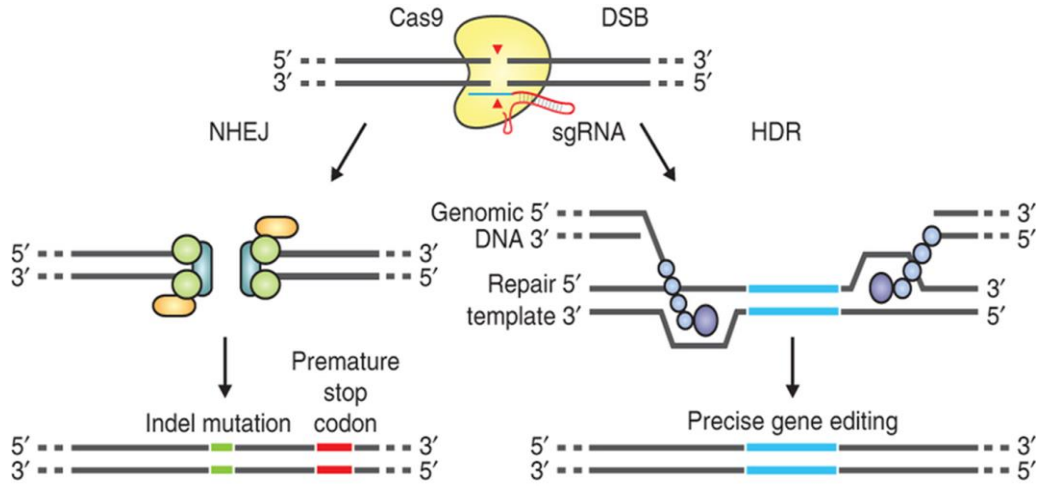

Figure 28: Recombination systems. DSBs induced by Cas9 can be repaired in one of these two ways. In the error-prone NHEJ pathway, the ends of DSB are processed by endogenous DNA repair machinery and rejoined, which results in random indel mutations at the site of junction. Indel mutations occurring within the coding region of a gene can result in frameshifts and can cause the creation of a premature stop codon, resulting in gene knockout. Alternatively, a repair template in the form of a ssODN can be supplied to active the HDR pathway, which allows high fidelity and precise editing (Ran et al., 2013).

Cas9 is a bi-lobed architecture protein with the gRNA nestled between the alpha-helical lobe and the nuclease lobe. Cas9 nucleases carry out strand-specific cleavage by using the conserved HNH and RuvC nuclease domains, which can be mutated and exploited for additional function (Sapranauskas et al. 2011). An aspartate-to-alanine (D10A) mutation in the RuvC catalytic domain allows the Cas9 nickase mutant (Cas9n) to nick rather than cleave DNA to yield single-stranded breaks, and the subsequent preferential repair through HDR (Jinek et al., 2012; Gasiunas et al., 2012; Cong et al., 2013) can potentially decrease the frequency of unwanted indel mutations from off-target DSBs. Appropriately offset sgRNA pairs can guide Cas9 to simultaneously nick both strands of the target locus to mediate a DSB, thus effectively increasing the specificity of target recognition (Ran et al., 2013). In addition, a Cas9 mutant with both DNA-cleaving catalytic residues mutated has been adapted to enable

transcriptional regulation in *Escherichia coli*, demonstrating the potential of functionalizing Cas9 for diverse applications, such as recruitment of fluorescent protein labels or chromatin- modifying enzymes to specific genomic loci for reporting or modulating gene function (Qi LS. et al., 2013).

Unintended off-target mutations pose a challenge to the application of any genome-editing technology. Also CRISPR/Cas9 system, even if very efficient, is not completely immune to errors. Understanding the possible weak sides could be helpful in order to prevent all potential off-target effects. Recently, a number of studies have examined potential off-target sites that differ from one to six positions from the on-target site in human cells (Pattanayak et al., 2014; Fu et al., 2013; Hsu et al., 2013). These reports have found cases of off-target mutations at sites that differ by as many as five positions within the protospacer region and that have an alternative PAM sequence (Semenova et al., 2011). Off-target mutations are generally more difficult to detect, requiring whole-genome sequencing to rule them out completely.

Recently, some improvements to the CRISPR/Cas9 system have been made to minimize off-targets mutations. Careful selection of cleavage site is obviously fundamental. One other potential strategy is to reduce the concentrations of gRNA and Cas9 expressed in human cells or to use a modified gRNA architectures (truncating the 3’ ends or by adding two extra guanine nucleotides to the 5´ end) which yields better on-target to off-target ratios but generally with lower efficiency on on-target genome editing (Pattanayak et al., 2014; Cho et al., 2013). Another way researchers have attempted to minimize off-target effects is with the use of “paired nickases” (Mali et al., 2013; Ran et al., 2013). This strategy uses D10A Cas9 mutant and two sgRNAs complementary to the adjacent area on opposite strands of the target site. While this induces DSBs in the target DNA, it is expected to create only single nicks in off-target locations and, therefore, result in minimal off-target mutations. However, the second gRNA can itself induce its own range of off-target mutations in the genome as multiple studies had shown (Kuzminoc et al. 2001; Cortes-Ledesma et al., 2006; Sander et al., 2014).

Though off-target effects will be difficult to eliminate from CRISPR genome editing, suggestions have been made for differentiating between phenotypes caused by on and off-target mutations. One option would be attempting to have a reporter

gene construct that is affected by the on-target mutation. Alternatively one could attempt a rescue of the wild type phenotype, which can be used to confirm the effects of knockout. Another possibility is to use sgRNAs targeted to different sites. Each sgRNA should have different off-target effects, so if an altered phenotype is present in all mutated strains it is more likely to be from the intended mutation (Sander et al., 2014). Moreover, it was recently identified some variants of Cas9, so called high-fidelity (SpCas9-HF1) and enhanced specificity (eSpCas9) variants, that substantially reduced off-target cleavage: both are trapped in an inactive state when bound to mismatched targets. So, Chen and colleagues, designing a new hyper-accurate Cas9 variant (HypaCas9), demonstrated a new approach to improve genome-wide specificity without compromising on-target activity in human cells (Chen et al., 2017).

Overall, the simplicity, high efficiency and broad applicability of the RNA-guided Cas9 system have positioned this technology to transform biological and biomedical research. Although the off-target effects of Cas9 remain to be defined on a genome-wide scale, much progress has already been made toward improving specificity, and further advances will undoubtedly come rapidly, given the intensity of research efforts in this area. It is recent All of these recent advances, and those to come, in developing and optimizing Cas9-based systems for genome and epigenome editing should propel the technology toward therapeutic applications, opening the door to treating a wide variety of human diseases.

CELL LINES

The K562 cell line used was obtained from the German Collection of Microorganisms and Cell Cultures (DSMZ, Braunschweig, Germany, www.dsmz.de).
The description in detail is provided in the Materials and Methods chapter of the first project (paragraph cell lines and cell culture, p.37).

PRIMARY HUMAN CELLS

For the evaluation of molecular targets and for cellular studies peripheral blood (PB) or bone marrow (BM) samples were obtained from PV, ET or PMF patients, diagnosed according to the World Health Organization (WHO) criteria, under a protocol approved by Institutional Review Board of Azienda Ospedaliera-Universitaria Careggi and after obtaining a written informed consent.

The purification of CD34 + cells from peripheral blood or cord blood (discarded from cord blood units) was performed using immunomagnetic separation according to the Miltenyi procedure (Miltenyi Biotec.). More details about the protocol on page 39.

LIQUID CULTURE AND REAGENTS

CELLS LINES. The K562 cells line were maintained in RPMI 1640 medium supplemented with 10% fetal bovine serum (FBS; Lonza, Verviers, Belgium), 1% L-glutamine and 1% Penicillin-Streptomycin. Cells were maintained at 37°C in 5% CO_2 humidified atmosphere.
The following reagents were purchased by Selleck (Selleckchem, Munich, Germany): Methotrexate (nonspecific dihydrofolate reductase (DHFR) inhibitor); Doxorubicin (inhibitor of DNA topoisomerase II); Mitoxantrone (type II topoisomerase inhibitor); Cytarabine (AraC, antimetabolic agent and DNA synthesis inhibitor); Daunorubicin (inhibitor of both DNA and RNA synthesis); and Oxaliplatin (DNA synthesis inhibitor).
As regard the transcription inhibitor actinomycin D, protein synthesis inhibitor cycloheximide (CHX) and calpain inhibitor I (ALLN, protease inhibitor) were obtained from Sigma (Sigma-Aldrich, St. Louis, MO).

CD34+ CELLS. CD34+ cells were plated at the concentration of $5x10^5$ cells/mL in Iscove's Modified Dulbecco's Medium (IMDM, Lonza, Belgium) with the addition of 20% human serum, 1% Penicillin/Streptomycin, 1% L-glutamine plus a cytokines cocktail allowing CD34+ proliferation: human SCF 50 ng/mL; FLT3L 50 ng/mL; human TPO 20 ng/mL; human IL-3 10 ng/mL; human IL-6 10 ng/mL.

TRANSFECTION

We generated *CALR* knock-out (KO) variants from donor CD34+ cells and BCR/ABL-mutated K562 and *CALR* Type 1 variants from K562. The plasmids for CRISPR-Cas9 were obtained from Applied StemCell (Euroclone).

To obtain the KO $1x10^6$ cells were transfected with the plasmid pCMV-Cas9-GFP expressing the endonuclease and a guide sequence complementary to exon 1 of the *Calreticulin* gene (**Figure 29**).

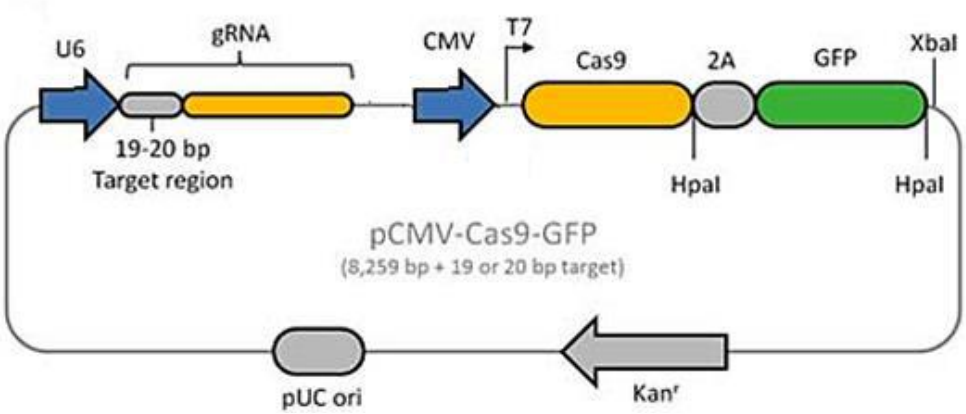

Figure 29: **All in One expression vector**. Four different gRNAs (selected basing on the best efficiency scores calculated by the Zhang Lab software), complementary to exons 1 (3 gRNAs) and 2 (1 gRNA) of the *Calreticulin* gene, were each introduced in 4 different expression vectors, followed by coding sequences for Cas9 endonuclease and Green Fluorescent Protein (GFP, used as gene reporter). All of these sequences were assembled into a single recombinant plasmid expressing the coding sequence of the gRNA under the control of the U6 promoter and the the Citomegalovirus promoter (CMV) for Cas9 and GFP sequences; two cutting sites for the HpaI restriction enzyme, flanking the two ends of the GFP sequence; a cutting site for the XbaI enzyme to allow plasmid linearization; a Kan^r sequence for Canamicin antibiotic resistance, and a procariotic origin of replication for the plasmid amplification. The plasmid thus designed has been defined as "all-in-one" because it hosts in a single vector the various components needed to promote genomic editing of interest.

Regarding the Type 1 variant we transfected $1x10^6$ cells with the following plasmids: pX330-hSpCas9-2A-puromycin plasmid expressing the endonuclease, pBT-U6-Cas9-2A-GFP containing the guideRNA (gRNA) plasmid with the sequence that is

complementary to a stretch of the genomic DNA and an additional single strand donor oligonucleotide (ssODN) allowing the knock-in of the specific mutation by homology directed repair (HDR). A 199nt ssODN, carrying the initial sequence of *CALR* exon 9 sequence (coding the 52 bp deletion), was designed and synthetized. To avoid Cas9/gRNA recognizes and cuts the ssODN, three silent mutations were designed within the ssODN which would not change the CALR amino acid sequences. In addition, it was added a stop codon, able to terminate the subsequent transcription and consequent translation of the molecule. Following Cas9 targeted cutting events, the cellular repair mechanisms will stochastically incorporate the ssODN by binding it to the end of the cut exon 9, thus generating a sequence corresponding to an exon 9 of 52 bp. Any ligation of the remaining sequence of exon 9 to the 3'end of the ssODN will not be transcribed and translated by the polymerases action due to the presence of the stop codon at the 3' end of the donor cDNA.

Plasmids were diluted into Plasmid Transfection Medium at optimized concentration and transfected using Amaxa Nucleoflector® (Lonza) according to the manufacturer's instructions. After 24 hours of incubation at 37°C in 5% CO_2 humidified incubator, single GFP-positive cells were sorted by using a FACS ARIA with the Diva onto individual wells of a 96 well plate containing complete medium. Single cell clones were allowed to proliferate and validated using PCR, Sanger sequencing, qRT-PCR and Western blot.

We performed CRISPR/Cas9 genome editing, to obtain *CALR* KO, also in CD34+ from cord blood: after the transfection we bulk sorted the GFP-positive cells into a tube containing the appropriate medium.

To confirm the results obtained with genome-edited cell lines, we also generated models of transient CALR- wild-type/Type1/Type2 expression by vectors transfection into CRISPR edited (CRISPRed) K562 *CALR* KO cell line. Briefly, in over-expression experiments, $1x10^6$ cells were transfected as previously described with the following plasmids: p-CMV3-(N)Flag-CALR wild-type; p-CMV3-(N)Flag-CALR Type1; p-CMV3-(N)Flag-CALR Type 2 and as control we used an empty vector (Mock).

CRISPRed K562 *CALR* KO cell line stably expressing CALR wild-type, Type1 and Type2 were generated transfecting cells with lentiviral vectors (ΔNGRF/GFP MA1) that was

performed by Prof. Manfredini and her group (University of Modena and Reggio-Emilia, Modena, Italy).

QUANTITATIVE REAL-TIME PCR (qRT-PCR)

The validation of the clones *CALR* KO from K562 was performed measuring the level of *CALR* messenger RNA (mRNA) by quantitative real-time PCR (qRT-PCR). Total RNA was extracted using TriPue Isolation Reagent (Roche Diagnostics) following the directions of the company. The RNA concentration and purity/integrity was determined with NanoDrop ND-1000 spectrophotometer (NanoDrop Techn., Wilmington, DE, USA) and reverse-transcribed to cDNA using one microgram of RNA.
cDNA was synthesized using High capacity cDNA Reverse Transcription kit (Applied Biosystems, Life Technologies; Carls-bad, CA) and qRT-PCR was carried out with SYBR Green PCR master mix (Applied Biosystems) on a StepOnePlus Real-time PCR System (Applied Biosystems) according to standard protocols.
The primers for the qRT-PCR analysis were as follows: for *CALR* (exon 2), forward 5'-CCTGATGCTTCAAAACCGGAAGACT- 3' and reverse 5'-CCGGGCTTCCACTCACCCTTGTA-3'; for *CALR* (exon 9), forward 5'-AACCCCGAGTATTCTCCCGA-3' and reverse 5'-TGGCCTGGCCGGGGA-3'; for *18S*, forward 5'-CGGCTACCACATCAAGGAA-3' and reverse: 5'-CGTGGAATTACCGCGGCT-3'. *18S* was used as internal control. Relative gene expression was calculated according to the comparative cycle threshold (Ct) method.

SANGER SEQUENCING OF *CALR*

CRISPR/Cas 9 on-target gene editing of K562 *CALR* Type1 (T1) cells was validated using Sanger sequencing. First genomic DNA was extracted using Maxwell DNA Purification Kits according to the Promega protocol (Promega, Madison, Wisconsin, USA). Conventional PCR amplification was performed using AmpliTaq Gold 360 PCR Master Mix (Thermo Fisher Scientific) and the primers for *CALR* exon 9 (forward 5'-AACCCCGAGTATTCTCCCGA-3' and reverse 5'-TGGCCTGGCCGGGGA-3') on Applied Biosystems 2720 Thermal Cycler instrument following the manufacturer's

protocol. The amplified DNA has been finally separated in agarose 2% gel and analyzed with Kodak 1 DLE 3.6 software.

The subsequent purification phase of PCR products was performed using QI-Aquick PCR purification Kit Qiagen according to manufacturer's instructions (Qiagen, Hilden, Germany). The purified specimens have been then hybridized and the reaction phases performed with Applied Biosystems 2720 Thermal Cycler. The following purification of hybridization products was performed with ZR DNA Sequencing Clean-up Kit (Zymo Research Corp, Irvine, CA, USA) and the samples were Sanger sequenced on ABI Prism Analyzer 310 instrument (Thermo Fisher Scientific). The analysis of the sequence was performed with Mutation Surveyor software (Softgenetics, State College, PA, USA).

ASSESSMENT OF THE VIABILITY, CELL CYCLE AND APOPTOSIS

The cell growth assay was performed as follow. Exponentially growing cells were washed three times with sterile PBS and plated in triplicate at $2x10^5$ cells/mL in complete medium. Cell viability was determined, at indicated time point, by Tripan blue dye exclusion assay using Biorad TC10 Automated Cell Counter (Biorad, Hercules, California, USA).

The cell cycle distribution was accomplished recovering $1x10^6$ cells after 18 hours of drugs treatment and washed twice with PBS by centrifugation at 1200 rpm for 5 minutes; subsequently the supernatant was aspirated, the cell pellet fixed with 500 µL of a 95% ethanol cold solution and then incubated on ice for 20 minutes. After washing with PBS, the cell pellet was resuspended in 500 µL of PBS containing 10 µg/mL of RNase (Roche) and incubated at 37°C for 20 minutes. The suspension was then transferred into a FACS tube and has been carried out a wash in PBS before addition of 500 µL of a propidium iodide (PI) solution at a concentration of 10 µg/mL and subsequent incubation on ice for 10 minutes. The addition of PI and subsequent incubation were performed protected from light. After incubation, we proceeded to the cytofluorimetric evaluation with FACS SCAN (Becton Dickinson) using the Cell Quest Pro software (Becton Dickinson) and a minimum of 30,000 events were acquired.

Regarding the quantification of apoptotic cells, it was performed using Annexin-V-FLUOS Staining kit (Roche, Basel, Switzerland). $1x10^6$ cells were removed from the wells after 24 hours of incubation with the various compounds and washed with PBS by centrifugation at 1200 rpm for 5 minutes. The pellet was resuspended in 100 µL of Incubation Buffer with the addition of 2µL of Annexin-V-FLUOS labeling solution (Roche) and 2 µL of Propidium iodide and incubated at room temperature for 15 minutes. Then 500 µL of Incubation Buffer were added and we proceeded to the evaluation of at least 20.000 events in a FACS SCAN flow cytometer (Becton Dickinson). Data were processed with Flow-Jo software (Tree Star, Ashland, OR, USA).

MEGAKARYOCYTIC DIFFERENTIATION

To achieve the growth of megakaryocytic cells, two-stage cultures were used during their *in-vitro* differentiation. A proliferative phase of expansion of the progenitor pool (first 7 days) and the second phase of differentiation (from day 7 to 14). We plated $2x10^5$ CD34+ cells/mL in IMDM medium with the addition of 20% BIT9500 (serum substitute, contains bovine serum albumin, insulin, and transferrin; StemCell Technologies Inc.), 1% Penicillin/Streptomycin, 1% L-glutamine plus the following cytokines: human SCF 50 ng/mL and human TPO 100 ng/mL for the first 7 days; only human TPO 10 ng/mL in the last phase (until day 14).

In-vitro megakaryocytic differentiation of the K562 cell line was induced plating $3×10^5$ cells/ml in complete medium with 10 nM phorbol 12-myristate 13-acetate (PMA; Sigma-Aldrich,) for 72 hours.

The cell differentiation was assessed by evaluating the expression of the early (CD41-PE, Milteny Biotec.) and late (CD61-FITC) megakaryocytic lineage markers. Fluorescence signals were detected and analyzed using FACS SCAN flow cytometer (Becton Dickinson). Data were processed with Flow-Jo software (Tree Star, Ashland, OR, USA). For this purpose aliquots of $1x10^5$ cells were labeled.

COLONY ASSAY

For the evaluation of the megakaryocytic colonies it was used MegaCult-C serum-free medium (Stem Cell Technologies Inc.). After 12 days of culture in an incubator at 37ºC and 5% CO_2, megakaryocytic colonies were recognized and counted (CFU-MK). More details about the protocol on Materials and Methods chapter of the first project (p.40).

WESTERN BLOTTING ANALYSIS

Harvested cells were lysed in RIPA lysis buffer (50 mM pH 7.4 Tris-HCl, 150 mM NaCl, 1% NP-40, 1 mM EDTA) containing a proteinase inhibitor cocktail (Halt Protease Inhibitor Cocktail 100X Kit, PIERCE, Rockford, IL, US) and treated by sonication (Microson XL-2000, Minisonix, Farmingdale, NY, USA) to obtain a total protein extract. For cytosol-nucleus fractionation, proteins were isolated by using the ProteoExtract Subcellular Proteome Extraction Kit (Merck Millipore, Darmstadt, Germany) as suggested by the manufacturer. As regard the cell culture supernatant, it was collected, at indicated time point, and concentrated using Vivaspin 20 centrifugal concentrators with a MWCO of 5,000 Da (Sigma–Aldrich) followed by spinning and addition of protease inhibitors.

Proteins were assayed by the BCA kit (Sigma-Aldrich) and resuspended in 4X Sample Buffer (Tris-HCl pH=6.8 250 mM, glycerol 10%, SDS 8%, Bromophenol blue) and β-mercaptoethanol. After heating at 95°C for 10 minutes, the samples were applied on a polyacrylamide gel 4-12% (Invitrogen-Life Technologies, Carlsbad, Ca, USA). After an electrophoretic separation (SDS-PAGE) with running buffer (Tris 15 g/L, glycine 72 g/L, SDS 5 g/L, H2O milli-Q) the proteins were blot on PVDF membranes using iBlot 7-minute Blotting System (Invitrogen). The membranes were subsequent blocked for one hour at room temperature with 5% BSA in a solution of Tris Buffered Saline with 0.1% Tween 20 detergent (TBST). The next incubation with the primary antibody took place overnight at 4°C with a 1:1000 dilution of the antibody in a solution of TBST with 1% BSA. After incubation, three washes of the membranes were carried out to remove the excess of unbound antibody with a solution of TBST. Then, an incubation in the HRP-

conjugated solution (with a dilution of 1:10000 in TBST with 1% BSA) was performed for one hour at room temperature. The membranes were successively rinsed 3 times for 5 minutes in TBST and incubated for 1 minute with ECL reagent. Western blotting images were acquired with ChemiDoc XRS+ (Bio-Rad, Hercules, CA, US) and analyzed with ImageJ software (50) for densitometric analysis.

The antibodies assayed in western blotting analysis were the following: Calreticulin (FMC75 clone; Abcam); GAPDH and H2AX (Cell Signalling); β-actin (Santa Cruz Biotechnology) and the primary antibodies against mutated calreticulin that we have developed in this project. Anti-rabbit HRP antibody was from Sigma-Aldrich and anti-mouse HRP antibody was from Millipore.

PRODUCTION OF RECOMBINANT MUTATED CALR

A synthetic form of CALR Type 1 (del52) was expressed in the BL21 DE3 RIPL and JM109 DE3 *Escherichia coli* strains by standard procedures; exponentially growing bacterial cultures were extracted and both the insoluble and the soluble fractions were collected and analyzed in a denaturing polyacrylamide gel electrophoresis.

ANTI-CALR ANTIBODY PREPARATION

A set of immunogenic peptides derived from the common mutated domain in the C-terminal of calreticulin was synthesized on the Symphony automatic peptide synthesizer (Protein Technologies, Tucson, AZ, USA), conjugated with keyhole limpet hemocyanin (*KLH*) and then purified on a Sephadex column by standard techniques; the conjugated peptides was used to immunize rabbits and mice in order to obtain respectively new polyclonal and monoclonal antibodies.

Peptide synthesis and animal immunization were performed at Primm srl. (Milano, Italy). The immunoglobulin fraction was purified by protein G-Sepharose 4 Fast Flow (GE Health Care Life Science, Uppsala, Sweden) column and then passed over a CNBr-activated Sepharose 4B containing the immobilized peptide to recover peptide-specific antibodies.

SANDWICH ELISA

The 96-flat bottom well ELISA plates (Nunc MaxiSorp, Thermo Fisher Scientific) were coated with the rabbit polyclonal antibodies (Abs) against mutated calreticulin in coating buffer and incubated at 4°C overnight. After washing three times with washing buffer, the well were blocked with 200 µL/well PBS containing 2% BSA for one hour at room temperature. Afterward, 50 µL/well of Type 1 and wild-type (Abcam) recombinant proteins, which were diluted with dilution buffer, were added and incubated at room temperature for one hour. After washing three times, the detecting antibody (anti- CALR mouse monoclonal Ab; FMC75 clone, Abcam) was added and incubated for one hour at room temperature. Successively, the plates were incubated with goat anti-rabbit conjugated with HRP (Sigma-Aldrich). After another washing, substrate TMB substrate was added into the plates and the absorbance were measured at 450 nm. The spectrophotometer used was the instrument ELISA EL808 (Biotek).

CONFOCAL MICROSCOPY

Cells were grown on glass coverslips, washed twice with 1 ml of PBS, fixed for 15 minutes in 3.7% paraformaldehyde in PBS and permeabilized with 0.1% Triton X-100 (Sigma) in PBS for 10 minutes. The cells were incubated in blocking buffer (3% BSA and 0.1% Triton X-100 in PBS) for 20 minutes at room temperature and then incubated overnight at 4° C with the antibody anti-CALR (F4-clone, Santa Cruz), anti-Flag (Sigma) and the primary antibodies against mutated calreticulin that we have developed in this project. Successively, the cells were incubated at room temperature for 1 hour with the anti-rabbit IgG Cy2-conjugated or anti-mouse IgG Cy3-conjugated secondary antibodies. Nuclei were stained with DAPI dye (4',6-diamidino-2-phenylindole; Life Technologies). Then, the cells were dried, mounted onto glass slides and examined by confocal microscopy using LSM 510 META Zeiss confocal microscope system (Carl Zeiss Inc., Jena, Germany). The collected images were analyzed by Confocor 2 (Zeiss) software.

STATISTICAL METHODS

The Mann-Whitney *U* or Fisher test was used for comparison using the SPSS software (StatSoft, Inc., Tulsa, OK, USA, www.statsoft.com) or Origin software (OriginiLab, Massachusetts, USA). Data were expressed as mean ± standard deviation (SD). The level of significance from two-sided tests was $p<0.05$.

RESULTS

GENERATION OF *CALRETICULIN* MUTANTS HUMAN HEMATOPOIETIC CELL LINES BY CRISPR/CAS9 GENOME-EDITING.

In order to obtain a valid tool to study *CALR* mutations in a hematopoietic setting, in this project we generated *CALR* mutants human hematopoietic cell lines by genome editing using CRISPR/Cas9 technology engineering the myeloid leukemia derived K562 cell line.

We first performed genome editing on the BCR/ABL-mutated K562 cells by targeting the exon 1 of *CALR* gene with the specific aim to generate a *Calreticulin* Knock-out (*CALR* KO) cell line. Further, we performed in K562 cells a trasfection of gRNA targeting exon 9 capable to generate break with non-complementary far-ends on nucleic acid sequence concomitantly to a "donor cDNA" with sticky hands to introduce a stop codon at the desired nucleotide in order to engineering genomic DNA sequence to obtain the traduction of *CALR* Type 1 (T1) variant (52 bp delection, the most common *CALR* mutation observed in patients with MPN). After transfection, cells were sorted by the GFP reporter expression whose gene was expressed downstream the gRNA by the introduced vectors and sorted cells were plated at density of single cell per well in a 96 wells plate containing proper culture medium. Single cell clones were allowed to proliferate and validated with qRT-PCR, PCR, Sanger sequencing e Western Blot.

To select *CALR* KO cells, the grown clones were screened by qRT-PCR for the absence of *CALR* trancript. 4 clones on the 51 evaluated showed no amplification of the *CALR* gene. About 23% showed a partial downregulation of the expression of the *CALR* gene in a range of 65% to 20% compared to control cells. These observations can be explained by a non-complete recombination effect of CRISPR/Cas9, probably not occurred on all encoding alleles for *calreticulin*.

As regard *CALR* T1, grown clones were pre-screened by conventional PCR and these resulting in a correct length PCR product (**Figure 30A,** 303 bp instead of 355 bp of the wild-type based on genome engineering prediction) were subjected to Sanger sequencing to confirm the correct mutated genome sequence. As shown in the **Figure 30B,** Sanger sequence of one K562 *CALR* T1 clone, of the total 99 clones analyzed, showed the desidered deletion of 52 bp genomic sequence and a residual sequence *CALR* wild-type (WT) problably due to a partial inefficiency of CRISPR/Cas9 recombination on the polyploid genome of K562.

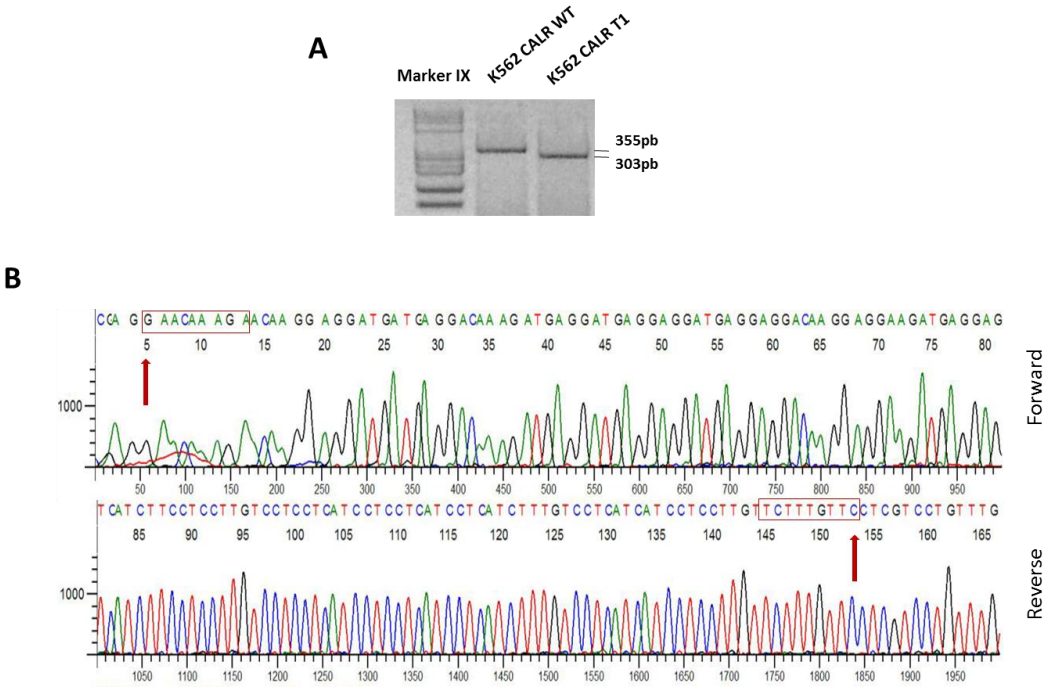

Figure 30: (A) Conventional PCR reaction, the amplifications were run on agar gel, and the potentially recombined samples selected on the basis of their expected molecular weight of 303 bp resulting from recombination mediated by gRNA/Cas9 and by the donor cDNA integration, amplified wild -types have an estimated molecular weight of 355 bp. **(B)** K562 CALR Type1 clone Sanger sequencing shows the expected recombined genomic sequence after CRISPR/Cas9 editing. Red arrow indicated the start of edited sequence.

Genome-edited K562 cells were assessed by qRT-PCR that showed an equal amount of *CALR* transcripts in WT and T1 cells, while no amplification was obtained in KO cells (**Figure 31A**). Western blotting analysis was performed probing cell lysates with an antibody targeting the N-terminal domain, therefore capable to detect both *CALR* WT and T1 mutant: as represented in the **Figure 31B** T1 lysates confirmed the presence of CALR protein with lower molecular weight compared to WT (55 kDa). Interestingly the lane with CALR T1 proteins shows only one band corresponding to

mutated protein, letting us speculate that residual CALR WT sequence and possible traslated protein corresponds to a very lower amount compared to the mutant protein. Of note, no bands were detected in K562 CALR KO lysates.

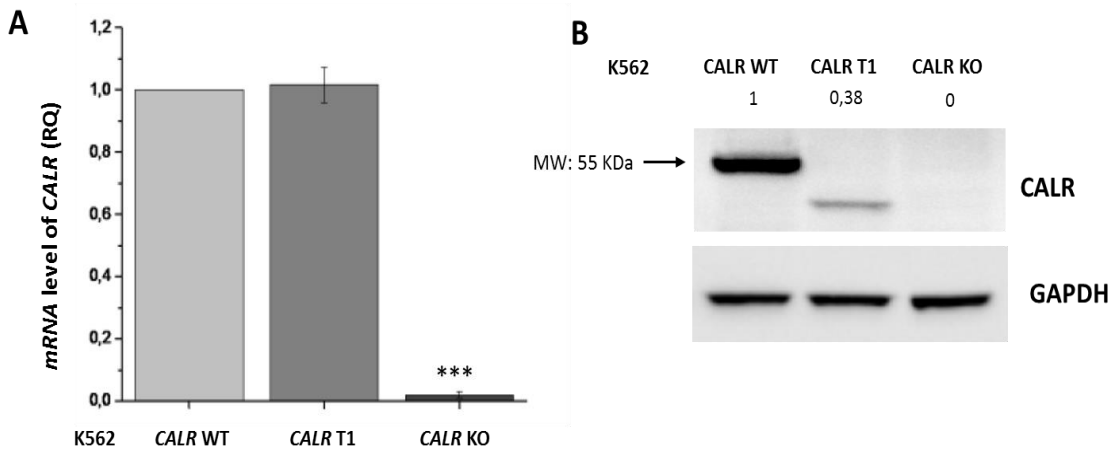

Figure 31: (A) *CALR mRNA* levels. Selected clones of edited K562 were assayed with qRT-PCR using primers that amplify a *CALR* exon 9 region external to mutated spot. As expected, reference K562 and CALR T1 variant show a similar *mRNA* amount in contrast to CALR KO clone the show no significant mRNA expression. P value was determined by unpaired two-tailed Student's T test (***p<0.01).
(B) Western blotting analysis on K562 CALR WT, CALR T1 and CALR KO. Whole lysates were probed with anti- N-terminal domain Ab (Abcam) and revealed with secondary Ab HRP-coniugated. CALR T1 shows one band of lower molecular weight compared to the expected CALR WT (55 KDa). No bands were detected in CALR KO lane. The numbers above each lane indicate results of densitometric analysis. Data are from one representative experiment out of three. GAPDH was used for loading normalization.

CHARACTERIZATION OF THE GENOME EDITED K562 CELL LINES

The characterization of genome edited cell lines was pursued by evaluating cell prolifetion, cell cycle and apoptoic.

As shown by the **(Figure 32A and 32B**), no significant differences in the proliferative rate and cell cycle of K562 *CALR* KO and T1 cells were observed in comparison to parental cells (K562 *CALR* WT).

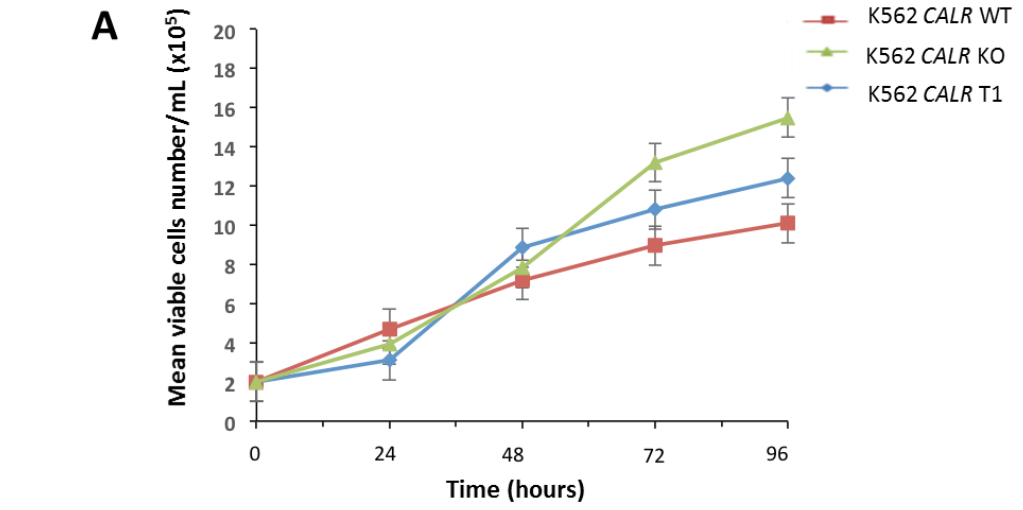

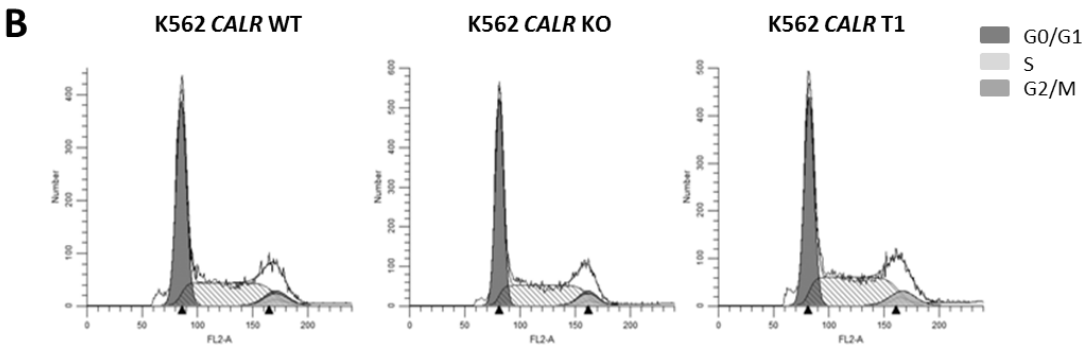

	G0/G1	S	G2/M
K562 *CALR* WT	47,54%	50,76%	46,75%
K562 *CALR* KO	38,72%	41,24%	45,25%
K562 *CALR* T1	13,73%	8%	8%

Figure 32: (A) Growth curves. Living cells were counted at indicated time point by Tripan blue dye exclusion assay using Biorad TC10 Automated Cell Counter. Data were expressed as the Means ± SD (n = at least three experiment). **(B)** Cell cycle analysis. DNA histograms were made by PI staining and FACS flow cytometry: the initial and middle peak represent G0-G1, S stage respectively, last is G2/M stage. DNA histograms were analyzed by Cell Quest Pro software cell cycle analysis software. Percent cells in different phases of the cell cycle are indicated in the table below.

These cells were also assayed for the capacity to resist chemotherapy. We tested the most common cytotoxic drugs that are traditionally used in the treatment of hematologic malignancies. The cell lines were treated with Doxorubicin, Oxaliplatin, Daunorubicin, Mitoxantrone and Cytarabine. We found that all the agents tested were able to induce apoptosis in µM range (data not shown). Of note, we observed a significant increase in apoptosis resistance of KO and T1 cells when treated with the type II topoisomerase inhibitor, Mitoxantrone (MTX). In particular, the *CALR* KO and *CALR* T1 cell lines are significantly more resistant to MTX-induced apoptosis than the wild-type counterpart: the IC_{50} value calculated for the K562 was 5µM (54% of

Annexin-V positive cells), while the percent value of Annexin V-positive cells was 30% and 35% respectively for the *CALR* KO and T1 cell lines have shown An-V positivity in a cell population equal to of the total ($p<0.05$) (**Figure 33**).

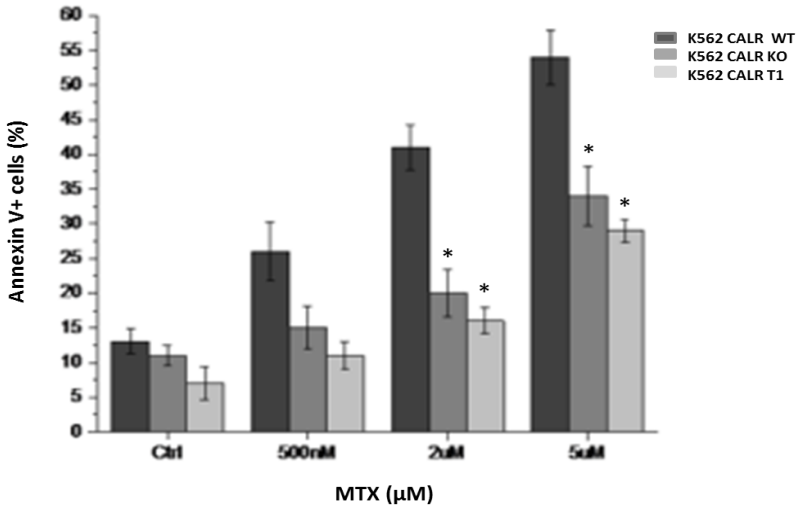

Figure 33: K562 *CALR* WT and genome-edited K562 cell lines were treated with varying drug amounts. Value were expressed as percent of Annessin V-positive cells. Controls (Ctrl) cells were treated with vehicle (DMSO) only. Values are Means ± SD of at least five separate experiments (*$p<0.05$).

EVALUATION OF THE *CALR* MUTANT STABILITY AND LOCALIZATION.

We observed significantly lower protein amounts of K562 CALR T1 than the CALR wild-type (WT) counterpart (**Figure 31B**) although *CALR mRNA* was simirarly expressed (**Figure 31A**). To evaluate the possibility of a lower stability of CALR mutant, we treated K562 CALR WT and T1 with Actinomycin D (an inhibitor of *mRNA* transcription), Cycloheximide (CHX, a protein synthesis inhibitor) and the calpain inhibitor I (ALLN, an inhibitor of the proteases and proteasome). At indicated time points, we assessed CALR stability by qRT-PCR and Western Blotting analysis.

Interestingly, we found that relative *mRNA* (**Figure 36A**) and protein levels (**Figure 36B**) of CALR T1 had a statistically significant decrease upon 6 hours treatment with Actinomycin D and CHX, respectively. After the calpain I inhibition, at the same time, we observed a considerable increase of the mutant protein level, while remained unchanged the wild-type form (**Figure 36C**).

Overall, these observation lead us to speculate an increased instability and turnover of mutated CALR (both at *mRNA* and protein level) than the wild-type counterpart.

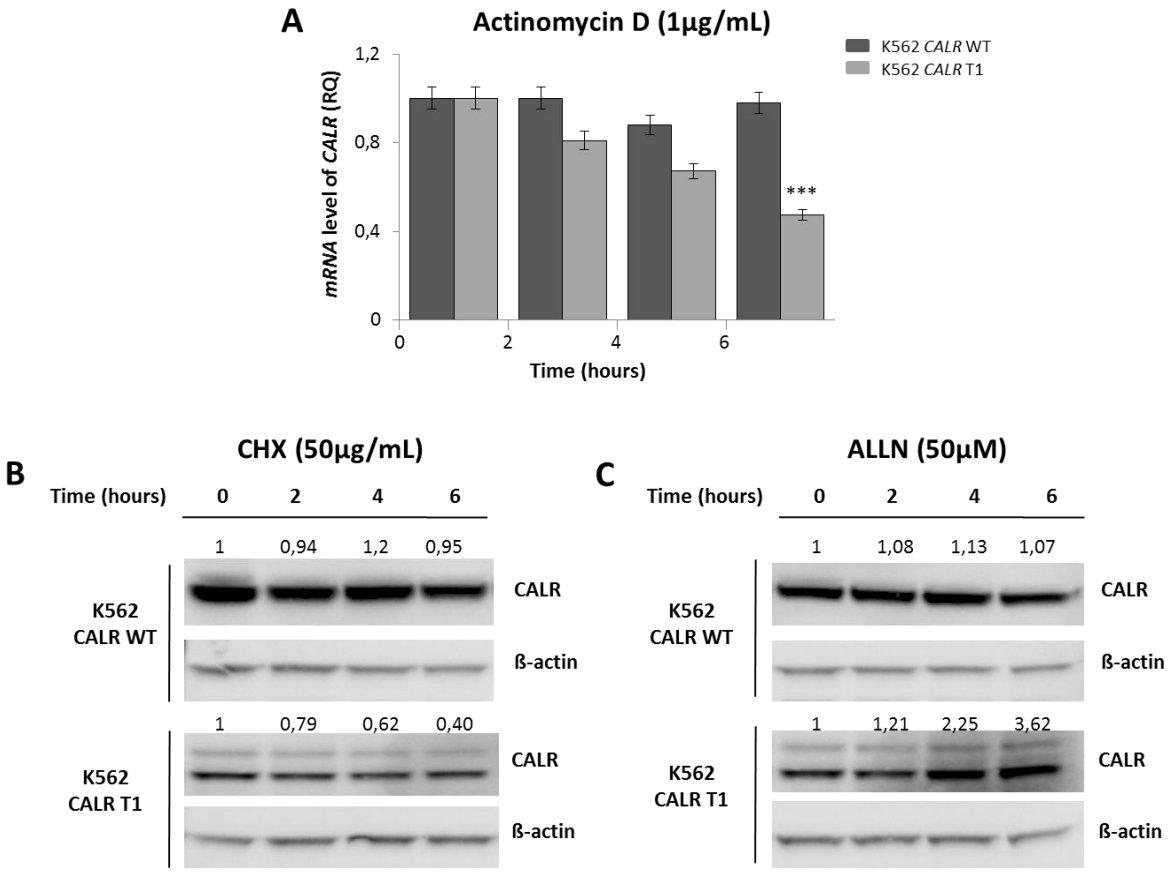

Figure 36: Mutated calreticulin *mRNA* and protein result more unstable than wild-type form. (A) Effect of the transcription inhibitor (Actinomicycin D) treatment of K562 CALR WT and K562 CALR T1 on *CALR mRNA* levels, assessed by qRT-PCR. As shown the treatment results in a significant decrease of mutant *mRNA* compared to wild-type. Values are Means ± SD of at least three separate experiments (***p<0.01). **(B-C)** Effects of the inhibition of translation by CHX (B) and inhibition of degradation by ALLN (C) on CALR protein levels, evaluated by Western Blot analysis. CHX and ALLN treatments results in a significant decrease and increase respectively of mutant protein compared to wild-type form. The numbers above each lane indicate results of densitometric analysis. Data are from one representative experiment out of three. B-actin was used for loading normalization.

Next, we performed a subcellular fractionation to define the subcellular localization of wild-type and mutant CALR. The distribution of all markers tested in the western blot as well as the density of each fraction are shown in the **Figure 37A**. Contrary to wild-type protein, found both in the cytoplasm and nuclear fractions, the mutated form remained largely in the cytosol, even though there was a lower total amount of Type 1 expressed at steady state in whole cell extracts.

To quantify these findings using a different model, we performed a transient transfection of Flag-tagged CALR- wild-type/Type1/Type2 vectors into CRISPRed K562 CALR KO cell line. We observed that both Type 1 and Type 2 mutant calreticulin localized preferentially in the cytoplasm and only a slight amount was left in the nucleus (**Figure 37B**). We then performed confocal microscopy to corroborate these observations. While we detected prominent cytoplasmic and nuclear staining for wild-type cells, the mutant form remained largely in the cytoplasm (**Figure 37C**).

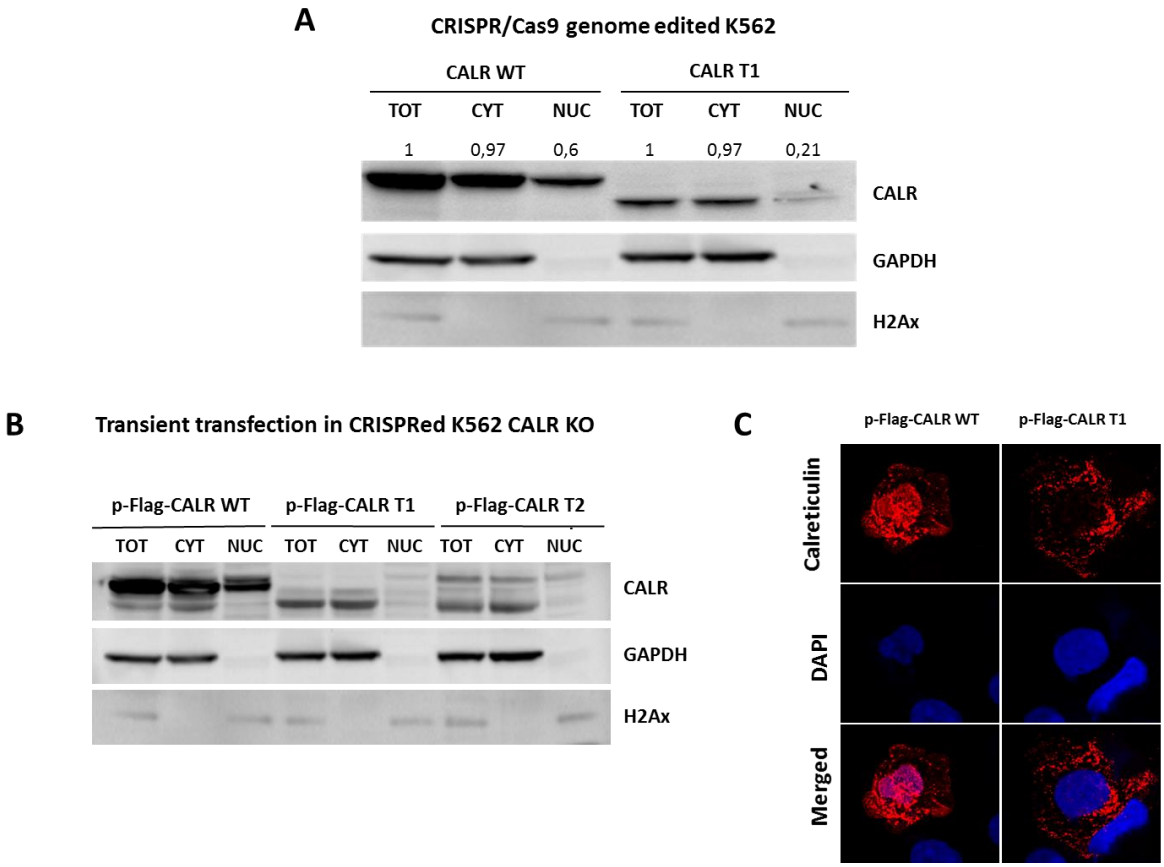

Figure 37: Subcellular fractionation of mutant calreticulin and confocal analysis. (A) Western blots from fractionation of the cytoplasmic and nuclear fractions of K562 *CALR* WT and genome edited K562 *CALR* T1. The numbers above each lane indicate results of densitometric analysis. Data are from one representative experiment out of three. GAPDH and H2Ax were used for loading normalization, as markers respectively of the cytoplasmic and the nuclear compartment. **(B)** Western blots from fractionation of the cytoplasmic and nuclear fractions of genome edited K562 *CALR* KO transiently transfected with Flag-calreticulin WT/T1/T2 plasmids. Data are from one representative experiment out of three. GAPDH and H2Ax were used for loading normalization, as markers respectively of the cytoplasmic and the nuclear compartment. **(C)** Confocal microscopy analysis was performed in CRISPed K562 CALR KO transiently transfected with Flag-calreticulin WT/T1 plasmids and stained with anti-N terminal CALR antibody. DAPI was used for nuclear staining. The collected images were analyzed by Confocor 2 (Zeiss) software. A representative experiment out of 5 is shown.

Both wild-type e mutant proteins were found in the cell surface (**Figure 38A**). Of note, collecting the supernatant and whole cellular lysates, we observed higher amounts of CALR Type1 proteins in the supernatant in comparison to both lysates and the wild-type counterpart (**Figure 38B**).

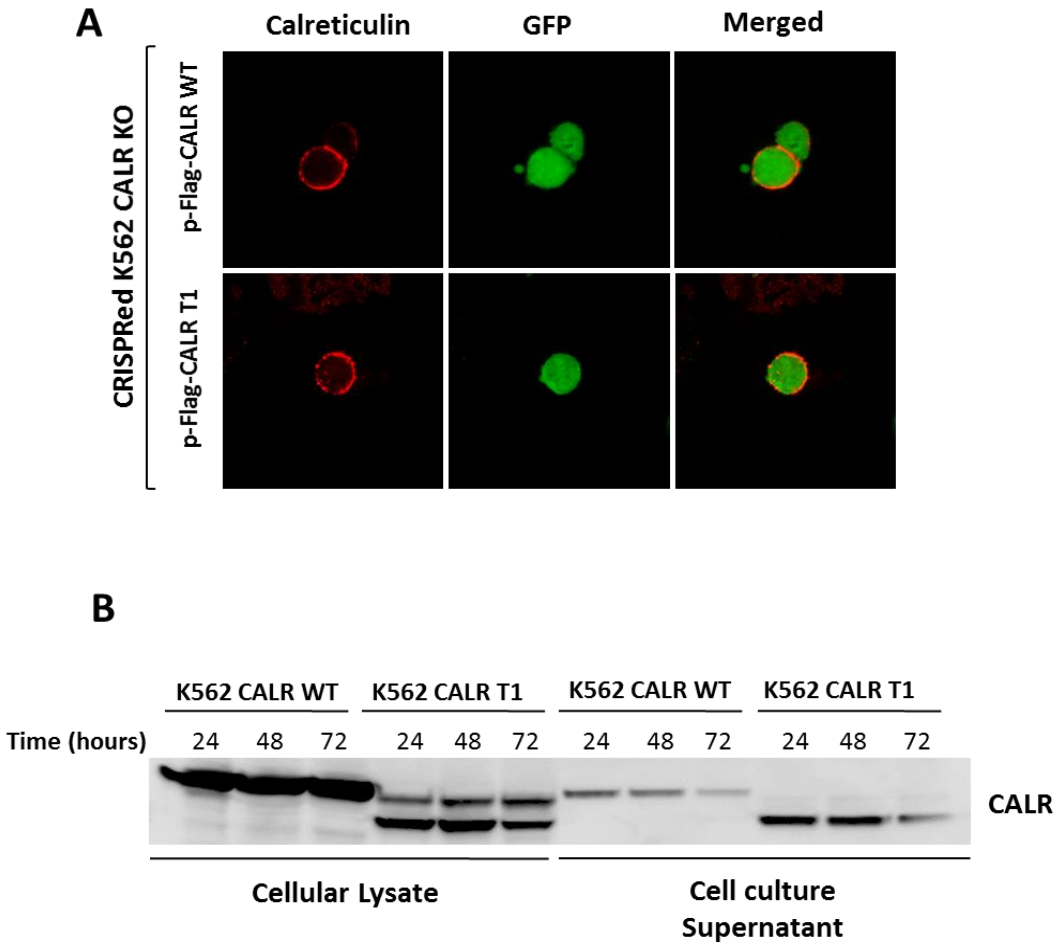

Figure 38: (A) Cell surface confocal analysis was performed in CRISPed K562 *CALR* KO transiently transfected with Flag-calreticulin WT/T1 plasmids and stained with anti-N terminal CALR antibody. A representative experiment out of 5 is shown**. (B)** Western blot of K562 and genome edited K562 CALR T1 whole cell lysate and cell culture supernatant. We collected each sample at indicated time (hours) points. Data are from one representative experiment out of three.

Overall, these findings indicate that CALR mutants are less easily detectable than their WT counterparts. This may be due either to a decreased protein stability of CALR mutants or an increased secretion in the extracellular compartment.

EFFECTS OF *CALR* MUTANT ON MEGAKARYOCYTOPOIESIS

CALR mutations are restricted to MPN subtypes displaying aberrant megakaryopoiesis, such as ET, PMF and post-essential thrombocythemia-myelofibrosis (post-ET PMF). Therefore, to deeply investigate the role of *CALR* mutations in the megakaryocytic (Mk) commitment, we cultured genome edited K562 cell lines with 10 nM of phorbol-myristate-acetate (PMA) for 72 hours. At that time is possible to observe significant changes in the cell morphology as well as the expression of CD41 and CD61 differentiation markers, evaluated by flow cytometry.

Interestingly, we found that CRISPRed K562 *CALR* KO and T1 cells showed accelerate and enhanced expression of CD41/CD61 compared to parental cells (2.25- and 3- fold higher respectively, $p<0.01$) (**Figure 39A**).

These data were further confirmed in K562 and K562 KO cells stably expressing CALR wild-type (WT), Type 1 (T1) and Type 2 (T2) generated transfecting cells with lentiviral vectors (kindly provided by Prof. Manfredini): the proportion of CD41/CD61 positive cells raised from 30% in WT cells to 55%, 62%, 70% respectively in T1, T2 and KO ($p<0.01$) (**Figure 39B**).

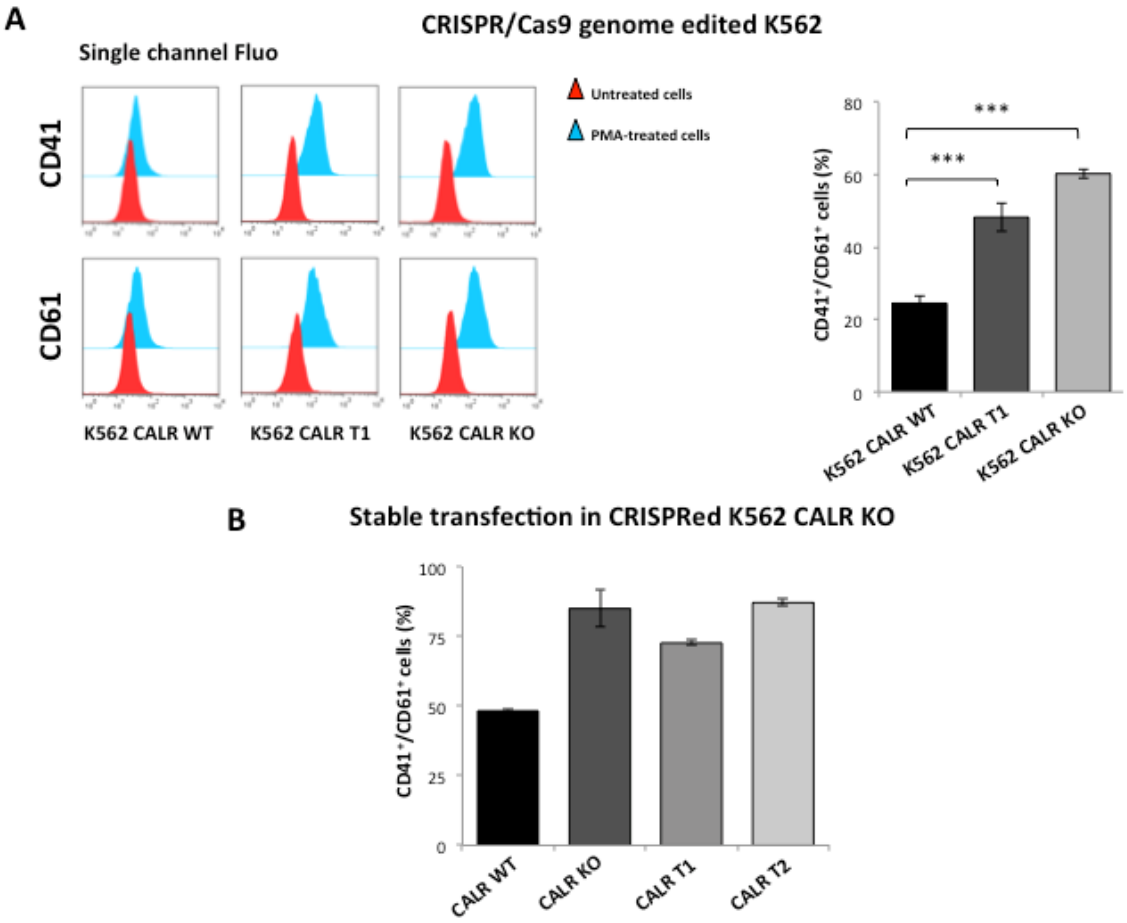

Figure 39: Induction of megakaryocytic commitment. (A) PMA stimulated K562 WT and genome edited K562 *CALR* T1 and *CALR* KO shows a various percentage of megakaryocytic commitment. On the left the histograms of the mean fluorescence intensity of CD41 and CD61 markers. On the right the percentages of cells CD41/CD61 positive cells. CALR T1 and KO cells show a 46% and 60% of cells expressing both Mk markers respectively, compared to a 22% double positive population in K562 CALR WT. **(B)** CRISPRed K562 *CALR* KO were transfected with lentiviral vector expressing CALR WT, CALR T1, CALR T2 and an empty vector used as control and cultured in Mk differentiating medium. Flow-cytometry analysis of Mk markers expression confirms CALR mutants and CALR KO cells with an increased capability of differentiation compared to CALR WT. Values are Means ± SD of at least three separate experiments (***p<0.01).

We also generated CRISPR/Cas9 *CALR* KO CD34+ cells from cord blood. Briefly, in this case, after the transfection we sorted GFP positive cells in bulk and we evaluated the efficiency of the genome editing with CRISPR by qRT-PCR to quantify the levels of *CALR* trancript (**Figure 40A**). We plated the cells in proper semisolid medium to allow megakaryocytic colonies growth: clonogenic assays showed that *CALR* KO CD34+ cells generated a number of CFU-Mk 7–fold higher than GFP negative (*CALR* WT) cells ($p<0.05$) (**Figure 40B**).

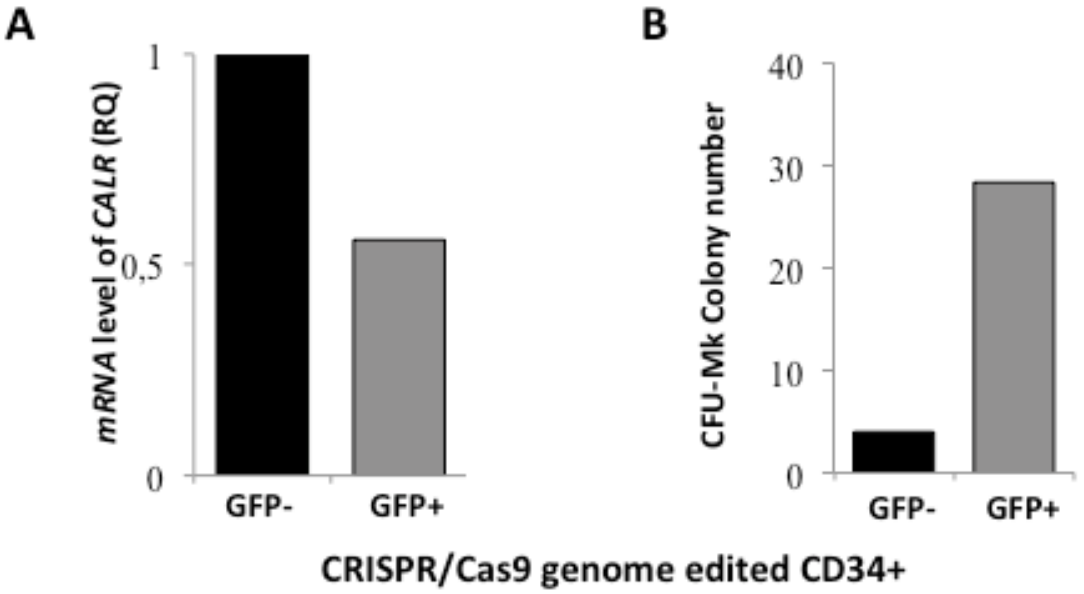

Figure 40: (A) *CALR mRNA* levels. We performed CRISPR/Cas 9 genome editing in CD34+ from cord blood: after the transfection we bulk sorted the GFP-positive cells into a tube containing the appropriate medium. GFP positive cells are validated with qRT-PCR to quantify the levels of CALR trancript. We obtained a reductions of about the 50% of *CALR mRNA*. **(B)** Clonogenic assays was performed with CD34+ GFP negative and positive cells. CFU-Mk colony number showed that *CALR* knock-down CD34+ cells generated a number of colonies 7–fold higher than GFP negative cells. Data are from one representative experiment out of three.

Overall, these data indicated that loss of wild-type CALR by CRISPR/Cas9-mediated target deletion in cell lines and primary CD34+ cells phenocopies the effects of *CALR* mutations on megakaryocytopoiesis.

GENERATION OF NEW ANTIBODIES AGAINST MUTATED CALRETICULIN.

All described *CALR* mutations cause a recurrent frameshift that results in a new C-terminal domain holding a common sequence of 36 aminoacidic. We previously developed a polyclonal antibody against a 17-peptide residue in the variant C terminus of mutated calreticulin that have proved able to label selectively BM sections from *CALR*-mutated MPN patients (Vannucchi et al., 2014).

Meantime, since the above mentioned polyclonal antibody volume was limited and with the additional purpose of generating a valid tool which could improve the knowledge of these mutations in MPN patients *ex-vivo*, we selected, by bioinformatic analysis, two novel immunogenic peptides suitable for immunization. These peptides

were used to immunize rabbits and mice aiming at producing polyclonal antibodies first and preliminary to the generation of monoclonal antibodies.

We developed and purified two new rabbit policlonal antibodies that were screened in ELISA assay against the synthetic peptides and the recombinant HIS-tagged CALR Type 1 (del52) protein that we have produced as well as the CALR wild-type one (commercially available). The screening provided evidences demostrating their binding to the mutated CALR only. Therefore, we performed confocal microscopy on genome edited K562 *CALR* KO transfected with Flag-tagged CALR- wild-type/Type1/Type2 vectors. The results showed the specificity and selectivity of these polyclonal antibodies for the mutated calreticulin (**Figure 41 and 42**).

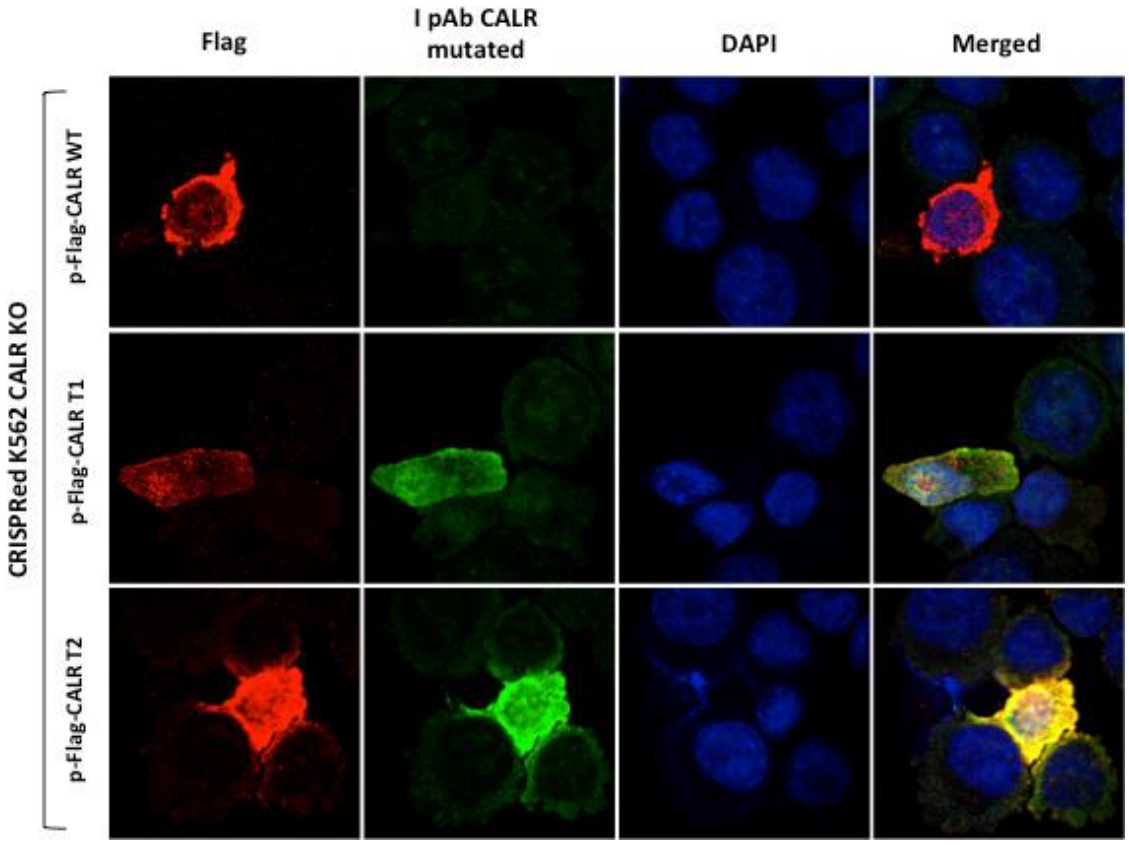

Figure 41: Confocal immunofluorescence microscopy was performed in previously described CRISPRed K562 *CALR* KO transiently transfected with Flag-calreticulin WT/T1/T2 plasmids and stained with anti-Flag and the **first rabbit polyclonal antibody anti-mutated CALR** that we had generated. Anti-rabbit IgG Cy2-conjugated or anti-mouse IgG Cy3-conjugated secondary antibodies were used. DAPI was used for nuclear staining. A representative experiment out of 5 is shown.

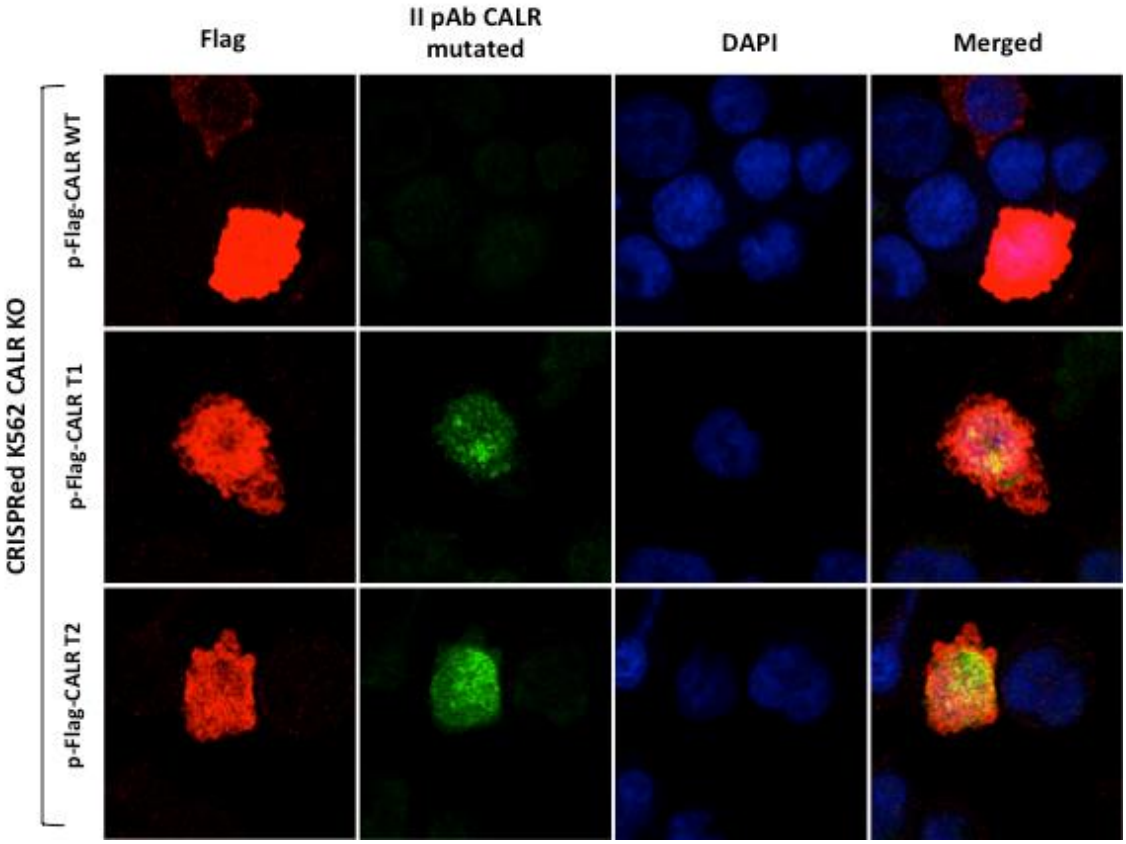

Figure 42: Confocal immunofluorescence microscopy was performed in previously described CRISPRed K562 CALR KO transiently transfected with Flag-calreticulin WT/T1/T2 plasmids and stained with anti-Flag and the **second rabbit polyclonal antibody anti-mutated CALR** that we had generated. Anti-rabbit IgG Cy2-conjugated or anti-mouse IgG Cy3-conjugated secondary antibodies were used. DAPI was used for nuclear staining. A representative experiment out of 5 is shown.

DISCUSSION

Mutations in the gene *calreticulin* have been recently reported in about 15-25% of patients with ET and PMF who are negative for the more common *JAK2*^{V617F} and *MPL* exon 10 mutations and have paved the way to a better understanding of MPN pathogenesis (Nangalia et al., 2013; Klampfl et al., 2013). The occasional simultaneous positivity for and *JAK2*^{V617F} and *CALR* mutation was reported to date in a handful of patients (Tefferi et al., 2014; Lundberg et al., 2014).

Known mutations of CALR are all located at exon 9 and, with the exception of a few non recurrent point mutations (Wu et al., 2014), all of these have been somatic deletions or insertions. The two commonest abnormalities (CALRdel52/Type 1 and CALRins5/Type 2) account for almost 80% of cases, while in the remaining 20% lesions are highly heterogeneous (Guglielmelli et al., 2014).

Although CALR mutated MPN patients seem to have a more benign prognosis in terms of survival and lower risk of thrombosis compared to JAK2 positive genotype (Rumi et al., 2014; Rotunno et al., 2014), the presence of these alterations leads to an aberrant megakaryopoiesis and a significant increase in the platelets number. Several studies showed how mutant CALR is highly expressed in the megakaryocyte lineage (Vannucchi et al., 2014), further confirmed by *in-vitro* and *in-vivo* researches (Marty et al., 2016; Elf et al., 2016; Shide et al., 2017).

Retrospective analysis on MPN *CALR*-mutated patients in clinical trials showed that they had benefited of JAK2-inhibition provided by Ruxolitinib therapy, supporting he involvment of JAK/STAT pathway with *CALR* mutations. Recent publications outlined the hypothesis that mutated CALR, owing to conformational changes imposed by novel C-terminus, is able to associate and active the thrombopoietin receptor (MPL) with subsequently activation of JAK2/STATs as well mitogen-activated protein kinase and phosphatidylinositol-3 kinase signaling (Balligand et al., 2016; Chachoua et al., 2016; Elf et al., 2016; Marty et al., 2016; Nivarthi et al., 2016; Araki et al., 2016). However, the molecular mechanism that links CALR mutations with MPNs is not fully understood.

Of note, it is necessary to underline the limitations of the available experimental tools employed till now to characterize these mutations: all models generated are hybrid cell systems in which the massive expression of the endogenous *CALR* gene, and hence wild-type, significantly mitigates the possible effects of the mutations ectopically introduced, whose expression is furthermore under the control a non-physiological promoter.

In this work, we aimed to create a model that overcome all the above mentioned limitations, allowing therefore mechanistic analysis of mutated *CALR* in a hematopoietic setting and its role in MPN pathogenesis.

We generated, by using the innovative CRISPR/Cas9 technology, *CALR* knock-out (KO) and *CALR* Type 1 (T1) variants starting from the BCR/ABL-mutated K562 cell line. CALR KO cell line could be a model to evaluate all the mechanisms involving calreticulin in the hematopoietic compartment, while the CALR T1 cell line represent the first *in-vitro* model expressing, by homologous recombination, the most common CALR mutation under the control of the endogenous promoter and without the "interference" of the wild-type (WT) gene. The efficiency of the CRISPR/Cas9 genome editing was also confirmed by Sanger sequencing analysis that corroborate the desired deletion of 52 bp in K562 CALR T1. We showed an equal amount of *CALR* transcripts in K562 WT and in genome edited K562 T1 cell lines, while no amplification was obtained in KO cells. As regard proteic level we confirmed the presence of CALR mutant protein demostrating a lower molecular weight compared to WT, while no CALR protein were detected in K562 KO.

By the characterization, genome edited K562 *CALR* KO and T1 showed no significant cell cycle and proliferation alterations compared to the wild-type cell line while we found a significant increased in the apoptosis resistance of KO and T1 cells when treated with chemotherapeutic agents in µM range, particularly upon treatment with Mitoxantrone. Such resistance, whose mechanism is still to be clarified, makes reason for the persistence of mutated clones that, whilst do not show a proliferative advantage, they are providing to be more able to resist the induction of apoptotic signals.

We observed a lower amounts of mutated protein than the wild-type counterpart, although mRNA was highly expressed. Our data suggest an increased

instability and turnover of mutated CALR compared to the wild-type, both at mRNA and protein level, that is in agreement with the findings reported by others colleagues (Chachoua et al., 2016; Han et al., 2016; Garbati et al., 2016).

The mutant calreticulin that remained in cells did not show marked changes in subcellular localization compared to wild-type calreticulin: it remained largely in the cytoplasm and it was found also in the cell surface, although, unlike the WT protein, only a slight proportion was in the nuclear fractions.

Interestingly we observed a greated amount of mutated protein in the cell culture supernatant that could explain our observations that Type 1 protein poorly expressed in cells.

CALR mutations are restricted to MPN subtypes displaying aberrant megakaryopoiesis, such as ET, PMF and post-ET PMF. The results provided by the megakaryocyte differentiation experiments clearly confirm the role of CALR alterations in these process. Our data suggest that CALR Type 1 and Type 2 increase megakaryocytic commitment, showing an higher expression of the typical differentiation markers CD41 and CD61 compared to control cell lines.

Interestingly, we observed that also the knock-out of the protein, in genome edited both cell lines and primary CD34+, resulted in promotion of megakaryocytopoiesis, mimicking the effects of CALR mutations.

Therefore, our data lead us to assert that the mutated protein, throught its structural confomational changes, might lose some of its physiologically functions and phenocopies the effects due to the absence of protein itself.

In this project, we wanted additionaly provide a tool which could improve the knowledge of these mutations in MPN patients *ex-vivo*. We exploited the fact that all exon 9 mutations result in a novel C-teminus of the protein with the acquisition of a minimum 36 amino acid stretch in plase of 27 amino acids that are lost from the normal sequence to generate novel immunogenic peptides. Therefore, we developed two polyclonal antibodies that proved able to label selectively and specificity mutated CALR only.

Overall, these data indicate that CALR-mutated models generated and specific anti-CALR mutated antibodies could be useful tools to study the pathogenic role of *CALR* mutations in MPNs and to develop new diagnostic and therapeutic strategies for future clinical applications.

REFERENCES

Abdel-Wahab O., Manshouri T., Patel J., Harris K., Yao J., Hedvat C., Heguy A., Bueso-Ramos C., Kantarjian H., Levine RL., Verstovsek S. *Genetic analysis of transforming events that convert chronic myeloproliferative neoplasms to leukemias*. Cancer Res. 2010. 70(2):447-452.

Adamson JW., Fialkow PJ., Murphy S., Prchal JF., Steinmann L.., *Polycythemia vera: stem-cell and probable clonal origin of the disease.* N Engl J Med. 1974; 290:1382.

Akada H., Yan D, Zou H, Flering S, Hutchison RE, Mohi MG. *Conditional expression of heterozygous or homozygous Jak2V617F from its endogenous promoter induces a polycithemia vera-like disease.* Blood. 2010. 115(17): 3589-3597.

Ahmed RZ., Rashid M., Ahmed N., Nadeem M. and Shamsi TS. *Coexisting JAK2V617F and CALR exon 9 mutations in myeloproliferative neoplasms- do they designate a new subtype?.* Asian Pacific J. Cancer Prev. 2016. 17(3): 923-926.

Araki M., Yang Y., Masubuchi N., Hironaka Y., Takei H., Morishita S., Mizukami Y., Kan S., Shirane S., Edahiro Y., Sunami y., Ohsaka A., Komatsu N. *Activation of the thrombopoietin receptor by mutant calreticulin in CALR-mutant myeloproliferative neoplasms.* Blood. 2016. 127(10):1307-1316.

Araki M., Komatsu N. *Novel Molecular mechanism of cellular transformation by a mutant molecular chaperone in myeloproliferative neoplasms*. Cancer Sci. 2017. 108(10):1907-1912.

Arber DA., Orazi A., Hasserjian R., Thiele J., Borowitz MJ., Le Beau MM., Bloomfiels CD., Cazzola M., Vardiman JW. *The 2016 revision to the World Health Organization classification of myeloid neoplasms and acute leukemia.* Blood. 2016; 127(20): 2391-405.

Ballingand T., Achouri Y., Pecquet C., Chachoua I., Nivarthi H., Marty C., Vainchenker W., Plo I., Kralovics R., and Constantinescu SN.. *Pathologic activation of thrombopoietin receptor and JAK2-STAT5 pathway by frameshift mutants of mouse calreticulin*. Leukemia. 2016. 30(8): 1775-1778.

Barbui T., Barosi G., Birgegard G., Cervantes F., Finazzi G., Griesshammer M., Harrison C., Hasselbalch HC., Hehlmann R., Hoffman R., Kiladjian JJ., Kröger N., Mesa R., McMullin MF., Pardanani A., Passamonti F., Vannucchi AM., Reiter A., Silver RT., Verstovsek S., Tefferi A.; European LeukemiaNet. *Philadelphia-negative classical myeloproliferative neoplasms: critical concepts and management recommendation from European LeukemiaNet*. J. Clin Oncol., Feb 20 2011; 29 (6): 761-770.

Barbui T, Thiele, J., Vannucchi, A.M., Tefferi, A. *Rationale for revision and proposed changes of the WHO diagnostic criteria for polycythemia vera, essential thrombocythemia and primary myelofibrosis.* Blood Cancer J. 2015. 5:e337.

Barbui T., Thiele j., Gisslinger H., Finazzi G., Vannucchi A.M., Tefferi A. *The 2016 revision of WHO classification of myeloproliferative neoplasms: Clinical and molecular advances*. Blood Reviews. 2016. 30: 453-459.

Barrangou, R., Fremaux C., Deveau H., Richards M., Boyaval P., Moineau S., Romero DA., Horvath P. *CRISPR provides acquired resistance against viruses in prokaryotes*. Science. 2007. 315: 1709–1712.

Bartalucci N., Bogani C., Vannucchi AM. *Preclinical models for drug selection in Myeloproliferative Neoplasms*. Curr Hematol Malign Rep. Springer. 2013. 8: 317-324.

Bartalucci N, Guglielmelli P, Vannucchi AM. *Rationale for Targeting the PI3K/Akt/mTOR Pathway in Myeloproliferative Neoplasms.* Clinical Lymphoma, Myeloma & Leukemia. 2013. 13(S2).

Bartalucci N., Tozzi L., Bogani C., Martinelli S., Rotunno G., Villeval JL, Vannucchi AM. *Co-targeting the PI3K/mTOR and JAK2 signalling pathways produces synergistic activity against myeloproliferative neoplasms*. J. Cell. Mol. Med. 2013; 17 (11): 1385-1396.

Bennet M., Strocek DF. *Recent advances in the bcr-abl negative chronic myeloproliferative diseases*. J Transl Med. 2006. 4: 41.

Bernal M., Jiménez P., Puerta J., Ruiz-Cabello F. and Jurado M. *Co-mutated CALR and MPL driver genes in patient with myeloproliferative neoplasm*. Ann. Hematol. 2017. 96(8): 1399-1401.

Berretta L., Gingras AC, Svitkin YV, Hall MN, Sonenberg N. Rapamycin blocks the phosphorylation of 4E-BP1 and inhibits cap-dependent initiation of translation. EBMO J., 1996; 15, 658-664.

Bhaya, D., Davison, M., and Barrangou, R. *CRISPR-Cas systems in bacteria and archaea: Versatile small RNAs for adaptive defense and regulation*. Annu. Rev. Genet. 2011. 45:273-297.

Blatt K., Herrmann H., Mirkina I., Hadzijusufovic E., Peter B., Strommer S., Hoermann G., Mayerhofer M., Hoetzenecker K., Klepetko W., Ghanim V., Marth K., Freder T., Wacheck V., Valenta R., Valent P. *The PI3-Kinase/mTOR-Targeting Drug NVP-BEZ235 Inhibits Growth and IgE-Dependent Activation of Human Mast Cells and Basophils*. PLoS ONE. 2012. 7(1): e29925.

Bogani C., Ponziani V., Guglielmelli P., Desterke C., Rosti V., Bosi A., Le Bousse-Kerdilès MC., Barosi G., Vannucchi AM. *Hypermethylation of CXCR4 promoter in CD34+ cells from patients with primary myelofibrosis*. Stem Cells. 2008. 26(8): 1920-30.

Bogani C., Bartalucci N., Martinelli S., Tozzi L., Guglielmelli P., Bosi A., Vannucchi AM., gruppo AGIMM. *mTOR inhibitors alone and in combination with JAK2 inhibitors effectively inhibit cells of Myeloproliferative Neoplasms*. Plos one. 2013. 1(8): e54826.

Brachmann SM., Kleylein-Sohn J., Gaulis S, Kauffmann A., Blommers MJ., Kazic-Legueux M., Hattenberger M., Stauffer F., Vaxelaire J., Romanet V., Henry C., Murakami M., Guthy DA., Sterker D., Bergling S., Wilson C., Brümmendorf T., Fritsch C., Garcia-Echeverria C., Sellers WR., Hofmann F., Maira SM. *Characterization of the mechanism of action of the pan class I PI3K inhibitor NVP-BKM120 across a broad range of concentrations.* Mol Cancer Ther. 2012; 11(8): 1747–57.

Brandts CH., Sargin B., Rode M., Biermann C., Lindtner B., Schwäble J., Buerger H., Müller-Tidow C., Choudhary C., McMahon M., Berdel WE., Serve H. *Constitutive activation of Akt by Flt3 internal tandem duplications is necessary for increased survival, proliferation, and myeloid transformation.* Cancer Res. 2005; 65(21):9643-50.

Brouns S.J., Jore MM., Lundgren M., Westra ER., Slijkhuis RJH., Snijders APL., Dickman MJ., Makarova KS., Koonin EV., and van der Oost J. *Small CRISPR RNAs guide antiviral defense in prokaryotes*. Science. 2008. 321(5891): 960-964.

Brush MH, Guardiola A, Connor JH, Yao TP., Shenolikar S. *Deactylase inhibitors distrupt cellular complexes containing protein phosphatases and deacetylases*. J Biol Chem. 2004. 279(9): 7685-7691.

Bumm TG., Elsea C., Corbin AS., Loriaux M., Sherbenou D., Wood L., Deininger J., Silver RT., Druker BJ., Deininger MW. *Characterization of murine JAK2V617F positive myeloproliferative disease.* Cancer Res. 2006; 66(23): 11156–65.

Buxhofer-Ausch V., Gisslinger H., Thiele J., Gisslinger B., Kvasnicka HM., Müllauer L., Frantal S., Carobbio A., Passamonti F., Rumi E., Ruggeri M., Rodeghiero F., Randi ML., Bertozzi I., Vannucchi AM., Antonioli E.,

Finazzi G., Gangat N., Tefferi A., Barbui T. *Leukocytosis as an important risk factor for arterial thrombosis in WHO-defined early/prefibrotic myelofibrosis: an international study of 264 patients.* Am J. Hematol. 2012. 87(7): 669-72.

Cabagnols X., Defour JP., Ugo V., Ianotto JC., Mossuz P., Mondet J., Girodon F., Alexandre JH., Mansier O., Viallard JF., Lippert E., Murati A., Mozziconacci MJ., Saussoy P., Vekemans MC., Knoops L., Pasquier F., Ribrag V., Solary E., Plo I., Constantinescu SN., Casadevall N., Vainchenker W., Marzac C., Bluteau O., *Differential association of calreticulin type 1 and type 2 mutations with myelofibrosis and essential thrombocythemia: relevance for disease evolution*. Leukemia. 2015. 29(1): 249-52.

Campbell PJ., Green AR. *The myeloproliferative disorders*. N Engl J Med. 2006; 355(23):2452-2466.

Cardoso BA., Belo H., Barat JT., Almeida AM. *The Bone Marrow-Mediated Protection of Myeloproliferative neoplastic cells to Vorinostat and Ruxolitinib Relies on the Activation of JNK and PI3K Signalling pathways.* PLoS One. 2015. 10(12): e014897.

Carte J., Wang R., Li H., Terns RM., and Terns MP. *Cas6 is an endoribonuclease that generates guide RNAs for invader defense in prokaryotes*. Genes Dev. 2008. 22(24): 3489-3496.

Cervantes F., Barosi G., Hernàndez-Boluda JC., Marchetti M., Montserrat E. *Myelofibrosis with myeloid metaplasia in adult individuals 30 years old or younger: Presenting features, evolution and survival*. Eur J Haematol. 2001. 66(5): 324-7.

Chachoua I., Pecquet C., El-Khoury M., Nivarthi H., Albu R-I. Marty C., Gryshkova V., Defour J-P. Vertenoeil G., Ngo A., Koay A., Raslova H., Courtoy PJ. Choong ML., Plo I., Vainchenker W., Kralovics R., Costantinescu SN. *Thrombopoietin receptor activation by myeloproliferative neoplasm associated calreticulin mutants*. Blood. 2016. 127(10):1325-1335.

Chao MP., Majeti R., Weissman IL. Programmed cell removal: a new obstacle in the road to developing cancer. Nat Rev Cancer. 2012. 12(1): 58-67.

Chen F., Pruett-Miller SM., Huang Y., Gjoka M., Duda K., Taunton J., Collingwood T.N., Frodin M., and Davis GD. *High-frequency genome editing using ssDNA oligonucleotides with zinc-finger nucleases. Nat*. Methods. 2011. 8(9): 753-755.

Chen JS., Dagdas YS., Kleinstiver BP., Welch MM., Sousa AA., Harrington LB., Sternberg SH., Joung K., Yildiz A., Doudna JA.. Enhanced proofreading governs CRISPR–Cas9 targeting accuracy. Nature. 2017. 550(7676): 407–410.

Cho SW., Kim S., Kim JM., and Kim JS. 2013. *Targeted genome engineering in human cells with the Cas9 RNA-guided endonuclease*. Nat. Biotechnol. 2013. 31(3): 230-232.

Cho SW., Kim S., Kim Y., Kweon J., Kim HS., Bae S., Kim JS. *Analysis of off-target effects of CRISPR/Cas-derived RNA-guided endonucleases and nickases*. Genome Res.. 2014. 24(1): 132–141.

Chou TC., Talaly P. *A simple generalized equation for the analysis of multiple inhibitions of Michaelis-Menten kinetic systems*. J Biol Chem. 1977. 252(18):6438-42.

Chou TC. *Drug combination studies and their synergy quantification using the Chou-Talalay method*. Cancer Res. 2010. 70(2): 440–6.

Ciccone M., Calin GA, Perrotti D. *From the Biology of PP2A to the PADs for therapy of hematologic malignancies.* Front Oncol. 2015. 5:21.

Cong L.., Ran FA., Cox D., Lin S., Barretto R., Habib N., Hsu PD., Wu X., Jiang W., Marraffini L.A., and Zhang F. *Multiplex genome engineering using CRISPR/Cas systems*. Science. 2013. 339(6121): 819-823.

Cortes-Ledesma F., Aguilera A. *Double-strand breaks arising by replication through a nick are repaired by cohesin-dependent sister-chromatid exchange*. EMBO Rep. 2006. 7(9):919-26.

Dameshek W. *Some speculation on the myeloproliferative syndromes*. Blood. 1951. 6: 372-5.

Deltcheva E., Chylinski K., Sharma CM., Gonzales K., Chao Y., Pirzada ZA., Eckert MR., Vogel J., and Charpentier E. *CRISPR RNA maturation by trans-encoded small RNA and host factor RNase III*. Nature. 2011. 471(7340): 602-607.

Denning GM., Leidal KG, Holst VA., Iyer SS., Pearson DW., Clark JR., Nauseef WM., Clark RA. *Calreticulin biosynthesis and processing in human myeloid cells: demonstration of signal peptide cleavage and N-glycosilation*. Blood. 1997. 90(1): 372-81.

DiCarlo JE., Norville JE., Mali P., Rios X., Aach J., and Church GM. *Genome engineering in Saccharomyces cerevisiae using CRISPR-Cas systems*. Nucleic Acids Res. 2013. 41:4336-4343.

Dilling BD., Germain G., Dudkin L., Jayaraman A.L., Zhang X., Harwood F., Houghtnn P. *4E-binding proteins, the suppressors of eukaryotic initiation factor 4E, are down-regulated in cells with acquired or intrinsic resistance to rapamycin*. J.Biol.Chem. 2002. 277(16): 13907-13917.

Dowling RJ, Topisirovic I, Alain T, Bidinosti M., Fonseca BD., Petroulakis E., Wang X., Larsson O., Selvaraj A., Liu Y., Kozma SC., Thomas G., Sonenberg N. *mTORC1-mediated cell proliferation, but not cell growth, controlled by the 4E-BPs*. Science. 2010. 328(5982): 1172-6.

Durrant ST., Nagler A., Vannucchi AM., Lavie D., Chuah C., Passamonti F., Gisslinger H., Le Coutre P., Gopalakrishna O., Mahuzier B., Mo S. and Martinez-Lopez J. An Open-Label, Multicenter, 2-Arm, Dose-Finding, Phase 1b Study of the Combination of Ruxolitinib and Buparlisib (BKM120) in Patients with Myelofibrosis: Results from HARMONY Study. Blood. 2015. 126(23): 827.

Elf S., Abdelfattah NS., Chen E. Perales-Paton J., A.Rosen E., Ko A., Peisker F., Florescu N., Giannini S., Wolach O., A.Morgan E., Tothova Z., Losman J-A., Schneider RK., Al-Shahrour F., Mullally A. *Mutant calreticulin requires both its mutant C-terminus and the thrombopoietin receptor for oncogenic transformation.* Cancer Discov. 2016. 6(4): 368-381.

Epstein E., Goedel A. *Hamorrhagische thrombozythamie bei vascularer schrumpfmilz (Hemorrhagic thrombocythemia with a vascular, sclerotic spleen).* Virchows Archiv A Pathol Anat Histopathol. 1934. 293: 233-248.

Feng Z., Zhang H., Levine AJ., Jin S. *The coordinate regulation of the p53 and mTOR pathways in cells.* Proc Natl Acad Sci U S A. 2005. 102(23): 8204-9.

Fiskus W., Verstovsek S., Manshouri T., Smith J.E., Peth K., Abhyankar S., McGuirk J., Bhalla K.N. *Dual PI3K/AKT/mTOR inhibitor BEZ235 synergistically enhances the activity of JAK2 inhibitor against cultured and primary human myeloproliferative neoplasm cells*. Haematologica. 2013. 98 (10): 1499-1509.

Foster JG, Blunt MD, Carter E, Ward SG*. Inhibition of PI3K signaling spurs new therapeutic opportunities in inflammatory/autoimmune diseases and hematological malignancies*. Pharmacol Rev. 2012. 64(4): 1027-54.

Friedland AE., Tzur YB., Esvelt KM., Colaiacovo MP., Church GM., Calarco JA. *Heritable genome editing in C. elegans via a CRISPR-Cas9 system*. Nat. Methods. 2013. 10(8): 741-743.

Fu Y., Sander JD., Reyon D., Cascio VM., Joung JK. *Improving CRISPR-Cas nuclease specificity using truncated guide RNAs.* Nat. Biotechnol. 2014. 32(3): 279-284.

Fu Y., Foden JA., Khayter C., Maeder ML., Reyon D., Joung JK., Sander JD. *High-frequency off-target mutagenesis induced by CRISPR-Cas nucleases in human cells*. Nat. Biotechnol. 2013. 31(9): 822–826.

Garbati MR., Welgan CA., Landefeld SH., Newell LF., Agarwal A., Dunlap JB., Chourasia TK., Lee H., Elferich J., Traer E., Rattray R., Cascio MJ., Press RD., Bagby GC., Tyner JW., Druker BJ., Dao KH. *Mutant calreticulin-expressing cells induce monocyte hyperactivity through a paracrine mechanism*. Am J Hematol. 2016. 91(2): 211-219.

Garneau JE., Dupuis M., Villion M., Romero DA., Barrangou R., Boyaval P., Fremaux C., Horvath P., Magadán AH., Moineau S. *The CRISPR/Cas bacterial immune system cleaves bacteriophage and plasmid DNA*. Nature. 2010. 468(7320): 67-71.

Gasiunas G., Barrangou R., Horvath P., Siksnys V. *Cas9-crRNA ribonucleoprotein complex mediates specific DNA cleavage for adaptive immunity in bacteria*. Proc. Natl. Acad. Sci. USA. 2012. 109(39): E2579–E2586.

Ghaffari S., Kitidis C., Zhao W., Marinkivic D., Fleming MD., Luo B., Marzalek J., Lodish HF. *AKT induces erythroid-cell maturation of JAK2-deficient fetal liver progenitor cells and is required for Epo regulation of erythroid-cell differentiation.* Blood. 2006. 107(5): 1888-1891.

Gold LI., Eggleton P., Sweetwyne MT., Van Duyn LB., Greives MR., Naylor SM., Michalak M., Murphy-Ullrich JE. *Calreticulin: non-endoplasmic reticulum functions in physiology and disease.* FASEB J. 2010. 24(3): 665–683.

Gratz SJ., Cummings AM., Nguyen JN., Hamm DC., Donohue LK., Harrison MM., Wildonger J., O'Connor-Giles KM. *Genome engineering of Drosophila with the CRISPR RNA-guided Cas9 nuclease*. Genetics. 2013. 194(4): 1029-1035.

Grimwade LF., Happerfield L., Tristram C., McIntosh G., Rees M., Bench AJ., Boyd EM., Hall M., Quinn A., Piggot N., Scorer P., Scott MA., Erber WN. *Phospho-STAT5 and phospho-Akt expression in chronic myeloproliferative neoplasms.* Br J Haematol. 2009. 147(4): 495-506.

Guertin DA., Sabatini DM. *Defining the role of mTOR in cancer*. Cancer Cell. 2007. 12(1):9-22.

Guertin DA., Stevens DM., Saitoh M., Kinkel S., Crosby K., Sheen JH., Mullholland DJ., Magnuson MA., Wu H., Sabatini DM. *mTOR complex 2 is required for the development of prostate cancer induced by Pten loss in mice*. Cancer Cell. 2009. 15(2): 148-59.

Guglielmelli P., Pancrazzi A., Bergamaschi G., Rosti V., Villani L.., Antonioli E., Bosi A., Barosi G., Vannucchi AM. GIMEMA--Italian Registry of Myelofibrosis; MPD Research Consortium. *Anaemia characterises patients with myelofibrosis harbouring Mpl mutation*. Br J Haematol. 2007. 137(3): 244-247.

Guglielmelli P., Zini R., Bogani C., Salati S., PancrazzI A., Bianchi E., Mannelli F., Ferrari S., Le Bousse-Kerdilès MC., Bosi A., Barosi G., Migliaccio AR., Manfredini R., Vannucchi AM. *Molecular profiling of CD34+ cells in idiopathic myelofibrosis identifies a set of disease-associated genes and reveals the clinical significance of Wilms' tumor gene 1 (WT1).* Stem Cells. 2007. 25(1): 165–173.

Guglielmelli P., Barosi G., Pieri L., Antonioli E., Bosi A., Vannucchi AM. *JAK2V617F mutational status and allele burden have little influence on clinical phenotype and prognosis in patients with post-polycythemia vera and post-essential thrombocythemia myelofibrosis.* Haematologica. 2009. 94(1): 144-146.

Guglielmelli P., Barosi G., Rambaldi A., Marchioli R., Masciulli A., Tozzi L., Biamonte F., Bartalucci N., Gattoni E., Lupo ML., Finazzi G., Pancrazzi A., Antonioli E., Susini MC., Pieri L., Malevolti E., Usala E., Occhini U., Grossi A., Caglio S., Paratore S., Bosi A., Barbui T., Vannucchi AM. AIRC-Gruppo Italiano Malattie Mieloproliferative (AGIMM) investigators. *Safety and efficacy of everolimus, a mTOR inhibitor, as single agent in a phase 1/2 study in patients with myelofibrosis.* Blood. 2011. 118(8): 2069-2076.

Guglielmelli P., Nangalia J., Green AR., Vannucchi AM. *CALR mutations in myeloproliferative neoplams: Hidden behind the reticulum*. Am J Hematol. 2014. 89(5): 453-456.

Guglielmelli P., Lasho TL., Rotunno G., Score J., Mannarelli C., Pancrazzi A., Biamonte F., Pardanani A., Zoi K., Reiter A., Duncombe A., Fanelli T., Pietra D., Rumi E., Finke C., Gangat N., Ketterling RP., Knudson RA., Hanson CA., Bosi A., Pereira A., Manfredini R., Cervantes F., Barosi G., Cazzola M., Cross NC., Vannucchi AM., Tefferi A. *The number of prognostically detrimental mutations and prognosis in primary myelofibrosis: an international study of 797 patients*. Leukemia. 2014. 28(9): 1804-10.

Guglielmellli P., Pacilli A., Rotunno G., Rumi E., Rosti V., Delaini F., Maffioli M, Fanelli T., Pancrazzi A., Pietra D., Salmoiraghi S., Mannarelli C., Franci A., Paoli C., Rambaldi A., Passamponti f., Barosi G., Barbui T., Cazzola M., Vannucchi AM. *Presentation and outcome of patients with 2016 WHO diagnosis of prefibrotic and overt primary myelofibrosis*. Blood. 2017. 129 (24): 3227-3236.

Guo L., Groenendyk J., Papp S., Dabrowska M., Knoblach B., Kay C., Parker JM., Opas M., Michalak M. *Identification of a N-domain histidine essential for chaperone function of calreticulin*. J Biol Chem. 2003. 278(50): 50645-53.

Hale C., Kleppe K., Terns RM., Terns MP. *Prokaryotic silencing (psi)RNAs in Pyrococcus furiosus.* RNA. 2008. 14(12): 2572-2579.

Han L., Schubert C., Kohler J., Schemionek M., Isfort S., Brummendorf TH., Koschmieder S., Chatain N. *Calreticulin-mutant proteins induce megakaryocytic signaling to transform hematopoietic cells and undergo accelerated degradation and Golgi-mediated secretion*. J Hematol Oncol. 2016. 9(1): 45.

Harutyunyan A., Klampfl T., Cazzola M., Kralovics R. *"p53 lesions in leukemic transformation."* N Engl J Med. 2011. 364(5): 488-490.

Harrison C., Kiladjian JJ., Al-Ali HK., Gisslinger H., Waltzman R., Stalbovskaya V., McQuitty M., Hunter DS., Levy R., Knoops L., Cervantes F., Vannucchi AM., Barbui T., Barosi G. *JAK inhibition with ruxolitinib versus best available therapy for myelofibrosis.* N Engl J Med. 2012. 366(9): 787-98.

Harrison CN., Vannucchi AM., Kiladjian JJ., Al-Ali HK., Gisslinger H., Knoops L., Cervantes F., Jones MM., Sun K., McQuitty M., Stalbovskaya V., Gopalakrishna P., Barbui T. *Long-term findings from COMFORT-II, a phase 3 study of ruxolitinib vs best available therapy for myelofibrosis*. Leukemia. 2016. 30(8): 1701-7.

Heuck G. *Zwei Falle von Leukamie mit eigenthumlichem Blut- resp. Knochenmarksbefund (Two cases of leukemia with peculiar blood and bone marrow findings, respectively).* Arch Pathol Anat Physiol Virchows. 1879. 78(3): 475-96.

Hietakangas V., Cohen SM. *Regulation of tissue growth through nutrient sensing.* Annu Rev Genet. 2009. 43:389-410.

Hirasawa T., Miyazawa M., Yasuda M., Shida M., Ikeda M., Kajiwara H., Matsui N., Fujita M., Muramatsu T., Mikami M. *Alterations of hypoxia-induced factor signaling pathway due to mammalian target of rapamycin (mTOR) suppression in ovarian clear cell adenocarcinoma: in vivo and in vitro explorations for clinical trial*. Int J Gynecol Cancer. 2013. 23(7): 1210-1218.

Hsu PD., Scott DA., Weinstein JA., Ran FA., Konermann S., Agarwala V., Li Y., Fine EJ., Wu X., Shalem O., Cradick TJ., Marraffini LA., Bao G., Zhang F. *DNA targeting specificity of RNA-guided Cas9 nucleases.* Nat. Biotechnol. 2013. 31(9): 827–832.

Hwang WY., Fu Y., Reyon D., Maeder ML., Tsai SQ., Sander JD., Peterson RT., Yeh JR., Joung, JK. *Efficient genome editing in zebrafish using a CRISPR-Cas system.* Nat. Biotechnol. 2013. 31:227-229.

Imai M., Araki M., Komatsu N. *Somatic mutations of calreticulin in myeloproliferative neoplams*. Int J Hematol. 2017. 105: 743-747.

Ishino Y., Shinagawa H., Makino K., Amemura M., Nakata A. *Nucleotide sequence of the iap gene, responsible for alkaline phosphatase isozyme conversion in Escherichia coli, and identification of the gene product.* J. Bacteriol. 1987. 169(12): 5429-5433.

Jacobs P., Maze S., Tayob F. *Myelofibrosis, splenomegaly, and portal hypertension*. Acta Haematol. 1985. 74:45.

James C., Ugo V., Le Couédic JP., Staerk J., Delhommeau F., Lacout C., Garcon L., Raslova H., Berger R., Bennaceur-Griscelli A., Villeval JL., Constantinescu SN., Casadevall N., Vainchenker W. *A unique clonal JAK2 mutation leading to constitutive signalling causes polycythaemia vera.* Nature. 2005. 434: 1144-1148.

Jinek M., Chylinski K., Fonfara I., Hauer M., Doudna JA., Charpentier E. *A programmable dual-RNA-guided DNA endonuclease in adaptive bacterial immunity.* Science. 2012. 337:816-821.

Jinek M., East A., Cheng A., Lin S., Ma E., Doudna J. *RNA-programmed genome editing in human cells.* Elife. 2013. 2: e00471.

Jore MM., Lundgren M., Van Duijn E., Bultema JB.,Westra ER., Waghmare SP.,Wiedenheft B., Pul U., Wurm R.,Wagner R., Beijer MR., Barendregt A., Zhou K., Snijders AP., Dickman MJ., Doudna JA., Boekema EJ., Heck AJ., van der Oost J., Brouns SJ. *Structural basis for CRISPR RNA-guided DNA recognition by Cascade.* Nat. Struct. Mol. Biol. 2011. 18(5): 529-536.

Jung HM., Patel RS, Phillips BL., Wang H., Cohen DM., Reinhold WC, Chang LJ, Yang LJ., Chan EK. *Tumor suppressor miR-375 regulates MYC expression via repression of CIP2A coding sequence through multiple repression of CIP2A coding sequence through multiple miRNA-mRNA interactions*. Mol Biol Cell. 2013. 24:1638-1648. S1631-1637.

Jung HM., Phillips BL., Chan EK. *miR-375 activates p21 and suppresses telomerase activity by coordinately regulating HPV E6/E7, E6AP, CIP2A, and 14-3-3ζ.*. Mol Cancer. 2014. 13:80.

Kapoor M., Srivinas H., Kandiah E. Gemma E., Ellgaard L., Oscarson S., Helenius A., Surolia A. *Interactions of substrate with calreticulin, an endoplasmic reticulum chaperone.* J Biol Chem. 2003. 278(8): 6194-200.

Karar J., Cerniglia GJ., Lindsten T., Koumenis C., Maity A. *Dual PI3K/mTOR inhibitor NVP-BEZ235 suppresses hypoxia-inducible factor (HIF)-1alpha expression by blocking protein translation and increases cell death under hypoxia*. Cancer Biol Ther. 2012. 13(11): 1102-1111.

Kharas MG., Fruman DA*. ABL oncogenes and phosphoinositide 3-kinase: mechanism of activation and downstream effectors.* Cancer Res. 2005. 65(6): 2047-53.

Khan I., Huang Z., Wen Q., Stankiewicz MJ., Gilles L., Goldenson B., Schultz R., Diebold L., Gurbuxani S., Finke CM., Lasho TL., Koppikar P., Pardanani A., Stein B., Altman JK., Levine RL., Tefferi A., Crispino JD. *AKT is a therapeutic target in myeloproliferative neoplasms*. Leukemia. 2013. 27(9): 1882-90.

Klampfl T., Gisslinger H., Harutyunyan AS., Nivarthi H., Rumi E., Milosevic JD., Them NC., Berg T, Gisslinger B, pietra D, Chen D, Vladimer GI, Bagienski K, Milanesi C, Casetti IC, Sant'Antonio E, Ferretti V, Elena C, Schischlik F, Cleary C, Six M, Schalling M, Schonegger A, Bock C, malcovati L, Pascutto C, Superi-Furga G, Cazzola M, Kralovics R. *Somatic mutations of calreticulin in myeloproliferative neoplasms*. New England Journal of Medicine. 2013. 369(25): 2379-2390.

Saeidi K. *Myeloproliferative neoplasms: Current molecular biology and genetics*. Critical Reviews in Oncology/Hematology. 2016. 98: 375-389.

Kralovics R., Stockton DW., Prchal TJ. *Clonal hematopoiesis in familial polycythemia vera suggests the involvment of multiple mutational events in the early pathogenesis of the disease*. Blood. 2003. 102(10): 3793-3796.

Kralovics R., Passamonti F., Buser AS., Teo SS., Tiedt R., Passweg JR., Tichelli A., Cazzola M., Skoda RC. *A gain-of-function mutation of JAK2 in myeloproliferative disorders.* N Engl J Med. 2005 Apr. 352:1779-1790.

Kroger NM., Deeg JH., Olavarria E., Niederwieser D., Bacigalupo A., Barbui T., Rambaldi A., Mesa R., Tefferi A., Griesshammer M., Gupta V., Harrison C., Alchalby H., Vannucchi AM., Cervantes F., Robin M., Ditschkowski M., Fauble V., McLornan D., Ballen K., Popat UR., Passamonti F., Rondelli D., Barosi G. *Indication and management of allogenic stem cell transplantation in primary myelofibrosis: A consensus process by an EBMT/ELN international working group.* Leukemia. 2015. 29(11): 2126-33.

Kubota Y., Ohnishi H., Kitanaka A., Ishida T., Tanaka T. *Constitutive activation of PI3K is involved in the spontaneous proliferation of primary acute myeloid leukemia cells: direct evidence of PI3K activation.* Leukemia. 2004. 18(8): 1438-40.

Kubovcakova L., Lundberg P., Grisouard J., Hao-Shen H., Romanet V., Andraos R., Murakami M., Dirhofer S., Wagner K., Radimerski T., Skoda RC. Differential effects of hydroxyurea and INC424 on mutant allele burden and myeloproliferative phenotype in a JAK2-V617F polycitemia vera mouse model. Blood. 2013. 121: 1188-1199.

Kundrapu K., Colenberg L., Duhe RJ. *Activation loop tyrosines allow the JAK2(V617F) mutant to attain hyperactivation*. Cell Biochem. Biophys. 2008. 52(2): 103–12.

Kuzminov A. *Single-strand interruptions in replicating chromosomes cause double-strand breaks.* Proc Natl Acad Sci. 2001;98:8241-6.

Lacout C., Pisani DF., Tulliez M., Gachelin FM., Vainchenker W., Villeval JL. *JAK2V617F expression in murine hematopoietic cells leads to MPD mimicking human PV with secondary myelofibrosis.* Blood. 2006. 108(5):1652-60.

Lasho TL., Pardanani A., McClure RF., Mesa RA., Levine RL., Gilliland DG., Tefferi A. *Concurrent MPL515 and JAK2V617F mutations in myelofibrosis: chronology of clonal emergence and changes in mutant allele burden over time.* Br. J. Haematol. 2006; 135(5): 683–687.

Lenz G., Staudt LM. *Aggressive lymphomas*. N Engl J Med. 2010. 362(15): 1417-29.

Levine RL., Wadleigh M., Cools J., Ebert B., Wernig G., Huntly B., Boggon T., Wlodarska I., Clark J., Moore S., Adelsperger J., Koo S., Lee J., Gabriel S., Mercher T., D'Andrea A., Frohling S., Dohner K., Marynen P., Vandenberghe P., Mesa R., Tefferi A., Griffin J., Eck M., Sellers W., Meyerson M., Golub T., Lee S. Gilliland DG. *Activating mutation in the tyrosine kinase JAK2 in polycythemia vera, essential thrombocythemia, and myeloid metaplasia with myelofibrosis.* Cancer Cell. 2005. 7(4): 387-39.

Levine RL., Gary Gilliland. *Myeloproliferative disorders.* Blood. 2008. 112(6): 2190-2198.

Li J., Spensberger D., Sook Ahn J., Anand S., Beer P., Ghevaert C., Chen E., Forrai A., Scott LM., Ferreira R., Campbell PJ., Watson SP., Liu P., Erber WN., Huntly B., Ottersbach K., Green AR. *JAK2 V617F impairs hematopoietic stem cell function in a conditional knock-in mouse model of JAK2 V617F-positive essential thrombocytemia*. Blood. 2010. 116(9): 1528-1538.

Li J., Kent DG., Chen E., Green AR. *Mouse models of myeloproliferative neoplasms: JAK of all grades.* Dis Model Mech. 2011. 4(3): 311–7.

Lin G., Gai R., Chen Z., Wang Y., Liao S., Dong R., Zhu H., Gu Y., He Q., Yang B. *The dual PI3K/mTOR inhibitor NVP-BEZ235 prevents epithelial-mesenchymal transition induced by hypoxia and TGF-β1.* Eur J Pharmacol. 2014. 729:45-53.

Lluis F., Cosma MP. *Somatic cell reprogramming control: signaling pathway modulation versus transcription factor activities*. Cell Cycle. 2009. 8(8): 1138-44.

Lundberg P., Karow A. Nienhold R., Looser R., Hao-Shen H., Nissen I., Girsberger S., Lehmann T., Passweg J., Stern M., Beisel C., Kralovics R., Skoda RC. *Clonal evolution and clinical correlates of somatic mutations in myeloproliferative neoplasms.* Blood. 2014. 123(14): 2220-2228.

Maira SM., Stauffer F., Brueggen J., Furet P., Schnell C., Fritsch C., Brachmann S, Chèene P, De Pover A, Schoemaker K, Fabbro D, Gabriel D, Simonen M, Murphy L, Finan P, Sellers W, Garcia-Echeverria C. *Identification and development of NVP-BEZ235, a new orally available dual PI3K/mTOR inhibitor with potent in vivo antitumor activity*. Mol Cancer Ther. 2008. 7:1851–1863.

Maira SM., Pecchi S., Huang A., Burger M., Knapp M., Sterker D., Schnell C., Guthy D., Nagel T., Wiesmann M., Brachmann S., Fritsch C., Dorsch M., Chène P., Shoemaker K., De Pover A., Menezes D., Martiny-Baron G., Fabbro D., Wilson CJ., Hoffman F., Garcia-Echeverria C., Sellers W., Voliva CF. *Identification and characterization of NVP-BKM120, an orally available pan-class I PI3-kinase inhibitor*. Mol Cancer Ther. 2012. 11(2): 317–28.

Mali P., Yang L., Esvelt KM., Aach J., Guell M., DiCarlo JE., Norville JE., Church GM. *RNA-guided human genome engineering via Cas9.* Science. 2013. 339(6121): 823-826.

Mali P., Aach J., Stranges PB., Esvelt KM., Moosburner M., Kosuri S., Yang L., Church GM. *CAS9 transcriptional activators for target specificity screening and paired nickases for cooperative genome engineering.* Nat. Biotechnol. 2013. 31(9): 833-838.

Marraffini LA. *CRISPR-Cas immunity in prokaryotes*. Nature. 2015. 526 (7571): 55–61.

Martin V., Groenendyk J., Steiner SS., Guo L., Dabrowska M., Parker JM., Müller-Esterl W., Opas M., Michalak M. *Identification by mutational analysis of amino acid residues essential in the chaperone function of calreticulin.* J Biol Chemc. 2006. 281(4): 2338-46.

Marty C, Lacout C, Martin A. Hasan S., Jacquot S., Birling MC., Vainchenker W., Villeval JL. *Myeloproliferative neoplasm induced by constitutive expression of JAKV617F in knock-in mice*. Blood. 2010. 116(5): 783-787.

Marty C., Pecquet C., Nivarthi H., El-Khoury M., Chachoua I., Tulliez M., Villeval J-L., Raslova H., Kralovics R., Costantinescu SN., Plo I., Vainchenker W. *Calreticulin mutant in mice induce an MPL-dependent thrombocytosis with frequent progression to myelofibrosis.* Blood. 2016. 127(10): 1317-1324.

Massa M., Rosti V., Ramajoli I., Campanelli R., Pecci A., Viarengo G., Meli V., Marchetti M., Hoffman R., Barosi G. *Circulating CD34+, CD133+ and vascular endothelial growth factor receptor 2-positive endothelial progenitor cells in myelofibrosis with myeloid metaplasia*. J Clin Oncol. 2005. 23(24): 5688-5695.

McGaffin G., Harper K., Stirling D., McLintock L. *JAK2 V617F and CALR mutations are not mutually exclusive; findings from retrospective analysis of a small patient cohort.* Br J Haematol. 2014. 167(2): 276-278.

Mèndez R, Myers MG Jr, White MF, Rhoads RE. *Stimulation of protein synthesis, eukaryotic translation initiation factor 4E phosphorylation, and PHAS-I phosphorylation by insulin requires insulin receptor substrate 1 and phosphatidylinositol 3-kinase*. Mol Cell Biol. 1996. 16(6):2857-64.

Michalak M., Groenendyk J., Szabo E., Gold LI, Opas M. *Calreticulin, a multi-process calcium-buffering chaperone of the endoplasmic reticulum.* Biochem J. 2009. 471(3): 651-666.

Mitra A., Ross JA., Rodriguez G., Nagy ZS., Wilson HL., Kirken RA. *Signal transducer and activator of transcription 5b (Stat5b) serine 193 is a novel cytokine-induced phospho-regulatory site that is constitutively activated in primary hematopoietic malignancies*. J Biol Chem. 2012. 287(20): 7685-7691.

Moulard O., Mehta J., Fryzek J., Olivares R., Iqbal U., Mesa RA. *Epidemiology of myelofibrosis, essential thrombocythemia, and polycythemia vera in the European Union*. Eur. J. Haematol., 2014. 92(4): 289-297.

Mullaly A, Lane SW, Ball B., Megerdichian C., Okabe R., Al-Shahrour F., Paktinat M., Haydu JE., Housman E., Lord AM., Wernig G., Kharas MG., Mercher T., Kutok JL., Gilliland DG., Ebert BL. *Physiological JAK2V617F expression causes a lethal myeloproliferative neoplasm with differential effects on hematopoietc stem and progenitor cells*. Cancer Cell. 2010. 17(6): 584-596.

Nakamura K., Zuppini A., Arnaudeau S., Lynch J., Ahsan I., Krause R., Papp S., De Smedt H., Parys JB., Muller-Esterl W., Lew DP., Krause KH., Demaurex N., Opas M., Michalak M. *Functional specialization of calreticulin domains.* J Cell Biol. 2001. 154(5): 961-72.

Nangalia J., Massie CE., Baxter EJ., Nice FL., Gundem G., Wedge DC., Avezov E., Li J., Kollmann K., Kent DG., Aziz A., Godfrey AL., Hinton J., Martincorena I., Joes AV., Guglielmelli P., Harding HP., Goudie CT., Ortmann CA., Loughran SJ., Raine K., Jones DR., Butler AP., Teague JW., O'Meara S., McLaren S., Bianchi M., Bloxham D., Maddison M., Robinson B., Hill K., Orchard K., Harrison CN., Cross NC., Ron D., Vannucchi AM., Papaemmanuil E., Campbell PJ., Green AR. *Somatic CALR Mutations in Myeloproliferative Neoplasms with Nonmutated JAK2. New England Journal of Medicine*. 2013. 369(25): 2391-2405.

Nangalia J., Nice FL., Wedge DC., Godfrey AL., Grinfield J., Thakker C., Massie CE., Baxter J., Sewell D., Silber Y., Campbell PJ., Green AR. *DNMT3A mutations occur early or late in patients with myeloproliferative neoplams and mutation influences phenotype*. Haematologica. 2015. 100(11): e438-42.

Nishioka C., Ikezoe T., Yang J., Yokoyama A. *Long-term exposure of leukemia cells to multi-targetd tyrosine kinase inhibitor induces activations of AKT, ERK and STAT5 signaling via epigenetic silencing of the PTEN gene*. Leukemia. 2010. 24(9): 1631-1640.

Nivarthi H., Chen D., Clearly C., Kubesova B., Jäger R., Bogner E., Marty C., Pecquet C., Vainchenker W., Constantinescu SN., Kralovics R. *Thrombopoietin receptor is required for the oncogenic function of CALR mutants*. Leukemia. 2016. 30(8): 1759-1763.

Ortmann CA., Kent DG., Nangalia J., Silber Y., Wedge DC., Grinfeld J., Baxter EJ., Massie CE., Papaemmanuil E., Menon S., Godfrey AL., Dimitropoulou D., Guglielmelli P., Bellosillo B., Besses C., Döhner K., Harrison CN., Vassiliou GS., Vannucchi A., Campbell PJ., Green AR. *Effect of mutation order on myeloproliferative neoplasm.* N Engl J Med. 2015. 372(7): 601-612.

Pandey R., Kapur R. *Targeting phosphatidylinositol-3-kinase pathway for the treatment of Philadelphia-negative myeloproliferative neoplasms*. Mol Cancer. 2015. 11;14:118.

Pardanani AD., Levine RL., Lasho T., Pikman Y., Mesa RA., Wadleigh M., Steensma DP., Elliott MA., Wolanskyj AP., Hogan WJ., McClure RF., Litzow MR., Gilliland DG., Tefferi A. *MPL515 mutations in myeloproliferative and other myeloid disorders: a study of 1182 patients.* Blood. 2006. 108(10): 3472-3476.

Pardanani A., Vannucchi AM, Passamonti F, Cervantes F, Barbui T, Tefferi A. *JAK inhibitor therapy for myelofibrosis: critical assessment of value and limitations.* Leukemia. 2011. 25(2): 218-25.

Park SH., Kim SY., Lee SM., Yi J., Kim IS., Kim HH., Chang CL., Lee EY., Song MK., Shin HJ., Chung JS. *Incidence, clinical features, and prognostic impact of CALR exon 9 mutations in essential thrombocythemia and primary myelofibrosis: an experience of a single tertiary hospital in Korea.* Ann Lab Med. 2015. 35(2): 233-37.

Passamonti F., Rumi E., Arcaini L., Boveri E., Elena C., Pietra D., Boggi S, Astori C., Bernasconi P, Varettoni M., Brusamolino E., Pascutto C., Lazzarino M. *Prognostic factors for thrombosis, myelofibrosis, and leukemia in essential thrombocythemia. A study of 605 patients*. Haematologica. 2008. 93(11): 1645-1651.

Passamonti F., Elena C., Schnittger S., Skoda RC., Green AR., Girodon F., Kiladjian JJ., McMullin MF., Ruggeri M., Besses C., Vannucchi AM., Lippert E., Gisslinger H., Rumi E., Lehmann T., Ortmann CA., Pietra D., Pascutto C., Haferlach T., Cazzola M. *Molecular and clinical features of the myeloproliferative neoplasm associated with JAK2 exon 12 mutations.* Blood. 2011. 117(10):.2813-6.

Passamonti F., Griesshammer M, Palandri F., Egyed M., Benevolo G., Devos T., Callum J., Vannucchi AM., Sivgin S., Bensasson C., Khan M., Mounedji N., Saydam G. *Ruxolitinib for the treatment of inadequately controlled polycythaemia vera without splenomegaly (RESPONSE-2): a randomised, open-label, phase 3b study*. Lancet Oncol. 2017. 18(1): 88-99.

Pattanayak V., Guilinger JP., Liu DR. *Determining the specificities of TALENs, Cas9, and other genome editing enzymes.* Methods Enzymol. 2014. 546: 47–78.

Perrotti D., Neviani P. *Protein phosphatase 2A: a target for anticancer theraphy.* Lancet Oncol. 2013. 14(6): e229-238.

Peterson TR., Laplante M., Thoreen CC., Sancak Y., Kang SA., Kuehl WM., Gray NS., Sabatini DM. *DEPTOR is an mTOR inhibitor frequently overexpressed in multiple myeloma cells and required for their survival.* Cell. 2009. 137(5): 873-86.

Pietra D., Rumi E., Ferretti VV., Di Buduo CA., Milanesi C., Cavalloni C., Sant'Antonio E., Abbonante V., Moccia F., Casetti IC., Bellini M., Renna MC., Roncoroni E., Fugazza E., Astori C., Boveri E., Rosti V., Barosi G., Balduini A., Cazzola M. *Differential clinical effects of different mutation subtypes in CALR-mutant myeloproliferative neoplams*. Leukemia. 2016. 30 (2): 431-438.

Pikman Y., Lee BH., Mercher T., McDowell E., Ebert BL., Gozo M., Cuker A., Wernig G., Moore S., Galinsky I., DeAngelo DJ., Clark JJ., Lee SJ., Golub TR., Wadleigh M., Gilliland DG., Levine RL. *MPLW515L is a novel somatic activating mutation in myelofibrosis with myeloid metaplasia*. PLoS Med. 2006. 3:e270.

Prchal JF., Axelrad AA. *Letter: Bone-marrow responses in polycythemia vera*. N Engl J Med. 1974. 290(24): 1382.

Qi LS., Larson MH., Gilbert LA., Doudna JA., Weissman JS., Arkin AP., Lim WA. *Repurposing CRISPR as an RNA-Guided Platform for Sequence-Specific Control of Gene Expression.* Cell. 2013. 152(5): 1173–1183.

Quintas-Cardama A., Vaddi K., Liu P., Manshouri T., Li J., Scherle PA., Caulder E., Wen X., Li Y., Waeltz P., Rupar M., Burn T., Lo Y., Kelley J., Covington M., Shepard S., Rodgers JD., Haley P., Kantarjian H., Fridman JS., Verstovsek S. *Preclinical characterization of the selective JAK1/2 inhibitor INCB18424: therapeutic implications for the treatment of myeloproliferative neoplasms*. Blood. 2010. 115(15): 3109-3117.

Quintas-Cardama A., Verstovsek S. *Molecular Pathways: Jak/Stat pathway: mutations inhibitors and resistance*. Clin Cancer Res. 2013. 19(8):1933-1940.

Rampal R., Al-Shahrour F., Abdel-Wahab O., Patel JP., Brunel JP., Mermel CH., Bass AJ., Pretz J., Ahn J., Hricik T., Kilpivaara O., Wadleigh M., Busque L., Gilliland DG., Golub TR., Ebert BL., Levine RL. *Integrated*

genomic analysis illustrates the central role of JAK-STAT pathway activation in myeloproliferative neoplasm pathogenesis. Blood. 2014. 123(22): e123-133.

Ran FA., Hsu PD., Lin CY., Gootenberg JS., Konermann S., Trevino AE., Scott DA., Inoue A., Matoba S., Zhang Y., Zhang F. *Double nicking by RNA-guided CRISPR Cas9 for enhanced genome editing specificity*. Cell. 2013. 154(6): 1380-1389.

Randi ML., Putti MC., Scapin M., Pacquola E., Tucci F., Micalizzi C., Zanesco L., Fabris F. *Pediatric patients with essential thrombocythemia are mostly polyclonal and V617FJAK2 negative.* Blood. 2006. 108(10): 3600-3602.

Ren H., Chen M., Yue P., Tao H., Owonokoko TK., Ramalingam SS., Khuri Fr., Sun SY. *The combination of RAD001 and NVP-BKM120 synergistically inhibits the growth of lung cancer in vitro and in vivo*. Cancer Letters. 2012. 325: 139-146.

Rosich L., Saborit-Villarroya I., Lopez-Guerra M., Xargay-Torrent S., Montraveta A., Aymerich M., Villamor N., Campo E., Pérez-Galan P., Roue G., Colomber D. *The phosphatidylinositol-3-kinase inhibitor NVP-BKM120 overcomes resistance signals derived from microenvironment by regulating the Akt/FoxO3a/Bim axis in chronic lymphocytic leukemia cells.* Haematologica. 2013; 98 (11): 1739-47.

Ross JA., Cheng H., Nagy ZS, Frost JA., Kirken RA. *Protein phosphatase 2A regulates interleukin-2 receptor complex formation and JAK3/STAT5 activation*. J Biol Chem. 2010. 285(6): 3582-3591.

Rotunno G., Mannarelli C., Guglielmelli P., Pacilli A., Pancrazzi A., Pieri L., Fanelli T., Bosi A., Vannucchi AM. *Impact of Careticulin Mutations on Clinical and Hematological Phenotype and Outcome in Essential Thrombocytemia*. Blood. 2014. 123(10): 1552-1555.

Rousseau D, Kaspar R, Rosenwald I, Gehrke L, Sonenberg N. *Translation initiation of ornithine decarboxylase and nucleocytoplasmic transport of cyclin D1 mRNA are increased in cells overexpressing eukaryotic initiation factor 4E*. Proc Natl Acad Sci U S A. 1996. 93(3): 1065-70.

Rumi E., Pietra D., Ferretti V., Klampfl T., Harutyunyan AS., Milosevic JD., Them NC., Berg T., Elena C., Casetti IC., Milanesi C., Sant'antonio E., Bellini M., Fugazza E., Renna MC., Boveri E., Astori C., Pascutto C., Kralovics R., Cazzola M. *JAK2 or CALR mutation defines subtypes of essential thrombocithemia with substantially different clinical course and outcomes.* Blood. 2014. 123(10): 1544-1551.

Rumi E., Pietra D., Pascutto C., Guglielmelli P., Martínez-Trillos A., Casetti I., Colomer D., Pieri L., Pratcorona M., Rotunno G., Sant'Antonio E., Bellini M., Cavalloni C., Mannarelli C., Milanesi C., Boveri E., Ferretti V., Astori C., Rosti V., Cervantes F., Barosi G., Vannucchi AM., Cazzola M. *Clinical effect of driver mutations of JAK2, CALR, or MPL in primary myelofibrosis*. Blood. 2014. 124(7): 1062-9.

Sander JD., Joung JK. *CRISPR-Cas systems for genome editing, regulation and targeting*. Nat Biotechnol. 2014. 32(4): 347–355.

Sapranauskas R., Gasiunas G., Fremaux C., Barrangou R., Horvath P., Siksnys V. *The Streptococcus thermophilus CRISPR/Cas system provides immunity in Escherichia coli.* Nucleic Acids Res. 2011. 39(21): 9275–9282.

Schaub FX., Looser R., Li S., Hao-Shen H., Lehmann T., Tichelli A., Skoda RC. *Clonal analysis of TET2 and JAK2 mutations suggests that TET2 can be a late event in the progression of myeloproliferative neoplasms*. Blood. 2010. 115(10): 2003–07.

Schnutgen F., Doerfliger N., Calléja C., Ending O., Chambon P., Ghyselinck NB. *A directional strategy for monitoring Cre-mediated recombination at the cellular level in the mouse.* Nat. Biotechnol. 2003. 21(5): 562-5.

Scott LM., Tong W., Levine RL., Scott M., Beer P., Stratton M., Futreal A., Erber W., McMullin MF., Harrison CN., Path MRC., Warren A., Gilliland G., Lodish HF., Green AR., Path FR. *JAK2 exon 12 mutations in polycythemia vera and idiopathic erythrocytosis.* N Engl J Med. 2007. 356:459-468.

Scott LM. *The JAK2 exon 12 mutations: a comprehensive review*. Am J. Hematol. 2011. 86(8): 668-76.

Semenova E., Jore MM., Datsenko KA., Semenova A., Westra ER., Wanner B., van der Oost J., Brouns SJ., Severinov K. *Interference by clustered regularly interspaced short palindromic repeat (CRISPR) RNA is governed by a seed sequence*. Proc. Natl. Acad. Sci. U S A. 2011. 108(25): 10098–10103.

Serra V., Markman B., Scaltriti M., Eichhorn P., Valero V., Guzman M., Botero ML., Llonch E., Atzori F., Di Cosimo S., Maira M., Garcia-Echeverria C., Parra JL., Arribas J., Baselga J. *NVP-BEZ235, a dual PI3K/mTOR inhibitor, prevents PI3K signaling and inhibits the growth of cancer cells with activating PI3K mutations*. Cancer Res. 2008. 68: 8022–8030.

Silvennoinen O., Hubbard SR. *Molecular insights into regulation of JAK2 in myeloproliferative neoplams.* Blood. 2015. 125(22): 3388-3892.

Shide K., Shimoda HK., Kumano T., Karube K., Kameda T., Takenaka K., Oku S., Abe H., Katayose KS., Kubuki Y., Kusumoto K., Hasuike S., Tahara Y., Nagata K., Matsuda T., Ohshima K., Harada M., Shimoda K. *Development of ET, primary myelofibrosis and PV in mice expressing* JAK2 V617F. Leukemia. 2008. 22(1): 87–95.

Shide K., Kameda T., Yamaji T., Sekine M., Inada N., Kamiunten A., Akizuki K., Nakamura K., Hidaka T., Kubuki Y., Shimoda H., Kitanaka A., Honda A., Sawaguchi A., Abe H., Miike T., Iwakiri H., Tahara Y., Sueta M., Hasuike S., Yamamoto S., Nagata K., Shimoda K. *Calreticulin mutant mice develop essential thrombocythemia that is ameliorated by the JAK inhibitor ruxolitinib.* Leukemia. 2017. 31(5): 1136-1144.

Shivaron V., Ivanova M., Tiu RV. *Mutated calreticulin retains structurally disordered C terminus that cannot bind Ca(2+): some mechanistic and therapeutic implications*. Blood Cancer J. 2014. 4:e185.

Skoda RC., Duek A., Grisouard J. *Pathogenesis of myeloproliferative neoplasms*. Exp Hematol. 2015. 43(8): 599-608.

Spivak JL. *Myeloproliferative neoplasms.* N Engl J Med. 2017. 376(22): 2168-2181.

Staerk J., Lacout C., Sato T., Smith SO., Vainchenker W., Costantinescu SN. *An amphipathic motif at the transmembrane cytoplasmic junction prevents autonomous activation of the thrombopoietin receptor*. Blood. 2006. 107(5): 1864-1871.

Steensma DP. *JAK2 V617F in myeloid disorders: molecular diagnostic techniques and their clinical utility: a paper from the 2005 William Beaumont Hospital Symposium on Molecular Pathology*. J Mol Diagn 2006. 8(4): 397–411.

Tahkandi H., Moore EM., Tomlinson B., Goebel. T., Sadri N. Co-occurrence of type I CALR and two MPL mutations in patient with primary myelofibrosis. Ann. Hematol. 2017. 96(8): 1399-1401.

Tapper W., Jones AV, Kralovics R, Harutyunyan AS, Zoi K, Leung W, Godfrey AL, Guglielmelli P, Callaway A, Ward D, Aranaz P, White HE, Waghorn K, Lin F, Chase A, Baxter EJ, Maclean C, Nangalia J, Chen E, Evans P, Short M, Jack A, Wallis L, Oscier D, Duncombe AS, Schuh A, Mead AJ, Griffiths M, Ewing J, Gale RE, Schnittger S, Haferlach T, Stegelmann F, Döhner K, Grallert H, Strauch K, Tanaka T, Bandinelli S, Giannopoulos A, Pieri L, Mannarelli C, Gisslinger H, Barosi G, Cazzola M, Reiter A, Harrison C, Campbell P, Green AR, Vannucchi A, Cross NC. *Genetic variation at MECOM, TERT, JAK2 and HBS1L-MYB predisposes to myeloproliferative neoplasms*. Nat. Commun. 2015. 6: 6691.

Tefferi A., Thiele J., Orazi A., Kvasnicka HM., Barbui T., Hanson CA., Barosi G., Verstovsek S., Birgegard G., Mesa R., Reilly JT., Gisslinger H., Vannucchi AM., Cervantes F., Finazzi G., Hoffman R., Gilliland DG.,

Bloomfield CD., Vardiman JW. *Proposals and rationale for revision of the World Health Organization diagnostic criteria for polycythemia vera, essential thrombocythemia, and primary myelofibrosis: recommendations from an ad hoc international expert panel*. Blood 2007. 110(4): 1092-7.

Tefferi A. *Essential Thrombocythemia, polycythemia vera, and myelofibrosis: current management and the prospect of targeted therapy.* Am J Hematol. 2008. 83(6): 491-7.

Tefferi A. Kantarjian H. and Pardanani AD., Mesa AR., Newton RC., Scherle PA., Burn T., Verstovsek S. *The clinical phenotype of myelofibrosis encompasses a chronic inflammatory state that is favorably altered by INCB018424, a selective inhibitor of JAK1/2.* Blood. 2008. 112(11): 2804.

Tefferi A. *Novel mutations and their functional and clinical relevance in myeloproliferative neoplasms: JAK2, MPL, TET2, ASXL1, CBL, IDH and IKZF1*. Leukemia. 2010. 24(6):1128-1138.

Tefferi A., Vainchenker W. *Myeloproliferative neoplasms: molecular pathophysiology, essential clinical understanding, and treatment strategies.* J. Clin Oncol. 2011. 29(5): 573-582.

Tefferi A., Wassie EA, Guglielmelli P., Gangat N., Belachew AA., Lasho TL., Finke C., Ketterling RP., Hanson CA., Pardanani A., Wolanskyj AP., Maffioli M., Casalone R., Pacilli A., Vannucchi AM., Passamonti F. *Type 1 versus Type 2 Calreticulin mutations in essential thrombocitemia: a collaborative study of 1027 patients*. Am J Hematol. 2014. 89(8): E121-4.

Tefferi A., Guglielmelli P., Larson DR., Finke C., Wassie EA., Pieri L., Gangat N., Fjerza R., Belachew AA., Lasho TL., Ketterling RP., Hanson CA., Rambaldi A., Finazzi G., Thiele J., Barbui T., Pardanani A., Vannucchi AM. *Long-term survival and blast transformation in molecularly annotated essential thrombocytemia, polycytemia vera, and myelofibrosis*. Blood. 2014. 124(16): 2507-2513.

Tefferi A., Lasho TL., Finke CM., Knudson RA., Ketterling R., Hanson CH., Maffioli M., Caramazza D., Passamonti F., Pardanani A. *CALR vs JAK2 vs MPL-mutated or triple-negative myelofibrosis: clinical, cytogenetic and molecular comparison*. Leukemia. 2014. 28(7): 1472-1477.

Tefferi A. *Myeloproliferative Neoplasms: A decade of discoveries and treatment advances.* Am J Hematol. 2016. 91(1): 50-58.

Tefferi A., Pardanani A. *Myeloproliferative neoplams: a contemporary review*. JAMA Oncol. 2015. 1(1): 97-105.

Tefferi A., Lasho TL., Guglielmelli P., Finke CM., Rotunno G., Elala Y., Pacilli A., Hanson CA., Pancrazzi A., Ketterling RP., Mannarelli C., Barracco D., Fanelli T., Paradanani A., Naseema G., Vannucchi AM. *Targeted deep sequencing in polycytemia vera and essential thrombocythemia*. Blood Adv. 2016. 1(1): 21-30.

Tefferi A., Lasho TL., Finke CM., Elala Y., Hanson CA., Ketterling RP., Gangat N., Pardanani A. *Targeted deep sequencing in primary myelofibrosis.* Blood Adv. 2016. 1(2): 105-111.

Tefferi A., Vannucchi AM. *Genetic Risk Assessment in Myeloproliferative Neoplasms*. Mayo Clin Proc. 2017. 92(8): 1283-1290.

Tenedini E., Bernardis I., Artusi V., Artuso L., Roncaglia E., Guglielmelli P., Pieri L., Bogani C., Biamonte F., Rotunno G., Mannarelli C., Bianchi E., Pancrazzi A., Fanelli T., Malagoli Tagliazucchi G., Ferrari S., Manfredini R., Vannucchi AM., Tagliafico E.; AGIMM investigators. *Targeted cancer exome sequencing reveals recurrent mutations in myeloproliferative neoplasms.* Leukemia. 2014. 28(5):1052-1059.

Teofili L., Giona F., Martini M., Cenci T., Guidi F., Torti L., Paulmbo G., Amendola A., Leone G., Foà R., Larocca LM. *The revised WHO diagnostic criteria for Ph-negative myeloproliferative diseases are not appropriate for the diagnostic screening of childhood polycythemia vera and essential thrombocythemia.* Blood. 2007. 110(9): 3384-3386.

Tiedt R., Hao-Shen H., Sobas MA., Looser R., Dirnhofer S., Schwaller J., Skoda RC. *Ratio of mutant JAK2-V617F to wild-type Jak2 determines the MPD phenotypes in transgenic mice.* Blood 2008. 111(8): 3931–3940.

Titmarsh GJ., Duncombe AS., McMullin MF., O'Ronke M, Mesa R, De Vocht F, Horan S, Fritschi L., Clarke M., Anderson LA. *How common are myeloproliferative neoplams? A systematic review and meta-analysis.* Am J Hematol. 2014. 89(6): 581-587.

Tiedt R., Hao-Shen H., Sobas MA., Looser R., Dirnhofer S., Schwaller J., Skoda RC. *Ratio of mutant JAK2-V617F to wild-type Jak2 determines the MPD phenotypes in transgenic mice*. Blood 2008. 111(8): 3931–3940.

Titmarsh GJ., Duncombe AS., McMullin MF., O'Ronke M, Mesa R, De Vocht F, Horan S, Fritschi L., Clarke M., Anderson LA. *How common are myeloproliferative neoplams? A systematic review and meta-analysis*. Am J Hematol. 2014. 89(6): 581-587.

Ugo V., Marzac C., Teyssandier I., Larbret F., Lécluse Y., Debili N., Vainchenker W., Casadevall N. *Multiple signaling pathways are involved in erythropoietin-independent differentiation of erythroid progenitors in polycythemia vera*. Exp Hematol. 2004; 32: 179–87.

Urnov FD., Rebar EJ., Holmes MC., Zhang HS., Gregory PD. *Genome editing with engineered zinc finger nucleases.* Nat. Rev.Genetics. 2010. 11(9): 636-646.
Vainchenker W., Delhommeau F., Constantinescu SN., Bernard OA. *New mutations and pathogenesis of myeloproliferative neoplasms.* Blood. 2011. 118(7): 1723-35

Vainchenker W., Constantinescu SN. *JAK/STAT signaling in hematological malignancies*. Oncogene. 2013. 32(21): 2601–2613.

Vainchenker W., Kralovics R. *Genetic basis and molecular pathophysiology of classical myeloproliferative neoplams*. Blood. 2017. 219(6): 667-679.

Vannucchi AM., Antonioli E., Guglielmelli P., Rambaldi A., Barosi G., Marchioli R., Marfisi RM., Finazzi G., Guerini V., Fabris F., Randi ML., De Stefano V., Caberlon S., Tafuri A., Ruggeri M., Specchia G., Liso V., Rossi E., Pogliani E., Gugliotta L., Bosi A., Barbui T. *Clinical profile of homozygous JAK2V617F mutation in patients with polycythemia vera or essential thrombocythemia.* Blood. 2007. 110(3): 840-846.

Vannucchi AM., Antonioli E., Guglielmelli P., Pancrazzi A., Guerini V., Barosi G., Ruggeri M., Specchia G., Lo-Coco F., Delaini F., Villani L., Finotto S., Ammatuna E., Alterini R., Carrai V., Capaccioli G., Di Lollo S., Liso V., Rambaldi A., Bosi A., Barbui T. *Characteristics and clinical correlates of MPL 515W-L/K mutation in essential thrombocythemia.* Blood. 2008. 112(3): 844–847.

Vannucchi AM., Pieri L., Guglielmelli P. *JAK2 Allele Burden in the Myeloproliferative Neoplasms: Effects on Phenotype, Prognosis and Change with Treatment.* Ther Adv Hematol. 2011. 2(1): 21-32.

Vannucchi AM., Rotunno G., Bartalucci N., Raugei G., Carrai V, Balliu m., Mannarelli C., Pacilli A., Calabresi L.., Fjerza R., Pieri L., Bosi A., Manfredini R., Guglielmelli P. *Calreticulin mutation-specific immunostaining in myeloproliferative neoplasms: pathogenetic insight and diagnostic value.* Leukemia. 2014. 28(9): 1811-1818.

Vannucchi AM., Kantarjian HM., Kiladjian JJ., Gotlib J., Cervantes F., Mesa RA., Sarlis NJ., Peng W., Sandor V., Gopalakrishna P., Hmissi A., Stalbovskaya V., Gupta V., Harrison C., Verstovsek S.; COMFORT Investigators. *A pooled analysis of overall survival in COMFORT-I and COMFORT-II, 2 randomized phase III trials of ruxolitinib for the treatment of myelofibrosis*. Haematologica. 2015. 100(9): 1139-45.

Vannucchi AM., *Ruxolitinib versus standard therapy for the treatment of polycythemia vera.* N Engl. J Med. 2015. 372(17): 1670-1671.

Vannucchi AM., Kiladjian JJ., Griesshammer M., Masszi T., Durrant S., Passamonti F., Harrison CN., Pane F., Zachee P., Mesa R., He S., Jones MM., Garrett W., Li J., Pirron U., Habr D., Verstovsek S. *Ruxolitinib versus standard therapy for the treatment of polycythemia vera*. N Engl J Med. 2015. 372(5): 426-35.

Vaquez HL. *Sur une forme speciale de cyanose s'accompagnant d'hyperglobulie excessive et peristante*. C.R. Soc. Biol. 1892. 44: 384-388.

Vardiman JW., Thiele J., Arber DA., Brunning RD., Borowitz MJ., Porwit A, Harris NL, Le Beau MM., Hellstrom-Lindberg E., Tefferi A., Bloomfield C. *The 2008 revision of the World Health Organization (WHO) classification of myeloid neoplasms and acute leukemia: rationale and important changes*. Blood. 2009. 114(5): 937-951.

Verma A., Kambhampati S., Parmar S., Platanias LC. *Jak family of kinases in cancer*. Cancer Metastasis Rev. 2003. 22(4): 423-34.

Verstovsek S., Kantarjian H., Mesa RA., Pardanani AD., Cortes-Franco J., Thomas DA., Estrov Z., Fridman JS., Bradley EC., Erickson-Viitanen S., Vaddi K., Levy R., Tefferi A. *Safety and efficacy of INCB018424, a JAK1 and JAK2 inhibito, in myelofibrosis*. N Engl J Med. 2010. 363(12): 1117-1127.

Verstovsek S., Mesa RA., Gotlib J., Levy RS., Gupta V., DiPersio JF., Catalano JV., Deininger M., Miller C., Silver RT., Talpaz M., Winton EF., Harvey JH Jr., Arcasoy MO., Hexner E., Lyons RM., Paquette R., Raza A., Vaddi K., Erickson-Viitanen S., Koumenis IL., Sun W., Sandor V., Kantarjian HM. *A double-blind, placebo-controlled trial of ruxolitinib for myelofibrosis*. N Engl J Med. 2012. 366(9): 799-807.

Vicari L., Martinetti D., Buccheri S., Colarossi C., Aiello E., Stagno F., Villari L., Cavalli M., Di Raimondo F., Gulisano M., De Maria R., Vigneri P. *Increased phospho-mTOR expression in megakaryocytic cells derived from CD34þ progenitors of essential thrombocythaemia and myelofibrosis patients*. Br J Haematol. 2012. 159(2): 237-40.

Yang J., Ikezoea T., Nishioka C., Nia L., Koefflerb HP., Yokoyama A. *Inhibition of mTORC1 by RAD001 (everolimus) potentiates the effects of 1,25-dihydroxyvitamin D3 to induce growth arrest and differentiation of AML cells in vitro and in vivo.* Exp Hematol. 2010. 38(8):666–676.

Yee KW., Zeng Z., Konopleva M., Verstovsek S., Ravandi F., Ferrajoli A., Thomas D., Wierda E., Apostolidou E., Albitar M., O'Brien S., Andreeff M., Giles FJ. *Phase I/II study of the mammalian target of rapamycin inhibitor everolimus (RAD001) in patients with relapsed or refractory hematologic malignancies*. Clin Cancer Res. 2006. 12(17): 5165-5173.

Xu Y., Jin J., Liu Y., Huang Z., Deng Y., You T., Zhou T., Si J., Zhuo W. *Snail-regulated MiR-375 inhibits migration and invasion of gastric cancer cells by targeting JAK2.* PLoS One. 2014. 9(7): e99516.

Xu X., Tan X., Tampe B., Sanchez E., Zeisberg M., Zeisberg EM. *Snail Is a Direct Target of Hypoxia-inducible Factor 1alpha (HIF1alpha) in Hypoxia-induced Endothelial to Mesenchymal Transition of Human Coronary Endothelial Cells*. J Biol Chem. 2015. 290(27): 16653-16664.

Wang H., Yang H., Shivalila CS., Dawlaty MM., Cheng AW., Zhang F., Jaenisch R. *One-step generation of mice carrying mutations in multiple genes by CRISPR/Cas-mediated genome engineering*. Cell. 2013. 153 (4): 910-918.

Wang R., Preamplume G., Terns MP., Terns RM., Li H. *Interaction of the Cas6 riboendonuclease with CRISPR RNAs: Recognition and cleavage.* Structure. 2011. 19(2): 257-264.

Wernig G., Mercher T., Okabe R., Levine RL., Lee BH., Gilliland DG. *Expression of JAK2V617F causes a polycythemia vera-like disease with associated myelofibrosis in a murine bone marrow transplant model.* Blood. 2006. 107(11): 4274–81.

Wiedenheft B., Sternberg SH., Doudna JA. *RNA-guided genetic silencing systems in bacteria and archaea*. Nature. 2012. 482(7385): 331-338.

Wolanskyi A., Schwager SM., McClure R., Larson DR., Tefferi A. *Essential thrombocythemia beyond the first decade: expectancy, long-term complication rates, and prognostic factors*. Mayo Clini Proc. 2006. 81(2): 159-166.

Wu Z., Zhang X., Xu X., Chen Y, Hu T., Kang Z., Li S., Wang H., Liu W., Ma X., Guan M. *The mutation profile of JAK2 and CALR in Chinese Han patients with Philadelphia chromosome-negative myeloproliferative neoplasms*. J Hematol Oncol. 2014. 7:48.

Zaleskas VM., Krause DS., Lazarides K., Patel N., Hu Y., Li S., Van Etten RA. *Molecular pathogenesis and therapy of polycythemia induced in mice by JAK2V617F*. PLoS One. 2006. 1: e18.

Zheng Y., Yang J., Qian J., Zhang L., Lu Y., Li H., Lin H., Lan Y., Liu Z., He J., Hong S., Thomas S., Shah J., Baladandayuthapani V., Kwak LW., Yi Q. *Novel phosphatidylinositol 3-kinase inhibitor NVP-BKM120 induces apoptosis in myeloma cells and shows synergistic anti-myeloma activity with dexamethasone*. J Mol Med 2012. 90(6): 695-706.